



UNIVERSITÄT  
BAYREUTH

Department of Plant Ecology

# Remote sensing-based Assessment of Gross Primary Production in Agricultural Ecosystems

Dissertation

to obtain the academic degree of Doctor of Natural Science (Dr. rer. nat.)

of the Bayreuth Graduate School for Mathematical and Natural Sciences of the University of Bayreuth

presented by

Bora Lee

born 15<sup>th</sup> March 1982 in Busan, Republic of Korea

Bayreuth, December 2014

---

This doctoral thesis was prepared at the Department of Plant Ecology, University of Bayreuth between April 2009 and December 2014 and was supervised by Prof. Dr. John Tenhunen, Dr. Hyojung Kwon, Prof. Dr. Bernd Huwe, and Prof. Dr. Sinkyu Kang.

This is a full reprint of the dissertation submitted to obtain the academic degree of Doctor of Natural Sciences (Dr. rer. nat.) and approved by the Bayreuth Graduate School of Mathematical and Natural Sciences (BayNAT) of the University of Bayreuth.

Date of submission: 11 December 2014

Date of defense : 3 March 2015

Acting Director: Prof. Dr. Franz Xaver Schmid

Doctoral Committee:

Prof. Dr. John Tenhunen (1<sup>st</sup> reviewer)

Prof. Dr. Christoph Thomas (2<sup>nd</sup> reviewer)

Prof. Dr. Cyrus Samimi (chairman)

Prof. Dr. Bernd Huwe

---

## Summary

Productivity in agricultural ecosystems is important to understand in terms of their role as a strong modifier of regional carbon balance, but also in their intended role of capturing carbon (energy) in the form of food products, e.g. agricultural yield. Gross primary production (GPP) of agricultural ecosystems is the amount of total carbon assimilated by the planted crops and the driver of useful biomass production. To assess the GPP of croplands, this study combines information from flux determinations with eddy covariance (EC) methodology, process-based modeling of carbon gain, and satellite remotely-sensed vegetation indices (VIs). The data is brought together synthetically for major crops found in agricultural landscapes of Gwangwon Province, South Korea, e.g., rice, soybean, maize, potato, and sugar beet as a surrogate for radish. The long term goal (beyond the current effort) is to utilize the results to assess carbon balances, agricultural production and yields in the landscape of Haeon Catchment, South Korea, which has been the focus of research in the TERRECO project (see acknowledgement).

This study focuses on relating two major variables determining GPP; leaf area index (LAI) of the crop and carboxylation capacity of the crop canopy ( $V_{c_{\text{uptake}}}$  - as first defined by Owen et al. 2007), to MODIS remotely sensed vegetation indices (VIs). Success in deriving such relationships will allow GPP to be remotely determined over the seasonal course of crop development. The relationship to VIs of both LAI and  $V_{c_{\text{uptake}}}$  were considered first by using the general regression approaches commonly applied in remote sensing studies, i.e., simple linear models or other statistical regression models. The results of GPP estimation from these general models were not adequate and led overall to underestimations. Therefore, a new alternative approach was developed to estimate LAI and  $V_{c_{\text{uptake}}}$  that used consistent development curves for each crop, i.e., relies on consistent biological regulation of plant development. In this case, the remote sensing maximum in VIs is used to identify timing of phenological development at the observed location. Depending on the maximum in VIs, seasonal change in the critical variables for structure and crop physiology may be estimated by synthesizing data from EC studies at multiple sites for each crop.

The relationship between observed GPP and modeled GPP based on the consistent development curves for LAI is remarkably improved over regression based values with  $R^2$  from 0.79 to 0.93. Modeled GPP based on the consistent development curve for both LAI and  $V_{c_{\text{uptake}}}$

agreed with  $R^2$  from 0.76 to 0.92 (within the 95% confidence interval) at the rice paddy sites. In the case of dry-land crops, the relationship between measured and modeled GPP based on the consistent development curve for LAI showed significantly improved results with  $R^2$  from 0.61 to 0.93 (within the 95% confidence interval), while measured vs. modeled GPP based on the consistent development curve for both LAI and  $V_{c_{\text{uptake}}}$  exhibited an  $R^2$  from 0.60 to 0.91 (within the 95% confidence interval).

Several unsolved problems remain with respect to GPP estimation that are associated with uncertainties in vegetation indices, unmatched scale for field size and remote sensing pixels, infrequent sampling of LAI at EC sites, and uncertainties whether LAI measurements correctly represent average crop structure within EC measurement footprints. Nevertheless, the results in this study demonstrate that improved linkages between the ground-based survey data, eddy flux measurements, process-based models, and remote sensing can be constructed to estimate GPP in agricultural ecosystems. This study suggests further that the consistent development curve concept and approach has potential for predicting GPP better than simple linear models, and therefore, to estimate critical parameters influencing carbon gain and agricultural yields with various crop types. Further and more detailed studies are required with accurately sampled spatial data in agricultural ecosystems in order to better calibrate LAI and physiological parameters such as  $V_{c_{\text{uptake}}}$  for use in models for GPP.

## Zusammenfassung

Es ist wichtig, die Produktivität von Agrarökosystemen zu verstehen, einerseits in ihrer Rolle als bedeutender Modifikator des regionalen Kohlenstoffhaushalts, zum anderen auch in der Bindung von Kohlenstoff (Energie) in Form von Lebensmitteln, z.B. dem landwirtschaftlichen Ertrag. Die Bruttoprimärproduktion (GPP) von Agrarökosystemen ist die Menge des gesamten, von den gepflanzten Feldfrüchten fixierten Kohlenstoffs und der Hauptparameter für die nutzbare Biomasseproduktion. Um die GPP von landwirtschaftlich genutzten Flächen zu messen, kombiniert die vorgelegte Studie Informationen aus Flux-Messungen mit der Eddy-Covarianz (EC)-Methode, prozess-basierter Modellierung des Kohlenstoffgewinns und satellitengesteuerter Erfassung von Vegetationsindizes (VIs). Die Daten wurden für die Hauptanbauprodukte in den Agrarlandschaften der Gangwon Provinz in Südkorea, insbesondere für Reis, Sojabohnen, Mais, Kartoffeln und Zuckerrüben (als Surrogat für Rettich), zusammengetragen und ausgewertet. Langfristiges Ziel (über die hier vorliegende Arbeit hinaus) ist es, die Ergebnisse für die Bestimmung des Kohlenstoffhaushalts, der Agrarproduktion und der Ernteerträge im Gebiet des Haeen Wassereinzugsgebiets in Südkorea zu nutzen (Hauptuntersuchungsgebiet des TERRECO-Projekts s. Danksagung).

Die vorliegende Studie konzentriert sich darauf, zwei Hauptvariablen zur Bestimmung der GPP: den Blattflächenindex (LAI) der Feldfrüchte und die Carboxilierungskapazität der Feldfruchtbestände ( $V_{c_{\text{uptake}}}$ - wie zuerst von Owen et al. 2007 definiert) mit den durch MODIS-Fernerkundung ermittelten Vegetationsindizes (VIs) in Verbindung zu setzen. Eine erfolgreiche Ableitung derartiger Abhängigkeiten wird es ermöglichen, mit Hilfe der Satelliten-Fernerkundung die GPP der verschiedenen Ackerkulturen im Laufe ihrer jahreszeitlichen Entwicklung zu bestimmen. Die Beziehung sowohl von LAI als auch  $V_{c_{\text{uptake}}}$  zu VIs wurde zuerst mit Hilfe allgemeiner Regressionsmethoden betrachtet, die gemeinhin bei Fernerkundungsstudien angewandt werden, insbesondere einfache lineare Modelle oder andere statistische Regressionsmodelle. Die Ergebnisse auf Basis der allgemeinen Modelle für die GPP-Bestimmung waren nicht adäquat und führten durchweg zu Unterschätzungen. Daher wurde ein alternativer Ansatz zur Abschätzung von LAI and  $V_{c_{\text{uptake}}}$  entwickelt, der konsistente Entwicklungskurven für jede Feldfrucht benutzt, d.h. der auf der konsistenten biologischen Regulation der Pflanzenentwicklung beruht. In diesem Fall wird das Maximum des VI der Fernerkundungsdaten benutzt, um das Stadium der

phänologischen Entwicklung an der beobachteten Lokalität zu identifizieren. In Abhängigkeit von den Maxima der VIs kann die saisonale Änderung der kritischen Variablen für Struktur und Physiologie der Ackerfrüchte durch die Synthese der Daten von EC-Studien für jede Feldfrucht an verschiedenen Standorten ermittelt werden.

Die Beziehung zwischen beobachteter GPP und modellierter GPP basierend auf den konsistenten Entwicklungskurven für LAI ist gegenüber regressionsbasierten Werten mit  $R^2$  zwischen 0.79 und 0.93 deutlich verbessert. Die modellierte GPP basierend auf den konsistenten Entwicklungskurven sowohl für LAI als auch für  $V_{\text{cuptake}}$  stimmte mit der gemessenen GPP mit  $R^2$  von 0.76 bis 0.92 (innerhalb des 95% Vertrauensbereichs) für die feuchten Reisstandorte überein. Im Falle der Trockenfeldfrüchte, zeigte die Beziehung zwischen modellierter und gemessener GPP basierend auf den konsistenten Entwicklungskurven für LAI signifikant verbesserte Ergebnisse mit  $R^2$  von 0.61 bis 0.93 (innerhalb des 95% Vertrauensbereichs), während der Zusammenhang zwischen gemessener und modellierter GPP basierend auf den konsistenten Entwicklungskurven sowohl für LAI and  $V_{\text{cuptake}}$  ein  $R^2$  von 0.60 bis 0.91 (innerhalb des 95% Vertrauensbereichs) ergab.

Hinsichtlich der GPP-Bestimmung bleiben einige ungelöste Probleme bestehen, die auf Unsicherheiten bei den Vegetationsindizes, nicht abgestimmten Skalen für die Fernerkundungs-Pixel für Ackerflächengrößen, lückenhafte Beprobung von LAI an EC-Standorten und der Frage, ob LAI-Messungen die durchschnittliche Struktur der Ackerkulturen innerhalb der EC-Fußabdrucke korrekt repräsentieren, beruhen. Dennoch zeigen die Ergebnisse dieser Studie, dass eine verbesserte Kopplung zwischen den Datenerhebungen im Feld, Eddy-Flux-Messungen, prozess-basierten Modellen und Fernerkundung erreicht werden kann, um die GPP in Agrarökosystemen zu bestimmen. Die vorgelegte Arbeit deutet außerdem darauf hin, dass Konzept und Ansatz der konsistenten Entwicklungskurven ein besseres Potential für die Vorhersage von GPP bietet als einfache statistische Modelle und damit auch für die Bestimmung kritischer Parameter, die Kohlenstoffgewinn und landwirtschaftliche Erträge bei verschiedenen Feldfrüchten beeinflussen. Für eine genauere Kalibrierung des LAI und physiologischer Parameter wie  $V_{\text{cuptake}}$  zur prozessbasierten Modellierung der GPP sind weitere und detailliertere Untersuchungen mit sorgfältig erhobenen räumlichen Daten aus Agrarökosystemen erforderlich.

---

## Acknowledgements

The completion of this dissertation was an extreme challenge for me. This study would not have been possible without the help and support from many individuals. I would like to express my deep appreciation and gratitude to my supervisory committee for their outstanding support and the motivation provided to me through to completion of this dissertation; and to Prof. John Tenhunen, for his patient guidance and mentorship, all the way from when I was first considering applying to the PhD program in the Department of Plant Ecology, through to submission of this thesis. I thank Dr. Hyojung Kwon, who taught me everything I needed to know about analysis of the data, understanding of the results, how to write the dissertation, and how to find the way through all the difficulties in Ph.D life. Thank you for the friendly and detailed discussions, clear guidance, and strong motivation. This study would not have been possible without your encouragement. My warm thanks to Prof. Bernd Huwe for discussions on statistics and many helpful recommendations. I thank Prof. Sinkyu Kang for his support of the field experiments carried out in Korea and discussions and advice on remote sensing.

Special thanks go to Frau Marga Wartinger, Friederike Rothe, Sandra Thomas, Bärbel Heindl-Tenhunen and Ralf Geyer who supported me with administrative work and computer programming. I received generous support about R programing and statistic from Prof. Björn Reineking. I also want to thank Dr. Dennis Otieno and Prof. Thomas Koellner for warm encouragement.

I thank all of the TERRECO members and doctoral students, the farmers of Haeon, and Mrs. Kwon and Mr. Park of Yellow Soil Guest House for the willingness to help solve so many problems. I am deeply grateful to Bumsuk Seo, for providing helpful discussions about statistics and programming. I thank Peng Zhao for providing eddy covariance data of Haeon, as well as friendly discussions and encouragement. Eunyoung, Youngsun, Saem, Kiyong and Heera, thank you all for sharing not only the field experiments but also lively moments in Korea and Germany. I would like to offer my special thanks to Emily Martin, Marianne Ruidisch, Svenja Bartsch, Steve Lindner, and Sebastian Arnold, who shared all the fun and adventure along with long days of field experiments. I also thank Cosmas Lambini for checking my summary. All done, thank you!

Finally, I thank my family and all my friends. Words cannot express how grateful I am to

my father, mother, brother, and my beloved husband for all of the sacrifices that you've made on my behalf.

**Grant information**

This research was supported by the Deutsche Forschungsgemeinschaft as an activity of the Bayreuth Center for Ecology and Environmental Research (BayCEER) in the context of the International Research Training Group TERRECO: Complex Terrain and Ecological Heterogeneity (GRK 1565/1) at the University of Bayreuth, Germany and by the Korean Research Foundation (KRF) at Kangwon National University, Chuncheon, South Korea.

# Contents

Summary . . . . .	i
Zusammenfassung . . . . .	iii
Acknowledgements . . . . .	v
Table of contents . . . . .	viii
List of figures . . . . .	xi
List of tables . . . . .	xviii
<b>1 Introduction</b>	<b>1</b>
1.1 General Introduction . . . . .	1
1.2 Objectives . . . . .	5
1.3 Hypotheses . . . . .	6
<b>2 State of the art</b>	<b>9</b>
2.1 Process-based CO <sub>2</sub> exchange models . . . . .	9
2.2 Eddy covariance methodology . . . . .	11
2.3 Vegetation indices from remote sensing . . . . .	12
2.4 Modeling GPP in agricultural ecosystems . . . . .	14
<b>3 Materials and Method</b>	<b>17</b>
3.1 Site descriptions . . . . .	17
3.1.1 Asian sites . . . . .	17
3.1.1.1 Haeon, South Korea (HK) . . . . .	17
3.1.1.2 Haenam, South Korea (HFK) . . . . .	18
3.1.1.3 Mase, Japan (MSE) . . . . .	18
3.1.2 European sites . . . . .	19
3.1.2.1 El Saler-Sueca, Spain (ESES2) . . . . .	19

3.1.2.2	Lonze, Belgium (BE-Lon)	19
3.1.2.3	Klingenberg, Germany (DE-Kli)	20
3.1.3	American site	20
3.1.3.1	Mead, Nebraska, U.S.A. (US-Ne3)	20
3.2	Algorithms of physiological process-based canopy gas exchange model	23
3.3	Physiological parameters of the canopy model and GPP estimation	26
3.4	Vegetation indices from remote sensing	27
3.5	Leaf area index estimates	29
3.6	Outlier removal	30
3.7	Statistical analysis	31
3.7.1	Model evaluation statistic	31
3.7.2	Sensitivity of variables	33
<b>4</b>	<b>Results: estimation of GPP for rice paddy sites</b>	<b>35</b>
4.1	Meteorological conditions at the study sites	35
4.2	LAI development	37
4.3	Dynamics of vegetation indices	38
4.4	LAI estimation	41
4.4.1	Estimating LAI from the seasonal course of VIs	41
4.4.1.1	Relationship between ground-measured LAI and VIs	41
4.4.1.2	Estimation of seasonal LAI	47
4.4.2	Estimation of LAI according to consistent phenological development	48
4.5	$V_{c_{uptake}}$ estimation by NDVI	51
4.6	GPP estimation with the best-fit model	57
<b>5</b>	<b>Results: GPP from dry-land crops</b>	<b>63</b>
5.1	Meteorological condition	63
5.2	LAI development	66
5.3	Dynamics of vegetation indices	67
5.4	GPP estimation of individual crop types	69
5.4.1	LAI estimation	70

5.4.2	$V_{\text{C}_{\text{uptake}}}$ estimation . . . . .	73
5.4.2.1	Seasonal changes of $V_{\text{C}_{\text{uptake}}}$ . . . . .	73
5.4.2.2	$V_{\text{C}_{\text{uptake}}}$ by two approaches . . . . .	76
5.4.3	GPP estimation with two models . . . . .	80
<b>6</b>	<b>Discussion</b>	<b>87</b>
6.1	Use of vegetation indices to estimate LAI of five crops . . . . .	87
6.2	Use of vegetation indecis to estimate $V_{\text{C}_{\text{uptake}}}$ for five crops . . . . .	89
6.3	Limitations due to the remotely sensed vegetation indices . . . . .	92
6.4	GPP estimation for agricultural ecosystems . . . . .	94
<b>7</b>	<b>Conclusion</b>	<b>97</b>
	<b>Appendices</b>	<b>99</b>
	<b>References</b>	<b>115</b>
	<b>Declaration/Erklärungen</b>	<b>133</b>

# List of Figures

**Figure 1.1** The location of Haeon Catchment in South Korea (a), and in relation to the watershed of Soyang Reservoir where crop cultivation in highland area (including Haeon) lead to "hotspots" of non-point pollution (b), (c) provides an overview of agricultural land use in Haeon Catchment (see also Seo et al., 2014). 4

**Figure 1.2** Flowchart illustrating the stepwise methodology implemented in this study. Step 1 relates to the estimation of a seasonal course for LAI based on either linear, exponential or “consistent seasonal development” relationship between the LAI observations and MODIS remotely sensed VIs (see text). Step 2 relates to the estimation of a seasonal course of  $V_{c_{uptake}}$  obtained by best-fit procedures using the seasonal LAI.  $V_{c_{uptake}}$  is along with meteorological information from eddy covariance sites and assuming that the PIXGRO algorithm correctly describe that photosynthetic process. The resulting time courses for  $V_{c_{uptake}}$  are examined in Step 3 in terms of potential linear or exponential relationship to MODIS remotely sensed VIs or as described by consistent seasonal development. Step 4 evaluates overall the efficiency of predicting GPP when both LAI and  $V_{c_{uptake}}$  are determined in dependence on MODIS VIs. These final results in estimating GPP are used to consider a strategy for linking VIs to GPP in regional and landscape studies of agricultural ecosystems. . . . . 8

**Figure 3.1** Detection of the outliers by two statistical methods as described in the text, i.e., generalized additive model (GAM) and detecting extreme value methods. Black closed circle are  $V_{c_{uptake}}$ , red closed circle are the extreme values, thick solid line is GAM, dashed line is the 99% confidence intervals, and thin solid line is standard deviation line. . . . . 32

- Figure 4.1** Seasonal time courses for meteorological variables measured at rice paddy sites that potentially influence GPP, i.e., can be considered driver variables for plant response as it affects carbon uptake, crop growth and primary production. Total global radiation ( $R_g$ ), mean air temperature ( $T_a$ ), mean maximum vapor pressure deficit (VPD), and total rainfall are given for 10-day intervals during the growth period for all rice paddy study sites. General site characteristics are given in Table 3.1. HK = Haeon (S. Korea), HFK = Haenam (S.Korea), MSE = Mase (Japan), and ESES2 = El Saler-Sueca (Spain). . . . . 36
- Figure 4.2** Seasonal time courses in the years indicated for change in leaf area index (LAI) of the studied rice paddies. HK = Haeon (S. Korea), HFK = Haenam (S.Korea), MSE = Mase (Japan), and ESES2 = El Saler-Sueca (Spain). . . . . 38
- Figure 4.3** MODIS vegetation indices for (a) NDVI and (b) EVI for the years indicated. HK = Haeon (S. Korea), HFK = Haenam (S.Korea), MSE = Mase (Japan), and ESES2 = El Saler-Sueca (Spain). Symbols indicate original VI data downloaded from the database (open circles), VI smoothed by TIMESAT method (closed circle), and estimated daily VI (solid line) from spline interpolation. The arrows below the NDVI/EVI values indicate the period of rice growth at each site. 39
- Figure 4.4** The relationship between measured LAI and NDVI or EVI for the years indicated and utilizing data from the entire growing season. HK = Haeon (S. Korea), MSE = Mase (Japan), and ESES2 = El Saler-Sueca (Spain). The solid line indicates the exponential equation established for the relationship as described in the text. The coefficients,  $R^2$  of the regression, and root mean square error (RMSE) are given. . . . . 42
- Figure 4.5** The relationship between measured LAI and NDVI for the years indicated where the data are separated into two phases, e.g., until maximum VIs are reached (Before) and after maximum VIs are attained (After). HK = Haeon (S. Korea), MSE = Mase (Japan), and ESES2 = El Saler-Sueca (Spain). The solid line indicates the exponential equation established for the relationship as described in the text. The coefficients,  $R^2$  of the regression, and root mean square error (RMSE) are given. . . . . 43

**Figure 4.6** The relationship between measured LAI and EVI for the years indicated where the data are separated into two phases, e.g., until maximum VIs are reached (Before) and after maximum VIs are attained (After). HK = Haeon (S. Korea), MSE = Mase (Japan), and ESES2 = El Saler-Sueca (Spain). The solid line indicates the exponential equation established for the relationship as described in the text. The coefficients,  $R^2$  of the regression, and root mean square error (RMSE) are given. . . . . 44

**Figure 4.7** The pooled relationships between measured LAI and NDVI or EVI utilizing data from the entire growing season. The regression for Asian sites includes the data from HK and MSE shown in previous figures, while the regression for the entire compliment of sites adds in the observations from ESES2. The solid line indicates the exponential relationship established for the relationships as described in the text. The coefficients,  $R^2$  of the regression, and root mean square error (RMSE) are given. . . . . 45

**Figure 4.8** The pooled relationships between measured LAI and NDVI or EVI where the data are separated into two phases, e.g., until maximum VIs are reached (Before) and after maximum VIs are attained (After). The regression for Asian sites includes the data from HK and MSE shown in previous figures, while the regression for the entire compliment of sites adds in the observations from ESES2. The solid line indicates the exponential relationship established for the relationships as described in the text. The coefficients,  $R^2$  of the regression, and root mean square error (RMSE) are given. . . . . 46

**Figure 4.9** Daily measured LAI (closed circle with solid line) and estimated LAI (dashed line) at rice paddies for the years indicated. HK = Haeon (S. Korea), MSE = Mase (Japan), and ESES2 = El Saler-Sueca (Spain). Estimates are calculated with an exponential fit to pooled data from all rice paddy sites, using observations over the entire season (upper right panel in Fig. 4.7) . . . . . 47

- Figure 4.10** A scaled general growth scale curve utilizing data from all rice paddy sites. The scaling results by dividing LAI observations by maximum LAI. The black closed circles indicate the relationship between the scaled LAI and DOY based on time shifts according to maximum NDVI. The solid line indicates the general growth curve determined with the generalized additive model (GAM). . . . . 49
- Figure 4.11** Daily measured LAI (closed circle with solid line) and estimated LAI (dashed line) obtained with the consistent phenological development approach (see text for stepwise procedure) at rice paddy sites for the years indicated. HK = Haeon (S. Korea), HFK = Haenam (S. Korea), MSE = Mase (Japan), and ESES2 = El Saler-Sueca (Spain). . . . . 51
- Figure 4.12** Seasonal change of  $V_{\text{uptake}}$  obtained with measured LAI ('Original', black closed circle) and with the consistent development LAI-NDVI model, ('estimated LAI', gray closed circle) of rice paddy sites for years indicated. HK = Haeon (S. Korea), HFK = Haenam (S.Korea), MSE = Mase (Japan), and ESES2 = El Saler-Sueca (Spain). . . . . 53
- Figure 4.13** The relationship between  $V_{\text{uptake}}$  and NDVI of rice paddies for the years indicated. HK = Haeon (S. Korea), MSE = Mase (Japan), and ESES2 = El Saler-Sueca (Spain). The correlations may be examined according to each month during the rice growing period, considering the order May (black closed circle), June (open square), July (closed triangle), August (open circle), and September (star). The coefficients and  $R^2$  of the regressions are given. . . . . 54
- Figure 4.14** Relationship between  $V_{\text{uptake}}$  and NDVI utilizing data from the entire growing season.  $V_{\text{uptake}}$  calculated using estimated LAI from the relationship shown in previous figures. The solid lines indicate the linear equation (black line) and exponential equation (gray line) established for the relationship as described in the text. The coefficients,  $R^2$  of the regression, and root mean square error (RMSE) are given. . . . . 56

**Figure 4.15** Seasonal time courses in  $V_{c_{\text{uptake}}}$  estimated using the best-fit linear model (Fig. 4.14 - gray closed circle) and  $V_{c_{\text{uptake}}}$  estimated using observed data (black closed circle) for the years indicated. HK = Haeon (S. Korea), HFK = Haenam (S.Korea), MSE = Mase (Japan), and ESES2 = El Saler-Sueca (Spain). . . . . 57

**Figure 4.16** A scaled general seasonal curve for  $V_{c_{\text{uptake}}}$  utilizing data from all rice paddy sites. The scaling results by dividing estimated  $V_{c_{\text{uptake}}}$  by maximum  $V_{c_{\text{uptake}}}$  for each site and year. The black closed circle indicates the relationship between the scaled  $V_{c_{\text{uptake}}}$  and DOY based on time shifts according to maximum NDVI. The solid line indicates the general seasonal curve determined by generalized additive model (GAM). . . . . 58

**Figure 4.17** Daily GPP estimation obtained with the linear regression model for  $V_{c_{\text{uptake}}}$  (gray solid line) and observed GPP (black solid line) of rice paddy sites for the years indicated. HK = Haeon (S. Korea), HFK = Haenam (S.Korea), MSE = Mase (Japan), and ESES2 = El Saler-Sueca (Spain). . . . . 61

**Figure 4.18** Daily GPP estimation with the general seasonal curve model for  $V_{c_{\text{uptake}}}$  (gray solid line) and observed GPP (black solid line) of rice paddy sites for the years indicated. HK = Haeon (S. Korea), HFK = Haenam (S.Korea), MSE = Mase (Japan), and ESES2 = El Saler-Sueca (Spain). . . . . 62

**Figure 5.1** Seasonal time courses for meteorological variables at dry-land crop sites that influence GPP, e.g., can be considered driver variables for plant response as it affects carbon uptake, crop growth, and primary production. Total global radiation ( $R_g$ ), mean air temperature ( $T_a$ ), mean maximum vapor pressure deficit (VPD), and total rainfall are given for 10-day intervals during the growth period. General site characteristics are given in Table 3.1. HK = Haeon (S. Korea) for potato, BE-Lon = Lonze (Belgium) for sugar beet (2004), DE-Kli = Klingenberg (Germany) for maize, and US-Ne3 = Nebraska-Mead (USA) for soybean (2002 and 2004) and maize (2003 and 2005). . . . . 64

- Figure 5.2** Seasonal time courses in the years indicated for change in leaf area index (LAI) of the studied dry-land crop sites. US-Ne3 = Nebraska (USA) for soybean (2002 and 2004) and maize (2003 and 2005), DE-Kli = Klingenberg (Germany) for maize, HK = Haeon (S. Korea) for potato, BE-Lon = Lonzeer (Belgium) for sugar beet (2004). . . . . 66
- Figure 5.3** MODIS vegetation indices for (a) NDVI and (b) EVI for the years indicated. US-Ne3 = Nebraska (USA) for soybean (2002 and 2004) and maize (2003 and 2005), DE-Kli = Klingenberg (Germany) for maize, HK = Haeon (S. Korea) for potato, BE-Lon = Lonzeer (Belgium) for sugar beet (2004). Symbols indicate original VI data downloaded from the database (open circles), VI smoothed by TIMESAT method (closed circle), and estimated daily VI (solid line) from spline interpolation. The arrows below the NDVI/EVI values indicate the period of crop growth at each site. . . . . 68
- Figure 5.4** General growth curves scaled from 0 to 1, utilizing data from each crop site and dividing by maximum observed LAI (black closed circle). The black closed circles indicate the relationship between the scaled LAI and DOY based on time shifts according to maximum VIs. The solid line indicates the general growth curve determined with the generalized additive model (GAM). . . . . 71
- Figure 5.5** Measured LAI (closed circle with solid line) and estimated daily LAI (dashed line) obtained with the consistent phenological development approach (see text for stepwise procedure) at dry-land crop sites for the years indicated. US-Ne3 = Nebraska (USA) for soybean (2002 and 2004) and maize (2003 and 2005), DE-Kli = Klingenberg (Germany) for maize, HK = Haeon (S. Korea) for potato, BE-Lon = Lonzeer (Belgium) for sugar beet (2004). . . . . 72
- Figure 5.6** Seasonal change of  $V_{\text{cuptake}}$  obtained with measured LAI ('Original', black closed circles) and with the consistent development LAI-NDVI model ('estimated LAI', gray closed circle) of dry-land crop sites for the years indicated. US-Ne3 = Nebraska (USA), DE-Kli = Klingenberg (Germany), HK = Haeon (S. Korea), BE-Lon = Lonzeer (Belgium). . . . . 75

- Figure 5.7** Relationships obtained between  $V_{c_{uptake}}$  and VIs for the years indicated and where the data are from the entire growing season. The lines indicate the linear equation (black line) and exponential equation (gray line) established for the relationship as described in the text. The coefficients and  $R^2$  of the regressions are shown. . . . . 77
- Figure 5.8** Seasonal development curves for  $V_{c_{uptake}}$  scaled from 0 to 1 by dividing daily values by the maximum in  $V_{c_{uptake}}$  and utilizing data from each dry-land crop sites. The time of each observation is shown in relation to maximum in recorded VI. The solid line indicates the general growth curve determined by generalized additive model (GAM). The dashed line indicates an upward adjustment to reproduce the observed maxima in  $V_{c_{uptake}}$ . . . . . 79
- Figure 5.9** Daily GPP estimation obtained with the linear regression model for  $V_{c_{uptake}}$  (gray solid line) and observed GPP (black solid line) of dry-land crop sites for the years indicated. US-Ne3 = Nebraska (USA), DE-Kli = Klingenberg (Germany), HK = Haeon (S. Korea), BE-Lon = Lonze (Belgium). . . . . 84
- Figure 5.10** Daily GPP estimation with the general seasonal curve model for  $V_{c_{uptake}}$  (gray solid line) and observed GPP (black solid line) of dry-land crop sites for the years indicated. US-Ne3 = Nebraska (USA), DE-Kli = Klingenberg (Germany), HK = Haeon (S. Korea), BE-Lon = Lonze (Belgium). . . . . 85
- Figure 5.11** Daily GPP estimation with the general seasonal re-scaled curve model for  $V_{c_{uptake}}$  (gray solid line) and observed GPP (black solid line) of dry-land crop sites for the years indicated. US-Ne3 = Nebraska (USA), DE-Kli = Klingenberg (Germany), HK = Haeon (S. Korea), BE-Lon = Lonze (Belgium). . . . . 86
- Figure 6.1** NDVI and EVI by TIMESAT (closed circle), daily NDVI by spline (solid line), and measured LAI (closed red circle with solid line) at dry-land crop sites for the years indicated. US-Ne3 = Nebraska (USA), DE-Kli = Klingenberg (Germany), HK = Haeon (S. Korea), BE-Lon = Lonze (Belgium). . . . . 93

# List of Tables

<b>Table 3.1</b>	Site information of rice paddy sites at Haeon and Haenam, South Korea, Mase, Japan and El Saler-Sueca, Spain and dry- land crops at Haeon, South Korea, Lonze, Belgium, Klingenberg, Germany, and Nebraska-Mead, U.S.A. Total $R_g$ is total global radiation, mean $T_a$ is mean air temperature, total P is total rainfall, planting and harvest date (day of year - DOY), maximum LAI and DOY of maximum LAI. Meteorological condition considers the period of crop growth (from the planting to the harvest). The eddy data of US-Ne3 2003 is available until DOY 243. . . . .	22
<b>Table 3.2</b>	Parameters for physiologically based canopy model. Parameter values are generalized from Harley and Tenhunen (1991), Falge et al. (1996), and Owen et al. (2007). . . . .	28
<b>Table 4.1</b>	Statistics for the correlation between measured LAI and estimated LAI comparing the exponential model (Fig. 4.9) and the LAI consistent development curve method (Fig. 4.11). $R^2$ is the determination of coefficient, RMSE is root mean square error, and CV is coefficient of variation. . . . .	50
<b>Table 4.2</b>	Statistics for the linear correlation between $V_{c_{uptake\_org}}$ and $V_{c_{uptake}}$ . $a$ is a slope, $b$ is a intercept, $R^2$ is the coefficient of determination, RMSE is root mean square error, and CV is coefficient of variation. . . . .	52
<b>Table 4.3</b>	Statistics for the linear correlation between $V_{c_{uptake\_org}}$ and $V_{c_{uptake}}$ obtained with the best-fit linear model (Fig. 4.14) with the coefficient of determination ( $R^2$ ), root mean square error (RMSE), and coefficient of variation (CV). . .	55

<b>Table 4.4</b> Summary of observed GPP and modeled GPP obtained with the linear regression model for $V_{c_{uptake}}$ from NDVI at all rice paddy sites with mean, standard deviation (STD), accumulated GPP (acc.GPP), difference between simulated GPP and observed GPP (%), slope (a), intercept (b), determination coefficients ( $R^2$ ), root mean square error (RMSE), coefficient of variation (CV), and modeling efficiency (MF). . . . .	59
<b>Table 4.5</b> Summary of observed GPP and modeled GPP with the general seasonal curve model for $V_{c_{uptake}}$ from NDVI at all rice paddy sites with mean, standard deviation (STD), accumulated GPP (acc.GPP), difference between simulated GPP and observed GPP (%), slope (a), intercept (b), determination coefficients ( $R^2$ ), root mean square error (RMSE), coefficient of variation (CV), and modeling efficiency (MF). . . . .	60
<b>Table 5.1</b> Statistics for the correlation between measured LAI and estimated LAI, where the LAI estimates are obtained with a general growth curve, $R^2$ is the coefficient of determination, RMSE is root mean square error, and CV is coefficient of variation. . . . .	70
<b>Table 5.2</b> Statistics for the linear relationship between $V_{c_{uptake\_org}}$ and $V_{c_{uptake}}$ obtained with the linear model from VIs (Fig. 5.7). $a$ is a slope, $b$ is a intercept, $R^2$ is the determination of coefficient, RMSE is root mean square error. . . . .	74
<b>Table 5.3</b> Statistics for the linear correlation between $V_{c_{uptake\_org}}$ and $V_{c_{uptake}}$ obtained with the seasonal development curve from VIs (Fig. 5.8). $a$ is a slope, $b$ is a intercept, $R^2$ is the determination of coefficient, RMSE is root mean square error. . . . .	76
<b>Table 5.4</b> Summary of observed GPP and modeled GPP with the best-fit linear model for $V_{c_{uptake}}$ from VIs for dry-land crop sites with mean, standard deviation (STD), accumulated GPP (acc.GPP), difference between simulated GPP and observed GPP (%), slope (a), intercept (b), determination coefficients ( $R^2$ ), root mean square error (RMSE), coefficient of variation (CV), and modeling efficiency (MF). . . . .	80

<b>Table 5.5</b>	Summary of observed GPP and modeled GPP with the general seasonal curve model $V_{c_{\text{uptake}}}$ for dry-land crop sites with mean, standard deviation (STD), accumulated GPP (acc.GPP), difference between simulated GPP and observed GPP (%), slope (a), intercept (b), determination coefficients ( $R^2$ ), root mean square error (RMSE), coefficient of variation (CV), and modeling efficiency (MF).	82
<b>Table 5.6</b>	Summary of observed GPP and modeled GPP with the general seasonal re-scaled curve model for $V_{c_{\text{uptake}}}$ for dry-land crop sites with mean, standard deviation (STD), accumulated GPP (acc.GPP), difference between simulated GPP and observed GPP (%), slope (a), intercept (b), determination coefficients ( $R^2$ ), root mean square error (RMSE), coefficient of variation (CV), and modeling efficiency (MF). . . . .	83

# Chapter 1

## Introduction

### 1.1 General Introduction

Among greenhouse gases, increasing atmospheric CO<sub>2</sub> is known to have the largest influence on global energy balance, and as such is the main driver of global warming, which in turn feeds back on global carbon balance (IPCC, 2014). The carbon balances of different terrestrial ecosystems have become increasingly important to understand in detail due to their significant role in climate change by regulation of CO<sub>2</sub> fluxes between the biosphere and the atmosphere (Christensen et al, 2007; Jonsson et al., 2007). In recent decades, the development and application of eddy covariance (EC) methods for monitoring carbon exchange between ecosystems and the atmosphere has revolutionized our understanding of the regulation of ecosystem carbon fluxes. As currently applied in FLUXNET (<http://fluxnet.ornl.gov>), the EC methodology measures net ecosystem CO<sub>2</sub> exchange (NEE) directly for a large "representative" area of a particular ecosystem type at high frequency and over long periods, along with meteorological conditions (Houghton and Woodwell, 1980; Baldocchi et al., 1988; Wang et al., 1995; Baldocchi et al., 1996). Observation of NEE have allowed us to identify environmental factors determining uptake (net photosynthesis, gross primary production or GPP) and losses of CO<sub>2</sub> (ecosystem respiration, carbon dioxide emissions or R<sub>eco</sub>) at tower footprint scale, typically ranging from hundreds of meters to several kilometers (Running et al., 1999; Valentini et al., 2003; Xiao et al., 2004). Flux measurements of CO<sub>2</sub> by the EC methodology provide us with reasonably accurate estimates of carbon exchange in response to local environmental conditions.

Combining EC flux measurements with process-based modeling allows the simulation of carbon uptake and losses over large spatial areas, in response to long-term climate records, and in the context of scenarios for future climate (Baldocchi et al., 2003). To support estimation of

global level CO<sub>2</sub> exchange between ecosystems and atmosphere, a network of EC tower stations has been established by the international FLUXNET project and now includes more than 500 towers across five continents (Baldocchi et al., 2001; Falge et al., 2001; Saigusa et al., 2002; Reichstein et al., 2005; Owen et al., 2007). FLUXNET covers a large range of climate and biome types at the local ecosystem level. The data from these monitoring studies allows us to improve carbon flux modeling along natural ecosystem and climatic gradients (Baldocchi et al., 2001). Satellite remote sensing is often used together with process-based models to accomplish this up-scaling of carbon fluxes to landscape, regional, continental and global levels, since eddy covariance measurements are spatially limited and detailed maps of ecosystem types are required (Goetz et al., 1999; Li et al., 2007; Wu et al., 2009; Oguto et al., 2013).

Agricultural land cover makes up 38% of terrestrial ecosystem extent, and approximately 24% of the Earth's land surface is cultivated cropland. Agroecosystems are important to understand not only in their role as a strong modifier of regional carbon balance, but also in their intended role of capturing carbon (energy) in the form of food products, e.g. agricultural yield (Cassman & Wood, 2005; Wilby et al., 2005; Smith et al., 2008). Gross primary production (GPP) of an agroecosystem is the amount of total carbon assimilated by vegetation in gross carbon uptake or photosynthesis of chlorophyll containing organs (Running et al., 1999; Smith et al., 2010). GPP is the driver of useful biomass production of crops, and is therefore closely related to crop yield as well as in calculating carbon balance (Reeves et al., 2005; Moureaux et al., 2008). In previous studies, quantifying crop yield based on primary production information has been demonstrated (Hicke et al., 2004; Ciais et al., 2010; Ruidisch et al., 2014).

Estimating the spatial distribution of GPP in agricultural landscapes is a necessary step for evaluating the influences of climate variation on crop yields and carrying out analyses related to food security (Tao et al., 2004). Determining the spatial variation of GPP, especially in agroecosystems, remains a significant challenge because it is influenced not only by local seasonal change in climate and water availability, but by varied management practices resulting from individual farmer's decision-making (Wattenbach et al., 2010). For example, the timing and characteristics of tillage, fertilizer and herbicide applications, and irrigation just to name a few factors, affect annual decomposition, carbon storage and soil nutrients, and CO<sub>2</sub> emissions in any particular crop field (Moors et al., 2010; Revill et al., 2013). The different crop-planting schedules for each crop field also play a major role in determining the seasonal course of GPP at landscape scale.

The agricultural landscape level of CO<sub>2</sub> exchange, including GPP and R<sub>eco</sub>, is strongly related to carbon and water balances as well as agricultural production as crop yield. The landscape

balances are determined by complex temporal and spatial variations in terrestrial ecosystem response along topographic and climate gradients (Tenhunen et al., 2009). As in the case of global level assessments, process-based models are often applied to many different ecosystem types (Adiku et al., 2006) in order to characterize CO<sub>2</sub> exchange at landscape scale (Ruidisch et al., 2014). Process-based models will only simulate balances and agricultural production with acceptable accuracy if they are supported by and adjusted to field observations, e.g., eddy covariance flux measurements, observations of biomass accumulation, and the information which explains land use and farming operations. Nevertheless, the extent to which direct observation may be carried out is limited. Thus, the work described here attempts to determine how the parameterization of process-based models, particularly with respect to carbon input to the system as GPP, can be aided *via* the use of remotely sensed vegetation indices.

The vegetation indices (VIs), especially Normalized Difference Vegetation Index (NDVI) and Enhanced Vegetation Index (EVI), depend strongly on the amount of chlorophyll and vegetation canopy structure that is viewed by the remote sensor, e.g., in the case of this thesis the sensor on the MODIS satellite platform. Utilized effectively, VIs allow us to monitor phenological events and seasonal changes in vegetation development (Huete et al., 1997; Myneni et al., 1997). In this study, I have investigated patterns found in NDVI and EVI evaluated at the greatest spatial resolution provided by MODIS (ca. 250 m x 250 m pixels). The work focuses on relatively high temporal resolution (daily) to examine phenological change in GPP and biomass accumulation in agricultural crop fields. New relationships between VIs and GPP and biomass are established, and will eventually be used to aid in parameterization of a process-based model at landscape scale (PIXGRO; cf. Ruidisch et al. 2014). The landscape of interest is located in the Haeon Catchment in Yanggu Gun, Gangwon-Do, South Korea where the dominant agricultural land use includes the dry-land crops potato, radish, beans and cabbage together with irrigated paddy rice (Fig. 1.1). The detailed information on landscape structure is described in section 3.1.1.1 and Seo et al. (2014).

While the overall interest in this study relates to spatial differentiation and climate influences on response and carbon balances at landscape level, the landscape level analysis is beyond the scope of the current work. As the first preliminary step in this analysis, relationships between VIs and vegetation development is studied at other field sites that have the same or similar crops as found in the Haeon Catchment. I have attempted to determine whether NDVI and EVI from MODIS at high spatio-temporal resolution can be related to canopy photosynthetic capacity, carbon uptake as GPP, and accumulation of the aboveground biomass of the crops. The work described below focuses on the one hand on seasonal timing in vegetation activity (crop

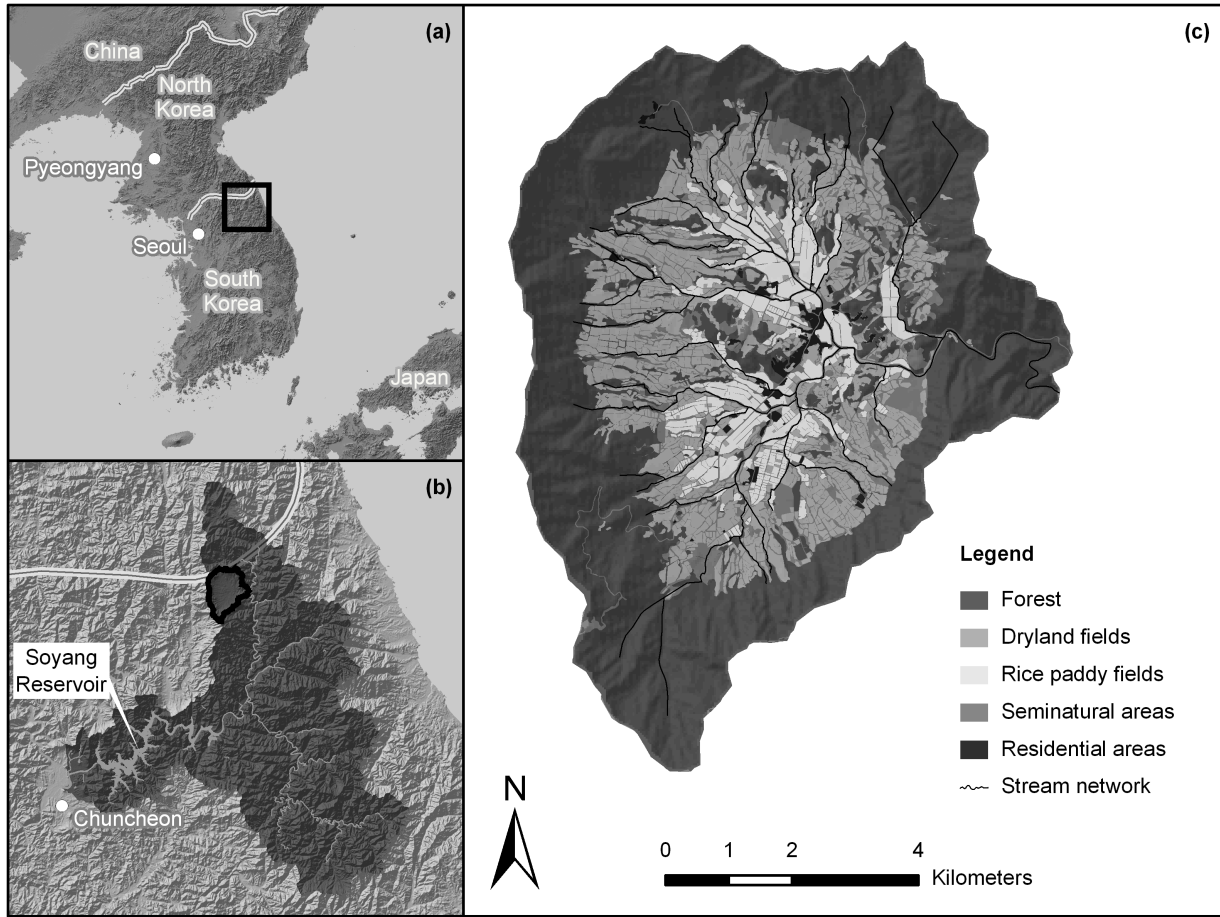


Fig. 1.1 The location of Haeon Catchment in South Korea (a), and in relation to the watershed of Soyang Reservoir where crop cultivation in highland area (including Haeon) lead to "hotspots" of non-point pollution (b), (c) provides an overview of agricultural land use in Haeon Catchment (see also Seo et al., 2014).

canopy phenology), and secondly on whether remote sensing may be used to help estimate the magnitude of land surface exchange fluxes. Both aspects are extremely important for improving the performance of the spatial simulation models.

As the process-based model, I have focused on the physiologically process-based canopy sub-model of PIXGRO (Tenhunen et al., 2009) that links flux observation from the eddy covariance studies with ecosystem physiology described as capacity for  $\text{CO}_2$  exchange (i.e., canopy content and activity of Rubisco) and plant phenology (i.e., leaf area index). PIXGRO is designed as a tool for bridging between measured gas exchange fluxes, derived parameters for carboxylation capacity, seasonal changes in biomass and structure in the case of herbaceous and crop plants, and crop yields, taking into account specific ecophysiological behavior of individual species (Adiku et al., 2006). The canopy sub-model of PIXGRO (named hereafter 'canopy model') calculates the dynamics of whole ecosystem  $\text{CO}_2$  and  $\text{H}_2\text{O}$  exchange (Reichstein, 2001). The canopy model includes the leaf photosynthesis model according to Farquhar and Caemmerer (1982) and stomatal conductance model according to Ball and Berry (1987). The equations as

modified for field applications as well as the evaluation of EC data are reported in detail by Harley and Tenhunen (1991), Adiku et al. (2006), Owen et al. (2007), and Ruidisch et al. (2014) and are summarized in Chapter 3.

Therefore, in this study, the main goal is to assess GPP at crop field sites, achieving critical parameterization of the PIXGRO model *via* a linkage of directly measured carbon exchange and increases in canopy biomass with remote sensing VIs from MODIS. Fig. 1.2 showed the research flow chart of this study. This study is a first step in the determination of parameters for a landscape model applied to agroecosystems that can be used to estimate carbon balance and emission of greenhouse gases by crops over the entire Haeon Catchment as aided *via* satellite remote sensing.

## 1.2 Objectives

The goal of this study is to quantitatively estimate the seasonal course of daily gross primary production (GPP) of crops with the model PIXGRO, achieving critical parameterization *via* a linkage between remote sensing VIs from MODIS and directly measured carbon exchange with eddy covariance methodology as well as measured increases in canopy biomass: and considering sites in Asia (Haeon Catchment, Haenam, and Mase), Europe (El Saler-Sueca, Lonze, and Klingenberg) and North America (Nebraska-Mead) in order to develop information that will subsequently allow a landscape scale evaluation of carbon balances in the Haeon Catchment. The stepwise objectives are:

- to organize a data base with half hourly information from the EC measurements that allow a parallel analysis of GPP of the major crops found in the Haeon Catchment (i.e., rice, soybean, maize, potato, and sugar beet as a surrogate for radish) in response to meteorological conditions
- to estimate for crop species from EC daily values the critical PIXGRO parameter  $V_{c_{uptake}}$  (cf. Owen et al., 2007) which together with leaf area index (LAI) controls canopy carbon fixation in response to multiple environmental factors
- to obtain daily vegetation indices (NDVI and EVI) from MODIS at 250 m resolution and to use them to examine crop phenology, e.g., the relationship between the observed LAI and VIs with approaches generally used by the remote sensing community as well as newly developed approaches

- to define the relationship between the daily VIs and modeling parameter  $V_{c_{\text{uptake}}}$ , that permits description of GPP in various crop types with approaches generally used by the remote sensing community as well as newly developed approaches
- to establish best-fit models to estimate GPP from VIs and ground observations of climate when essential observations of  $\text{CO}_2$  exchange and LAI are non-existent
- to consider a strategy based on the results from selected EC sites for linking VIs to GPP in regional and landscape studies

Fig. 1.2 illustrates the stepwise methodology of this study. Step 1 is carried out to obtain a statistically-based regression model to estimate the seasonal course of LAI. This is obtained by relating the observed LAI and VIs. Linear and exponential relationships were considered, as well as a new model based on consistent phenological development of individual crops. The seasonal course of LAI obtained as dependent on VIs, as well as the actual measured course of change in LAI and a constant LAI at maximum measured, were used to estimate the seasonal course of the parameter  $V_{c_{\text{uptake}}}$  along with meteorological information from eddy covariance method and assuming that the PIXGRO algorithm correctly describe the photosynthetic process (Step 2). The critical parameter  $V_{c_{\text{uptake}}}$  is estimated for observed data *via* fitting of the PIXGRO model to observed GPP. Differing results with the alternative methods for inputting LAI are described in the results section. The relationship between  $V_{c_{\text{uptake}}}$  and the daily VIs are considered in Step 3. Again alternative descriptions have been examined. Step 4 provides an overall examination of the efficiency of the procedure, inputting LAI and  $V_{c_{\text{uptake}}}$  from the best-fit models and estimating GPP to compare with measurements. Finally, the results in estimating GPP are used to consider a strategy for linking VIs to GPP in regional and landscape studies of agricultural ecosystems.

### 1.3 Hypotheses

- Fitting of the physiologically-based PIXGRO canopy model to GPP obtained from EC crop sites allows definition of the seasonal course of the critical parameter  $V_{c_{\text{uptake}}}$ .
- The seasonal course of the parameter  $V_{c_{\text{uptake}}}$  along with meteorological information allows efficient description of GPP (e.g., reproduces the observed data efficiently).
- $V_{c_{\text{uptake}}}$ , which is estimated using seasonal observation of LAI development together with observed GPP and meteorology, performs better in estimating GPP than  $V_{c_{\text{uptake}}}$  using a

constant LAI.

- Estimating GPP by best-fit model for  $V_{c_{\text{uptake}}}$  and LAI in dependence on VIs from MODIS allows accurate GPP predictions with PIXGRO.
- Despite differences in climate across geographical regions, general relationships between VIs and  $V_{c_{\text{uptake}}}$  or LAI can be established for the same crop species and can be used to estimate GPP in agriculture ecosystems.

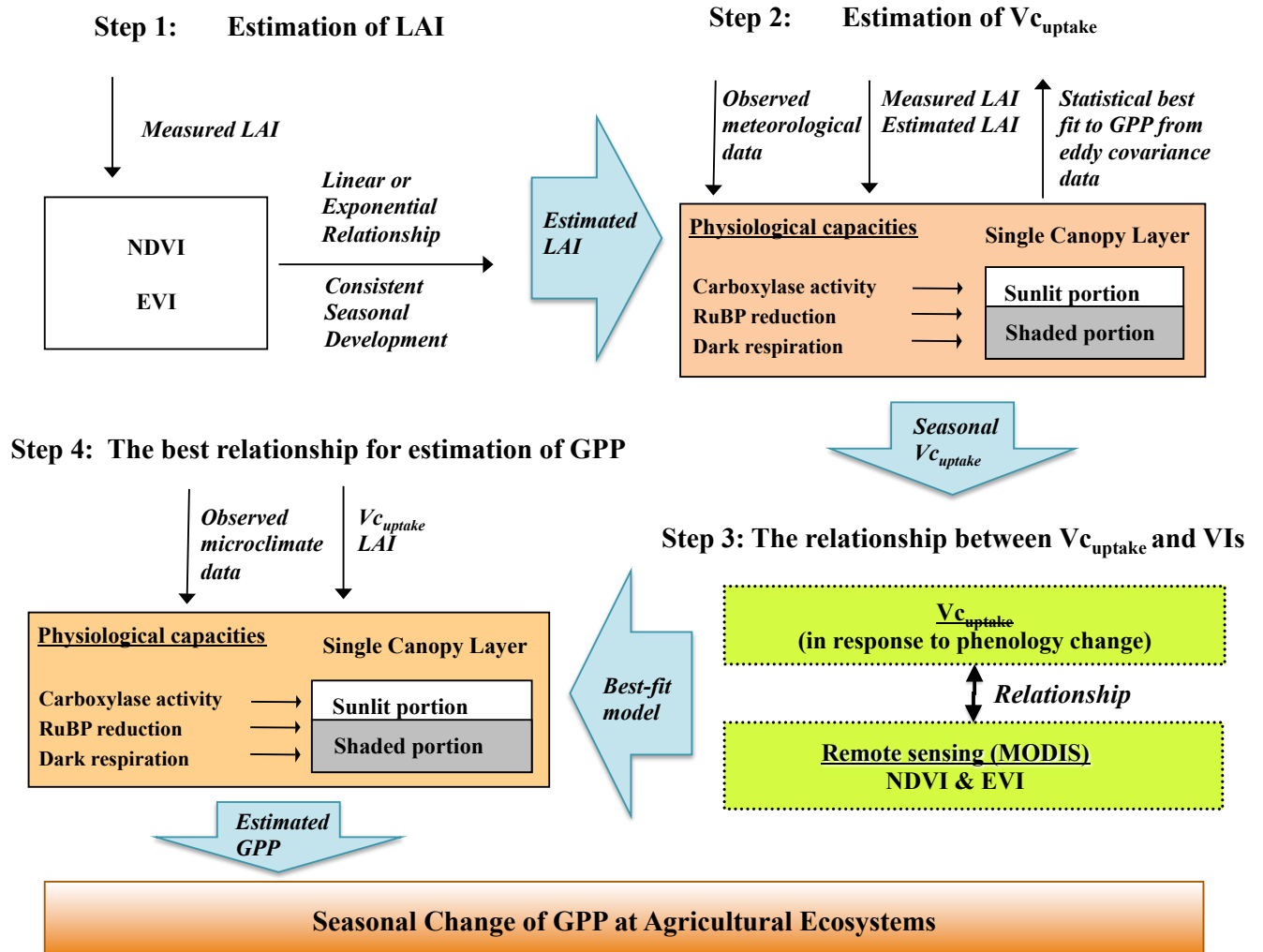


Fig. 1.2 Flowchart illustrating the stepwise methodology implemented in this study. Step 1 relates to the estimation of a seasonal course for LAI based on either linear, exponential or “consistent seasonal development” relationship between the LAI observations and MODIS remotely sensed VIs (see text). Step 2 relates to the estimation of a seasonal course of  $V_{c_{uptake}}$  obtained by best-fit procedures using the seasonal LAI.  $V_{c_{uptake}}$  is along with meteorological information from eddy covariance sites and assuming that the PIXGRO algorithm correctly describe that photosynthetic process. The resulting time courses for  $V_{c_{uptake}}$  are examined in Step 3 in terms of potential linear or exponential relationship to MODIS remotely sensed VIs or as described by consistent seasonal development. Step 4 evaluates overall the efficiency of predicting GPP when both LAI and  $V_{c_{uptake}}$  are determined in dependence on MODIS VIs. These final results in estimating GPP are used to consider a strategy for linking VIs to GPP in regional and landscape studies of agricultural ecosystems.

# Chapter 2

## State of the art

### 2.1 Process-based CO<sub>2</sub> exchange models

The carbon balance of terrestrial ecosystems is determined by the long-term differences in gross primary production (GPP) and ecosystem respiration fluxes and in some cases the additional transport of carbon into or out of the system (Schulze, 2006). GPP refers to the total uptake of carbon dioxide in photosynthesis or CO<sub>2</sub> assimilation, which is the main driver of subsequent ecosystem processes, including plant growth and agricultural yields. GPP depends momentarily on continual change in environmental factors, e.g., light, temperature, air humidity, air turbulence and CO<sub>2</sub> concentration, and on ecosystem physiology, e.g., nitrogen and proteins supporting leaf carboxylation capacity, structure that exposes photosynthetically active materials to light, and stomatal restrictions on CO<sub>2</sub> diffusion (Farquhar and Sharkey, 1982; H. Muraoka and H. Koizumi, 2005; Schulze, 2006). To quantify and predict the overall response of plant stand GPP and ecosystem respiration to time dependent changes in physiological and environmental factors, process-based CO<sub>2</sub> exchange models have been widely implemented at different scales (Tenhunen et al., 1976; Farquhar et al., 1980; Falge et al., 1996; Muraoka et al., 2005). The importance of using process-based models relates to a desire to 1) understand better the processes which change over time, and 2) to best build a potential for extrapolating modeling results to other locations and for use under altered climate conditions.

Farquhar et al. (1980) described a model for the fundamental processes influencing photosynthesis at leaf level, assuming that either ribulose biphosphate carboxylase-oxygenase kinetics or RuBP regeneration determine CO<sub>2</sub> uptake rate. The influence of temperature on the enzymatic components of the Calvin cycle is also taken into consideration. The “Farquhar Model” is widely accepted as theoretically sound, and the respective equations are generally included

into all process-based models for GPP in current use. Nevertheless, GPP is simultaneously determined by additional physiological processes and by physical diffusion of  $\text{CO}_2$  to the chloroplasts. While practical physiologically-based descriptions for stomatal conductance (determining  $\text{CO}_2$  diffusion) have not been achieved, the close coupling of conductance to net photosynthesis rate (Schulze and Hall, 1982) has allowed stomatal responses to be described with correlation equations both at leaf and plant canopy levels (Ball et al., 1987; Tenhunen et al. 1990; Leuning, 1995; Falge et al. 1996; Owen et al. 2007). At plant stand or ecosystem level, such models treat the canopy as one big leaf (Sellers et al., 1992) where the integrated response can be determined experimentally via eddy covariance measurements. On the other hand, such a "big leaf" has a certain mass, or represents a finite amount of leaf area, which changes over time. Different parts of this leaf area are exposed to very different radiation over the course of the day. As a compromise between simplicity (big leaf) and spatial distribution of response (gradients influencing different leaf clusters), the sunlit and shaded leaf areas have been estimated and have been treated separately in almost all models (Pury and Farquhar, 1997; Wang and Leuning, 1998; Chen et al., 1999; Owen et al. 2007).

Harley and Tenhunen (1991) modified the leaf  $\text{CO}_2$  exchange model of Farquhar (1980) to emphasize practical field applications and field-based parameterization via chamber gas exchange measurements (Harley et al., 1989; Harley and Tenhunen, 1991). Considering the plant canopy as a big leaf, Li et al. (2008) applied the same equations to measurements obtained with large plant chambers. Development of eddy covariance methodology provides  $\text{CO}_2$  gas exchange data sets for larger spatial areas, in various ecosystem types and over long-term periods (Baldocchi et al., 1996). In relation to these data, the single leaf models have been extended to describe ecosystem level GPP (Baldocchi and Meyers, 1998, Owen et al. 2007).

The process-based models require reliable input parameters related to physiology and phenology of vegetation. Carboxylation capacity is the most important parameter and there have been many studies emphasizing the importance of accurate estimates of carboxylation capacity (Farquhar and Sharkey, 1982; Tenhunen et al., 1990; Leuning, 1995; Falge et al., 1996; Owen et al., 2007). Maximum carboxylation capacity ( $V_{c_{\max}}$ ) at canopy level depends on the amount of photosynthetically active biomass present, the physical arrangement of this biomass with respect to light interception, and the investment by plants in enzymatic components of the carbon fixation cycle, (Falge et al., 1996; Wilson et al., 2000; Wang et al., 2001; Baldocchi et al., 2001; Kumagai et al., 2006; Owen et al., 2007; Wang et al., 2007; Wang et al., 2008; Tenhunen et al., 2009; Muraoka et al., 2012). Reichstein et al. (2003) and Wang et al. (2007) estimated the  $V_{c_{\max}}$  and the maximum electron transport rate at canopy level using inverse modeling methods.

Owen et al. (2007) described GPP based on eddy covariance observations and modeling. A single “physiological parameter” ( $V_{c_{\text{uptake}}*1}$  in the terminology of Owen et al. 2007, while this study simply uses  $V_{c_{\text{uptake}}}$ ) describing canopy carboxylation capacity was identified to allow comparison of  $\text{CO}_2$  uptake by many different ecosystem types. Instead of using the notation of  $V_{c_{\text{max}}}$  at the leaf level,  $V_{c_{\text{uptake}}}$  describes the maximum rate of carboxylation capacity at the canopy level as determined from EC data.  $V_{c_{\text{uptake}}}$  has to date been studied in only a few crop-lands (Owen et al., 2007). In these determinations, a constant maximum LAI was assumed due to lack of measured seasonal changes in LAI. The current work attempts to provide new insight on seasonal changes in  $V_{c_{\text{uptake}}}$  within various agricultural ecosystem types, and it includes the important influences of seasonal changes in LAI.

## 2.2 Eddy covariance methodology

Assessments of  $\text{CO}_2$  exchange of plant parts, of ecosystem compartments and even of small ecosystem monoliths has been a primary focus of biosphere ecological studies since the International Biological Program (1964). In IBP, energy flows as represented in carbon compounds and biogeochemical cycles were estimated for various types of ecosystems of the terrestrial biosphere at different temporal and spatial scales. To appropriately accomplish such goals, it was required that carbon flux measurement should be carried out on hourly, daily, seasonal, and yearly time scales and across plot-, regional, and global scales (Baldocchi, 2003). Despite the ability of traditional chamber methods to examine instant and diurnal variations of NEE, and to determine environmental controls on NEE for a particular object under study (Keller et al., 1986; Harley and Sharkey, 1991; Li et al., 2008), the chamber method has inherent limitations due to alteration of the local environment and lack of spatial representation (Baldocchi, 1988; Long et al., 1996). Furthermore, it is impossible to conduct continuous measurements at the ecosystem level (Long et al., 1996).

In recent years, the eddy covariance (EC) method has been developed as a widely used-technique to measure overall ecosystem carbon exchange (Baldocchi et al., 1988; Moncrieff et al., 1997a; Papale et al., 2006). The EC method is based on micrometeorological theory and interprets observations of the covariance between vertical wind velocity and scalar gas concentration fluctuations (cf. Baldocchi et al., 1988). Advantages of the EC method, e.g. the ability to continuously measure carbon exchange across a spectrum of time scales from hours to years and to obtain spatially-integrated data at ecosystem level without disturbing natural conditions (Baldocchi et al., 1988; Wofsy et al., 1993; Schmid, 1994; Foken and Wichura, 1996;

Baldocchi, 2003), have led to their wide use. The increasing numbers of EC flux tower sites has produced flux observation networks at regional (e.g., AmeriFlux, EuroFlux, and AsiaFlux) and global (i.e., FLUXNET) scales, which coordinate the flux observational data and provide an organized and standardized flux data resource, along with the micrometeorological drivers ([www.fluxdata.org](http://www.fluxdata.org)), to the research community.

Currently, over 500 tower sites are operated on a long-term and continuous basis, covering deciduous and coniferous forests, tropical and boreal forests, crops, grasslands, chaparral, wetlands, tundra, etc. Establishment of regional and global databases of the EC measurements of carbon, water, and energy fluxes provide opportunities to examine terrestrial carbon, water, and energy cycles. Nevertheless, it is still the case that most tower sites observe fluxes from forests and grasslands. Only a few sites study croplands in part due to the difficulties and uncertainties related to calculating the cropland carbon budget (see Osborne et al., 2010). Among those sites, rice (Saito et al., 2005; Kwon et al., 2010), sugar beet (Moureaux et al., 2006), winter wheat and triticale (Ammann et al., 1996; Anthoni et al., 2004; Baldocchi, 1994; Moureaux et al., 2008; Béziat et al., 2009), and sunflower, rapeseed or maize for silage (Béziat et al., 2009) have been investigated. Maize/soybean rotations in North America have also received great attention (Baker and Griffis, 2005; Bernacchi et al., 2005; Hollinger et al., 2005; Pattey et al., 2002; Suyker et al., 2005; Suyker et al., 2004; Verma et al., 2005). Data from these cropland sites provide important input to the current work.

## 2.3 Vegetation indices from remote sensing

Satellite remote sensing is often used together with process-based models and detailed maps of ecosystem distribution to accomplish the up-scaling of carbon fluxes to landscape, regional, continental and global scales (Goetz et al., 1999; Xiao et al., 2008; Wu et al., 2009; Oguto et al., 2013). Since the first earth observation satellites were launched in the mid-1970s, surface reflectance data and information on vegetation cover has been compiled in order to advance our understanding of ecosystems (NASA Langley Research Center Atmospheric Science Data Center ([LaRC ASDC] <http://eosweb.larc.nasa.gov>). Vegetation indices were first used by Rouse et al. (1973) at the Remote Sensing Center of Texas A& M University. Vegetation indices are mathematical relationships obtained by combining spectral reflectance values from the spectral bands measured by sensors on board satellites (Bannari et al., 1995). Generally, vegetation indices (VIs) have been related to the ratio between red and near infrared (NIR) reflectance. Visible radiation in the red (620-670 nm) is absorbed by chlorophyll while the mesophyll leaf

cellular structures reflect NIR (841-876 nm) (Pettorelli et al., 2005).

The remotely sensed vegetation indices of ecosystem canopies allow monitoring of phenological events and seasonal change in vegetation development (Sellers 1985; Running et al., 1988; Myneni et al., 1995) from regional (Chen et al., 1999; Kimball et al., 1999; Kang et al., 2003) to global scale (Running et al., 1999; Huete et al., 2002). The Normalized Difference Vegetation Index (NDVI) is most widely used (Rouse et al., 1974; Myneni et al., 1995), which depends strongly on the amount of chlorophyll and other pigments exposed to the view of the satellite (Huete et al., 1997). NDVI is calculated using red and near-infra-red wavelengths as

$$NDVI = (\rho_{NIR} - \rho_{red}) / (\rho_{NIR} + \rho_{red}) \quad (2.1)$$

is surface reflectance in near infrared and red sensor bands, respectively (Running et al., 2004). NDVI is tightly correlated with LAI development over the growing season (Xiao et al., 2002), allowing the monitoring of phenology (R. Lee et al., 2002; Vina et al., 2004), validation of production models (White and Running, 2009; Peng et al., 2012), and determination of vegetation cover density (Jiang et al., 2006). NDVI has been reported to correlate directly with vegetation productivity in a number of studies (Garmon et al., 1995; Nemani et al., 2003; Wang et al., 2004) and with phenology in many ecosystem types (Lee et al., 2002; Zhang et al., 2003; Wang et al., 2005; Sakamoto et al., 2005; Zhang et al., 2005; Soudani et al., 2012).

The enhanced vegetation index (EVI) was developed by Huete et al. (1999) at the University of Arizona. EVI has improved sensitivity to vegetation canopy structure and exhibits high correlation with vegetation cover in areas with dense vegetation (Huete et al., 2002; Wardlow and Egbert, 2010), calculated using the blue, red, and NIR reflectance values and canopy background adjustment factor ( $L$ ) (Huete et al., 1997).

$$EVI = G(\rho_{NIR} - \rho_{red}) / (\rho_{NIR} + C1\rho_{red} - C2\rho_{blue} + L) \quad (2.2)$$

$L$  is the canopy background adjustment factor that accounts for differential red and NIR radiant transfer through the canopy,  $C1$  and  $C2$  are the coefficients of the aerosol resistance term, which uses the blue band to correct for aerosol influences in the red band. EVI attempts to de-couple canopy reflectance from background reflectance ( $L$ ) and reduce atmosphere influences by including blue band reflectance, which is more sensitive to atmosphere aerosols than red reflectance (Huete et al., 2002). Including the factor  $L$  and blue reflectance reduces soil background effect and residual atmospheric contamination which has often been shown to limit the use of NDVI (Huete et al., 1994). EVI has been used to monitor vegetation phenology in

forested areas (Zhang et al., 2003) and to estimate vegetation photosynthesis together with process-based models (Xiao et al., 2004).

VIIs in addition to NDVI and EVI have been suggested. The best known are the following: Huete (1988) suggested the soil adjusted vegetation index (SAVI) which was modified by Chehbouni et al. (1994; MSAVI). SAVI allows the minimization of soil brightness effects (Huete, 1988; Huete and Liu, 1994). SAVI has been used to determine LAI where soil background reflectance is a major problem (Darvishzadeh et al., 2008; Li et al., 2008). The ratio vegetation index (RVI) uses the simple ratio between red and NIR (Pearson and Miller, 1972), a “perpendicular vegetation index” (PVI) has been used to distinguish vegetation from soil background (Richardson and Wiegand, 1977), the green NDVI (GNDVI) attempts improvements by including green band information (Gitelson et al., 1996), and the global environment monitoring index (GEMI) was developed to obtain a global scale index without soil effects (Pinty and Verstraete, 1992). Many additional indices have been proposed by researchers of the remote sensing community. In this study, NDVI and EVI were used to describe plant phenology and carboxylation capacity due to their broad application in other studies, i.e., to possibly allow for comparisons. As discussed in Chapter 6, however, extension of the studies may be possible with the use of additional VIIs.

## 2.4 Modeling GPP in agricultural ecosystems

Modeling GPP in agroecosystems is a necessary step in evaluating the influences of climate variation on crop yield and understanding potentials to meet the growing demand for food (Tao et al., 2004; Dorigo et al., 2007). Previous studies of carbon balances in croplands have examined GPP with the EC method as described above, have sampled LAI and biomass over the course of the growing season (Suyker et al., 2005), have attempted to consider crop history and crop rotation (Aubinet et al., 2009), and have examined managements effects (Kutsch et al., 2010, Ceschia et al., 2010). Various models have been developed in order to scale up carbon assimilation, and these have been validated via EC measurements (Hoyaux et al., 2008; Peng et al., 2012; Gitelson et al., 2012). Yan et al. (2009) used a satellite-based photosynthesis model to estimate crop GPP with EVI derived model parameters, comparing the results with EC data. Revill et al. (2013) established a technique of combining flux measurements with earth observation data to simulate LAI, carbon fluxes, and the yield of European cropland.

The studies of quantifying GPP in agroecosystems have aimed at accurate estimations with the inclusion of various information related to direct field data sampling, use of inventory data,

application of the EC methodology, utilizing different types of remote sensing, and synthesizing results with process-based models at different spatial and temporal resolutions. However, GPP estimation in agroecosystems is often limited due to incompatibility in the spatial scales of flux measurements and resolution of satellite data. Therefore, quantifying GPP in agroecosystems at landscape scale remains a challenge due to gradients in local climate, fragmentation of land cover dependent on field structure and management effects.



# Chapter 3

## Materials and Method

### 3.1 Site descriptions

Study sites were selected where the crops were the same or similar to those grown in Haean Catchment, South Korea. Using available data, the collected data came from various climate zones. These included South Korea (Haean Catchment and Haenam) and Japan (Mase) in Asia, Spain (El Saler-Sueca), Belgium (Lonze), and Germany (Klingenberg) in Europe, and Nebraska, U.S.A. (Mead) in North America. Meteorological conditions and site characteristics are summarized in Table 3.1. The flux data for GPP recorded in the databases provide the material for analysis in this thesis (see further section 3.1.1, 3.1.2, and 3.1.3).

#### 3.1.1 Asian sites

All the Asian sites are under the influence of monsoon climate resulting in more than 50% of annual precipitation occurred during a summer monsoon period. The summer monsoon period is followed by a subsequent typhoon season, mainly in September and October.

##### 3.1.1.1 Haean, South Korea (HK)

Haean Catchment is a typical erosion mountain basin in South Korea located northeast of Chuncheon, Gwangwon Province in Yanggu County (38° 17' N, 128° 08' E, 450 - 1200 m a.s.l.). Total area of the catchment is 64 km<sup>2</sup>, which consists of 58% forested mountain area, 30% agricultural area, and 12% as residential, riparian, field margins, and farm road area according to land surveys (Fig. 1.1, Arnhold et al., 2012). The agricultural area is characterized as a mosaic patchwork of fields, with a dominance of dry-land fields (22% of the total area) and the remaining as rice paddy fields (8%). Rice paddies (*Oryza sativa* L., cv. Odae) are cultivated at

less than 500 m a.s.l. in the catchment, whereas the main dry-land crops (e.g, potato, radish, beans and cabbage) are planted from 500 to 750 m a.s.l. (Choi et al., 2010). Annual mean temperature is ca. 8.5 °C and annual precipitation is 1577 mm (Table 3.1; Choi et al., 2010; Kettering et al., 2012).

Measurements of CO<sub>2</sub> exchange with the eddy covariance (EC) method were conducted in 2010 at rice paddy and potato (*Solanum tuberosum* L.) sites. Rice was transplanted on day of year (DOY) 144 and harvested on DOY 290, whereas potato was sown on DOY 116. The aboveground plant parts of potato had died by DOY 240, while the tubers were harvested on DOY 273. The EC system ran during three time periods at the rice paddy site and the potato site, respectively (i.e., DOY 177-186, 203-223, and 242-274 at the rice paddy site and DOY 152-175, 187-203, and 225-240 at the potato site; Zhao et al., 2012). Leaf area index (LAI) as an indicator of phenological plant stage was measured by plot harvests and using a leaf area meter (LI-3000A, LI-COR Inc., USA) throughout the measurement period at the rice paddy site of EC measurements. LAI for potato was measured in a potato field directly adjacent to the EC measurement site during the biomass growth period (DOY120 - 243).

### 3.1.1.2 Haenam, South Korea (HFK)

The Haenam site is located in the southwestern part of the Korean Peninsula within Haenam-gun, Jeollanamdo (34° 33' 18" N, 126° 34' 7" E, 14 m a.s.l.). Haenam is a typical rice (*Oryza sativa* L.) farming region and one of the largest rice cultivating areas in Korea (Kim et al., 2011; Statistics Korea, 2010). The study site was covered the mixture of rice paddies and various seasonal crops such as beans, sweet potato, Indian millet, and sesame (Lee et al., 2003). Annual mean temperature is ca. 13.3 °C and annual precipitation is ca. 130 mm. The EC measurements have been conducted since 2002 as one of the main KoFlux sites ([http://asiaflux.net/?page\\_id=13](http://asiaflux.net/?page_id=13)). In this study, the EC flux and meteorological data in 2008 were used. For further information on the EC measurement, see Kwon et al., 2010. Seasonal LAI at the Haenam site was unavailable.

### 3.1.1.3 Mase, Japan (MSE)

The Mase site is located in a rural area (36° 03' 14" N, 140° 01' 38" E, 15 m a.s.l.) of Tsukuba City in central Japan, which is about 50 km northeast of Tokyo. The size of rice (*Oryza sativa* L.) paddy was ca. 2 km<sup>2</sup>, and the rice paddy was managed as a single rice-cropping field following practices common in the area (Saito et al., 2005). The transplanting

and harvesting dates of the rice were shown in Table 3.1. Annual mean temperature is ca. 13.7 °C and annual precipitation is ca. 1200 mm (<http://www.asiaflux.net/network/>) were included. In this study, the EC flux and meteorological data from 2002 to 2005 obtained from AsiaFlux (<https://db.cger.nies.go.jp/asiafluxdb/>) were included. LAI was measured with an optical area meter (AAM-7, Hayashi Denkoh, Tokyo, Japan). Further information of EC and LAI measurements are described in Saito et al. (2005).

### 3.1.2 European sites

The sites in European occur under different climate conditions. El Saler, which is under sub-arid Mediterranean climate, has a hot summer with almost no rain and cold winter with substantial rain. Lonze occurs under a temperate maritime climate dominated all year around by the polar front and often with overcast weather, while Klingenberg is subjected to continental/sub-continental climate with a warm summer and cold winter.

#### 3.1.2.1 El Saler-Sueca, Spain (ESES2)

The El Saler Sueca site is located in the protected wetland area of La Albufera Natural Park in the Valencia region of Spain (39° 16' 32" N, 0° 18' 55" E, 10 m a.s.l.). The rice paddy at El Saler Sueca is within a large rice paddy field (ca. 15 km<sup>2</sup>) where the management of rice farming has not changed for over 200 years (Kutsch et al., 2010; Moors et al., 2010). The sowing and harvesting dates of the rice are shown in Table 3.1. Annual mean temperature is 17.9 °C and annual precipitation is 550 mm (Kutsch et al. 2010). The EC flux, meteorological data, and LAI of El Saler Sueca in 2007 and 2008 were obtained from CarboEurope cropland network (<http://www.carboeurope.org/>; Table 3.1). LAI was measured using sampled plants. Further details about the site, agricultural management, and measurements including EC methodology are described in Kutsch et al. (2010) and Moors et al. (2010).

#### 3.1.2.2 Lonze, Belgium (BE-Lon)

The Lonze site is located about 45 km southeast of Brussels, Belgium (50° 33' 08" N, 4° 44' 42" E, 165 m a.s.l.) on a flat plateau. Annual mean temperature is about 10.8 °C and annual precipitation is about 800 mm (Moureaux et al., 2006). The site has been cultivated more than 70 years primarily with cereals, potato, and sugar beet. In 2004, sugar beet (*Beta vulgaris* L.) was sown on DOY 121 and harvested on DOY 273 (Table 3.1; Moureaux et al., 2006). In the context of analysis of the Haeon landscape in South Korea, sugar beet is considered as

a surrogate for the important crop radish, since the growth form is similar and radish data are non-existent. We used the EC flux, meteorological data, and LAI in 2004 obtained from CarboEurope-IP ecosystem network (<http://www.carboeurope.org/>). LAI of sampled plants was estimated using a camera and a picture analyser (Windias, Delta-T Devices, Cambridge, UK). For detailed information on the Lonze site, see Moureaux et al., 2006 and Aubinet et al., 2009.

### 3.1.2.3 Klingenberg, Germany (DE-Kli)

The Klingenberg site is located in Saxonia, Germany (50° 53' 34" N, 13° 31' 21" E, 468 m a.s.l). Annual mean temperature is ca. 7.3 °C and annual precipitation is ca. 850 mm (Kutsch et al., 2010). The site has been cultivated since 1975, mainly with barley, rapeseed, and maize (Ceschia et al., 2010). In 2007, maize (*Zea mays*, L ), which is C4 crop, was sown on DOY 143 and harvested on DOY 268 (Table 3.1). Maize is cultivated in Gwangwon Province, which includes Haeen Catchment, and it account for 40% of total maize cultivated in South Korea. LAI was measured by plot harvests and with a leaf area meter (LI-3000A, LI-COR Inc., USA). The EC system was utilized at the site since 2004. The EC flux data and meteorological data from 2007 from the CarboEurope-IP ecosystem network (<http://www.carboeurope.org/>) were used in this study.

## 3.1.3 American site

### 3.1.3.1 Mead, Nebraska, U.S.A. (US-Ne3)

Nebraska site is located in the Agricultural Research and Development Center, University of Nebraska in USA (41° 10' 46" N, 96° 26' 22" W, 362 m a.s.l.). It is a rainfed agricultural area and planted with rotation of maize (*Zea mays*, L ) and soybean (*Glycine max* [L] Merr.) over two year periods. The data from the years of 2002 and 2004 at the Nebraska site were selected for analysis of soybean GPP. In the case of maize, the data from the years of 2003 and 2005 were used. The planting days in study years of soybean or maize differed by 14 to 17 days, but the harvest dates were similar (Table 3.1). The Nebraska site is subjected to a humid continental climate; annual mean temperature is ca. 10.1 °C and annual precipitation is ca. 784 mm (<http://www.fluxdata.org:8080/SitePages/>). The EC flux data used in this study were those obtained with natural rainfall as Haeen Catchment. LAI was determined using a leaf area meter (Model LI3100C: Li-Cor Inc., Lincoln, NE) at 10- to 14-day intervals until harvest (Suyker et al., 2010). The EC flux, meteorological data, and LAI were downloaded

from AmeriFlux (<http://ameriflux.ornl.gov/>). Additional information about the site can be found on the web site, but see also Suyker et al. (2010).

Table 3.1. Site information of rice paddy sites at Haeon and Haenam, South Korea, Mase, Japan and El Saler-Sueca, Spain and dry- land crops at Haeon, South Korea, Lonze, Belgium, Klingenberg, Germany, and Nebraska-Mead, U.S.A. Total  $R_g$  is total global radiation, mean  $T_a$  is mean air temperature, total P is total rainfall, planting and harvest date (day of year - DOY), maximum LAI and DOY of maximum LAI. Meteorological condition considers the period of crop growth (from the planting to the harvest). The eddy data of US-Ne3 2003 is available until DOY 243.

Crop	Site	Year	Site information		Meteorological condition			Planting Harvest		Max LAI
			Country	Coordinates	Elevation (m)	Total $R_g$ (MJ/m <sup>2</sup> )	Mean $T_a$ (°C)	Total P (mm)	(DOY)	(DOY)
Rice	Haeon	2010	S.Korea	38.29 N, 128.13 E	446	1712.5 (6.8)	20.4 (4.1)	1165	144	290
	Haenam	2008	S.Korea	34.92 N, 126.95 E	14	2050.1 (6.9)	25.5 (3.5)	706	140	280
	Mase	2002	Japan	36.05 N, 140.03 E	13	2355.9 (7.7)	22.0 (4.4)	593	122	262
		2003	Japan	36.05 N, 140.03 E	13	2049.2 (6.6)	20.3 (3.3)	545	122	262
		2004	Japan	36.05 N, 140.03 E	13	2384.4 (7.3)	22.7 (4.3)	547	123	254
Potato	El Saler	2005	Japan	36.05 N, 140.03 E	13	2236.6 (6.4)	21.8 (4.5)	647	122	256
		2007	Spain	39.28 N, -0.32 E	10	3223.7 (5.9)	22.8 (1.9)	437	134	270
		2008	Spain	39.28 N, -0.32 E	10	3262.5 (6.4)	22.1 (2.8)	121	132	278
		2010	S.Korea	38.28 N, 128.12 E	440	1534.2 (7.6)	21.4 (3.4)	660	116	273
		2004	Belgium	50.55 N, 4.74 E	165	2974.2 (6.1)	14.3 (3.9)	411	90	273
Sugar beet	Lonze	2002	NE, USA	41.18 N, -96.44 E	362	2995.8 (6.7)	22.2 (5.2)	372	140	282
	Mead	2004	NE, USA	41.18 N, -96.44 E	362	2638.6 (5.9)	20.2 (4.0)	311	154	285
	Klingenberg	2007	Germany	50.89 N, 13.52 E	475	2075.9 (6.7)	15.0 (3.7)	471	143	268
Maize	Mead	2003	NE, USA	41.18 N, -96.44 E	362	2509.7 (6.1)	21.8 (4.1)	178	133	286
		2005	NE, USA	41.18 N, -96.44 E	362	2882.3 (6.5)	21.8 (5.8)	365	116	290

## 3.2 Algorithms of physiological process-based canopy gas exchange model

The canopy model for predicting GPP in comparison to data from EC sites is designed to calculate short-term ecosystem  $\text{CO}_2$  exchange (Tenhunen et al., 1994; Reichstein et al., 2003a; Wang et al., 2003). The model is single-layered model. It estimates light interception and  $\text{CO}_2$  exchange rates of canopy foliage for sun and shaded light classes half-hourly which is then compared to EC measurements (Owen et al., 2007). The model is driven by meteorological data, e.g., global radiation ( $R_g$ ), air temperature ( $T_a$ ), vapor pressure deficit (VPD), wind speed, air pressure, and atmospheric  $\text{CO}_2$  concentration, and requires estimated values for LAI.

Total shortwave radiation on the sunlit leaves is the sum of direct, sky diffuse and multiple scattered radiation, whereas on the shaded leaves, it is only the sum of sky diffuse, and multiple scattered radiation (see Eq. 2, 3, 4, and 5 in Owen et al., 2007). The foliage orientation function ( $G$ ) was set at 0.5 and the influence of clumping ( $\Omega$ ) at 0.9 for croplands in these equations. In order to account for the effect of the canopy on light interception, we expanded LAI to plant area index (PAI), which is the sum of LAI and stem area index (SAI) (i.e.,  $\text{PAI} = \text{LAI} + \text{SAI}$ ). SAI of the crop is calculated as 14% of LAI, whereas SAI of the rice is set at 0.01 (see details in Owen et al., 2007).

Simulation of gross photosynthesis follows Farquhar and von Caemmerer (1982), as modified for practical field applications by Harley and Tenhunen (1991). It is based on Ribulose-1,5-bisphosphate-carboxylase-oxygenase (Rubisco) enzyme reactions, where the rate of  $\text{CO}_2$  fixation is limited by either the regeneration of Ribulose-1,5-bisphosphate (RuBP) at low light intensity and/or high internal  $\text{CO}_2$  concentration or by Rubisco activity and  $\text{CO}_2/\text{O}_2$  concentration at saturated light and low internal  $\text{CO}_2$  concentration. The key parameter of the model is Rubisco maximum carboxylation rate ( $V_{c_{\max}}$ ) at 25 °C, while all temperature dependencies are fixed in relation to this rate. When comparing predicted GPP to EC measured values, a best fit is obtained for this key parameter. RuBP reduction capacity, dark respiration capacity, and light utilization efficiency of the canopy are assumed to be proportional to  $V_{c_{\max}}$ . Given that fixed temperature dependencies and process proportionalities are used, and that assumptions are made about canopy structure and light interceptions, a lumped parameter,  $V_{c_{\text{uptake}}}$ , that is

assumed to control overall carbon fixation rather than direct enzyme related parameter  $V_{c_{max}}$  is obtained from the statistical fitting procedure.

The model formulation follows Farquhar and Von Cammerer (1982) further, net photosynthesis ( $P_{net}$ ) is obtained using

$$P_{net} = (1 - \frac{\Gamma^*}{c_i}) \min(w_c : w_j) - 0.5R_d \quad (3.1)$$

where  $\Gamma^*$  is  $CO_2$  compensation point in the absence of mitochondrial respiration,  $w_c$  is the carboxylation rate supported by Rubisco enzyme,  $w_j$  is the carboxylation rate supported by the actual electron transport rate,  $R_d$  is the respiration occurring in mitochondria without light.  $c_i$  is the internal  $CO_2$  concentration based on Fick's Law for molecular diffusion of  $CO_2$  through the stomata and boundary layer, and is calculated from the following equation.

$$c_i = c_s - \frac{1.6P_{net}}{g_s} \quad (3.2)$$

where  $c_s$  is the  $CO_2$  concentration at the surface of the leaf and  $g_s$  is the stomatal conductance according to modified Ball-Berry equation (Ball et al., 1987; Harley and Tenhunen, 1991).

$$g_s = g_{s,min} + g_{fac} \frac{(P_{net}R_d)rH}{c_s} \quad (3.3)$$

where  $g_{s,min}$  is the minimum stomatal conductance,  $r_H$  is relative humidity,  $g_{fac}$  is a constant representing stomatal sensitivity in relation to  $CO_2$  assimilation. It has been evaluated for different species from chamber experiments (Tenhunen, 1990; Sala and Tenhunen, 1994, 1996).

$w_c$  is the carboxylation rate supported by Rubisco enzyme, calculated as:

$$w_c = \frac{V_c c_i}{c_i + K_c(1 + O/K_o)} \quad (3.4)$$

where  $V_c$  is the maximum rate of carboxylation,  $K_c$  is the Michaelis constant for carboxylation,  $K_o$  is the Michaelis constant for oxygenation, and  $O$  is the oxygen concentration of the air [ $210 \text{ cm}_3 \text{ O}_2 (\text{L air})^{-1}$ ]. As the dependency of temperature,  $V_c$  is calculated as:

$$V_c = \frac{V_{c_{max}} e^{\Delta H_a(T_k - 298/298RT_k)}}{1 + e^{(\Delta ST_k - \Delta H_d)/RT_k}} (1 + e^{298\Delta S - \Delta H_d/298R}) \quad (3.5)$$

where  $V_{c_{\max}}$  is the maximum rate of carboxylation capacity at 25 °C,  $\Delta H_a$  is the activation enthalpy of carboxylation,  $T_k$  is the estimated the leaf temperature in the current model iteration step,  $R$  is the universal gas constant,  $S$  is an enthalpy term for deactivation, and  $\Delta H_a$  is the deactivation enthalpy of carboxylation.  $w_j$  is calculated as:

$$w_j = \frac{P_m c_i}{c_i + 2.0\Gamma^*} \quad (3.6)$$

where  $P_m$  is the maximum potential rate of RuBP production.  $P_m$  is calculated following the Smith equation (cf. Tenhunen et al., 1976):

$$P_m = \frac{\alpha I}{\sqrt{1 + (\alpha^2 I^2 / P_m^2 l)}} \quad (3.7)$$

where  $\alpha$  is the average leaf light utilization efficiency without photorespiration,  $I$  is the incident PPFD, and  $P_{m_l}$  is the CO<sub>2</sub> and light saturated temperature dependent potential RuBP regeneration rate as described in Falge (1997).

As indicated above, rather than using the notation of  $V_{c_{\max}}$  at the leaf level,  $V_{c_{\text{uptake}}}$  is referred to as the estimate of the maximum rate of carboxylation capacity at the canopy level when fitting the model to EC data. Estimated  $V_{c_{\text{uptake}}}$  is extracted by minimizing the sum of residual least squares i.e., the Levenberg-Marquardt algorithms of the PV-WAVE routine in the comparison of model predictions with EC observations at half hour intervals. The light utilization efficiency,  $\alpha$ , can also be estimated from the EC data as an additional fitting parameter. In this study, however, we assumed  $\alpha$  to be proportional to  $V_{c_{\text{uptake}}}$  following Owen et al. (2007). The relationship of  $\alpha$  and  $V_{c_{\text{uptake}}}$  is

$$\alpha = \min(0.0008V_{c_{\text{uptake}}}, 0.06) \quad (3.8)$$

$V_{c_{\text{uptake}}}$  estimation was carried out on a daily basis over the course of the growing season for each crop data set. We determined that the predicted  $V_{c_{\text{uptake}}}$  was occasionally unrealistically high during the early growing season ( $>200 \mu\text{mol m}^{-2} \text{ leaf area s}^{-1}$ ) when LAI was low ( $<1$ ) but GPP was positive ( $>50 \mu\text{mol m}^{-2} \text{ leaf area s}^{-1}$ ). This results from errors in the flux determination or in LAI estimation; values that are critical in the analysis of CO<sub>2</sub> uptake (it may occur, for example, if the flux footprint is different from the area used in LAI estimation). In order to

eliminate artificially high estimates of  $V_{c_{\text{uptake}}}$ , the current work includes only flux data where LAI is  $> 1$  in the model fitting procedure. More information on the physiologically-based model can be found in Owen et al. (2007).

The photosynthesis sub-model has been developed based on C3 plant photosynthesis. C4 plants are known to have less photorespiration than C3 plant due to the  $\text{CO}_2$  concentration mechanism of the C4 cycle (Edwards and Walker, 1983; Taiz and Zeiger, 1991). In these plants, atmospheric  $\text{CO}_2$  is initially fixed into C4 acids in the mesophyll cells. The acids are transported to the bundle sheath cells where they are decarboxylated. Decarboxylation of the C4 acids increases  $\text{CO}_2$  concentration in the chloroplasts to levels much higher than in the external atmosphere (Edwards and Walker, 1983). Dai et al. (1993) reported intercellular  $\text{CO}_2$  concentration for maize that was about 3.2-fold higher than in the C3 plant wheat. Based on this experiment, atmospheric  $\text{CO}_2$  concentration in Eq. 3.2 was set 3 times higher (1000 ppm) for analysis of the EC data from the C4 plant maize.

### 3.3 Physiological parameters of the canopy model and GPP estimation

The leaf physiological parameters applied as constants and those controlling temperature dependencies were obtained in previous studies on leaf physiology. These values are identified and shown in Table 3.2 (from Tenhunen et al., 1990; Harley and Tenhunen, 1991; Falge et al., 1996; Sala and Tenhunen, 1996). These parameters describe temperature and light dependencies and response of stomata (Tenhunen et al., 1990). Gross primary production (GPP) is calculated with the single-layered canopy sub-model as described in 3.2.1. Inputs to the model are half-hourly global radiation, air temperature, relative humidity and precipitation. Matrices for all meteorological drivers are prepared previous to analysis runs (estimated in separate routines and stored outside of the model) and are input to the model according to the half-hourly simulation time step. Of primary concern in this study was estimation of a single key parameter,  $V_{c_{\text{uptake}}}$ , that describes change in overall canopy  $\text{CO}_2$  uptake capacity.

Seasonal variation of  $V_{c_{\text{uptake}}}$  was estimated *via* model fitting with the detailed canopy sub-model and EC GPP data (Owen et al., 2007). The method was performed using the functions

NLINLSA and NONLINREGRESS of PV-WAVE statistical program package. These functions used a modified Levenberg-Marquardt algorithm that is a method for minimizing a sum of weighted squared residuals to solve nonlinear parameter problems, such as estimation of  $V_{c_{\text{uptake}}}$  (PV-WAVE IMSL Mathematics Reference, 2010; Transtrum and Sethna, 2012). A common least-squares minimization is expressed as:

$$C(\theta) = \frac{1}{2} \sum_{m=1}^M r_m(\theta)^2 \quad (3.9)$$

where  $N \leq M$ ,  $r: \mathbb{R}^N \rightarrow \mathbb{R}^M$  is an  $M$ -dimensional nonlinear vector function of  $N$  parameters  $\theta$ . Function  $r_m(\theta)$  followed the form

$$r_m(\theta) = \frac{(y(t_m, \theta) - y_m)}{\sigma_m} \quad (3.10)$$

$\theta$  is the parameter,  $y(t_m, \theta)$  is a model of the observed data,  $y_m$ , that depends on unknown parameters  $\theta$ , one or more independent variables  $t$ , and uncertainty in observed data,  $\sigma$ . The terms in Eq. 3.10 are known as the residuals, the parameter values that minimize  $C(\theta)$  are known as the best fit parameters. Consistent seasonal trends in the key physiological parameter describing  $\text{CO}_2$  uptake capacity,  $V_{c_{\text{uptake}}}$ , are found for functional crop types, e.g., root crops and rice as a grain crop (Li et al., 2010), which aids in parameterization according to the land use.

### 3.4 Vegetation indices from remote sensing

Remote sensing vegetation indices (NDVI and EVI) are determined by light reflected from the crop surface. NDVI and EVI depend on properties, which are determined on the one hand *via* change in crop canopy structure (leaf area index) but also *via* physiological factors, i.e., the pigmentation change that may be correlated with the levels of investment in photosynthesis metabolism. NDVI and EVI from 2001 to 2011 were obtained from daily gridded L3G (level-3) composite data at 250 m resolution that is embedded in the MODIS/terra surface reflectance products (MOD13G1) obtained from the Warehouse Inventory Search Tool (WIST, <https://wist.echo.nasa.gov/>). MOD13Q1 provides 16-day composite vegetation condition derived from blue (459-479 nm), red (620-670 nm), and near-infra-red (NIR, 841-876 nm) surface

Table 3.2. Parameters for physiologically based canopy model. Parameter values are generalized from Harley and Tenhunen (1991), Falge et al. (1996), and Owen et al. (2007).

Parameter	Description	Crops
Veg.typ	Vegetation type	3
$\Omega$	Modified to consider the influence of clumping	0.9
alpha	Initial slope of the light response curve (leaf level light-use efficiency)	
	$[\text{mol CO}_2 \text{ m}^{-2} \text{ Leaf surface} (\text{mol Photonen m}^{-2} \text{ horizontal area})^{-1}]$	0.045
$\Delta H_a(J_{\max})$	Activation enthalpy for maximum rate of electron transport	40000
$\Delta H_d(J_{\max})$	Deactivation enthalpy for maximum rate of electron transport	200000
$\Delta S(J_{\max})$	Entropy factor for maximum rate of electron transport	655
$\Delta H_a(V_{c_{\max}})$	Activation enthalpy for maximum rate of carboxylation	69000
$\Delta H_d(V_{c_{\max}})$	Deactivation enthalpy for maximum rate of carboxylation	198000
$\Delta S(V_{c_{\max}})$	Entropy factor for maximum rate of carboxylation	660
$E_a(R_d)$	Activation energy for mitochondrial (dark) respiration	58000
$E_a(\tau)$	Activation energy for enzyme specificity factor	-28990
$f(\tau)$	Scaling factor for enzyme specificity factor	2339.53
$E_a(K_O)$	Activation energy for Michaelis-Menten constant for oxygenation	35900
$f(K_O)$	Scaling factor for Michaelis-Menten constant for oxygenation	248
$E_a(K_C)$	Activation energy for Michaelis-Menten constant for carboxylation	59500
$f(K_C)$	Scaling factor for Michaelis-Menten constant for carboxylation	404
gfac	Bell-Berry stomatal conductance factor	12

reflectance in the sinusoidal projection. The normalized difference vegetation index (NDVI) is calculated using red and near-infra-red wavelengths as in Eq. 2.1. NDVI depends strongly on the amount of chlorophyll and other pigments exposed to the view of the satellite (Huete et al., 1997).

Enhanced Vegetation Index (EVI) (Huete et al., 2002), is calculated using the blue, red, and NIR reflectance values and canopy background adjustment factor ( $L$ ) (Huete et al., 1997).  $L$  and blue reflectance value for EVI reduce soil background effect and residual atmospheric contamination that has known to the limit applications of NDVI (Huete et al., 1994). EVI can be calculated as in Eq. 2.2. I adopted  $L=1$ ,  $C1=6$ ,  $C2=7.5$ , and  $G$  (gain factor)=2.5 as recommended by Huete et al. (2002).

The original values of VIs include frequency noise components due to clouds, water, snow, shadow, bidirectional effects, high solar or scan angles and transmission errors which are identified in a series of quality control indicators. In the initial studies reported here, the TIMESAT program developed by Jonsson and Eklundh (2004) for smoothing VIs was applied. TIMESAT is an open source software, which provides three different smoothing functions: asymmetric Gaussian, double logistic, and adaptive Savitzky-Golay filtering, to fit the time-series satellite sensor data. VIs were smoothed as final NDVI and EVI by the adaptive Savitzky-Golay filtering method at rice paddy sites and dry land crop sites. The adaptive Savitzky-Golay filtering is calculated locally to achieve the smallest estimated mean square error; it is able to follow complex fluctuations that occur with rapid increase and decreases in the reflectance data (Jonsson and Eklundh, 2004). Agricultural crops are able to change their physical and physiological condition over short time intervals. In this study, VIs at a daily time step, which was same temporal resolution as modeled GPP, was calculated using a spline as a polynomial interpolation.

### 3.5 Leaf area index estimates

The measurement of leaf area index (LAI) was conducted during the growing season at most of the EC measurement sites, Haeon (rice and potato), Mase, El Saler, Lonze, Klingenberg, and Nebraska. LAI measurement was not conducted at Haenam. Since measured LAI has in previous studies been shown to be correlated with spectral reflectance (Xiao et al., 2002; Pontauiller et al., 2003; Stenberg et al., 2004; Fan et al., 2008), two VIs were applied to estimate LAI, e.g., NDVI

and EVI. It was also tested whether features of reflectance at the beginning of the growing season are different than during at the senescence period. Therefore, two correlation models for LAI were developed at each site and for the growing season of the crop. The first model equation considered the relationship between measured LAI and VIs over the entire course of the season (indicated as E in the results tables), and the second model combined two equations, including the relationship between measured LAI and before and after maximum VIs (indicated as BA in the results tables). The relationships are shown for rice at the individual sites (HK, MSE, and ESES2) in Fig. 4.4 and Fig. 4.5, the continental sites (HK and MSE) and entire rice paddy in Fig. 4.7 and Fig. 4.8 (Chapter 4). Dry-land crop results are shown according to crop type (soybean, maize, potato, and sugar beet) in Chapter 5. Additionally, a new method for estimation of the seasonal course in LAI was developed which focuses on and requires only the identification of the time at which maximum NDVI and EVI is attained (see results).

### 3.6 Outlier removal

Outlier values for  $V_{c_{\text{uptake}}}$  may be indicative of errors in observation or in model-based analyses (Loo, 2010). Estimated  $V_{c_{\text{uptake}}}$  occasionally was extremely large (e.g.,  $\leq 500 \mu\text{mol m}^{-2} \text{ leaf area s}^{-1}$ ), much larger than most values determined for  $V_{c_{\text{uptake}}}$  (ranging from 0 to  $100 \mu\text{mol m}^{-2} \text{ leaf area s}^{-1}$ ). In order to remove the  $V_{c_{\text{uptake}}}$  outliers, we applied two statistical methods based on 1) the generalized additive model (GAM) and 2) detecting extreme value methods.

GAM, which has been widely used in ecological research, is based on the backfitting algorithm by combining different smoothing and fitting functions to find the best fit for the generalized data. Using a local regression and smoothing splines (Hastie and Tibshirani, 1990; Yee et al., 1991; Liu et al., 2008), the smoothed  $V_{c_{\text{uptake}}}$  ( $V_{c_{\text{uptake\_gam}}}$ , Fig. 3.1, thick solid line) was obtained where the values of the estimated  $V_{c_{\text{uptake}}}$  are determined from the 99 % confidence intervals (Fig. 3.1, dashed line). The confidence intervals are determined by standard deviation (STD) of  $V_{c_{\text{uptake\_gam}}}$ . The upper level of the confidence intervals is set by STD of  $V_{c_{\text{uptake\_gam}}}$  add  $V_{c_{\text{uptake\_gam}}}$ , whereas lower level is set by STD of  $V_{c_{\text{uptake\_gam}}}$  minus  $V_{c_{\text{uptake\_gam}}}$  (Fig. 3.1, thin solid line). The data outside of the confidence range, are considered as outliers and are removed.

The method of detecting extreme value determines outliers with reference to the approximant

( $\rho$ ) of the distribution of the observation, which is computed by probability plot (Quantile-Quantile plot) positions using a cumulative distribution function (Loo, 2010). After generating a model distribution of  $V_{\text{uptake}}$  with cumulative density,  $F(Y|\theta)$  (where  $Y$  is a random variable and  $\theta$  is a vector of parameter specifying  $F$ ), a criterium of outlier detection limit is determined and  $\rho$  of  $V_{\text{uptake}}$  is calculated. When  $V_{\text{uptake}}$  is either above or below with respect to  $\rho$ , it is categorized as an outlier (see Loo, 2010 for more detail information).

The two methods were applied to  $V_{\text{uptake}}$  data using R (Version 2.15.2), and the results from both methods were in good agreement (Fig. 3.1). The detected outliers by GAM, which lay above the upper level of confidence intervals, matched well with those by the detecting extreme values method in different years and at different measurement sites. Based on the concurring results and the complexity in the algorithms of GAM, it was decided to use the method of the detecting extreme values.

## 3.7 Statistical analysis

### 3.7.1 Model evaluation statistic

Several statistics are used to evaluate the accuracy of GPP estimation. Coefficient of determination ( $R^2$ ) is used to measure correlation between the modeled and the observed, and root mean squared error (RMSE) is used to measure the difference between the modeled and observed:

$$RMSE = \sqrt{1/N \sum_{i=1}^N (\hat{y}_i - y_i)^2} \quad (3.11)$$

where  $\hat{y}_i$  is the modeled and  $y_i$  is the observed. Coefficient of variation of the RMSE, CV (RMSE) is defined as the RMSE normalized to the mean of observation and is calculated as:

$$CV(RMSE) = RMSE/\bar{y} \quad (3.12)$$

where  $\bar{y}$  is the mean of the observed. Assessment of modeling efficiency (ME) was conducted to evaluate the model performance by comparing model simulation and observation (Janssen and Hauberger, 1995). ME measures correlation between the modeled and the observed as well

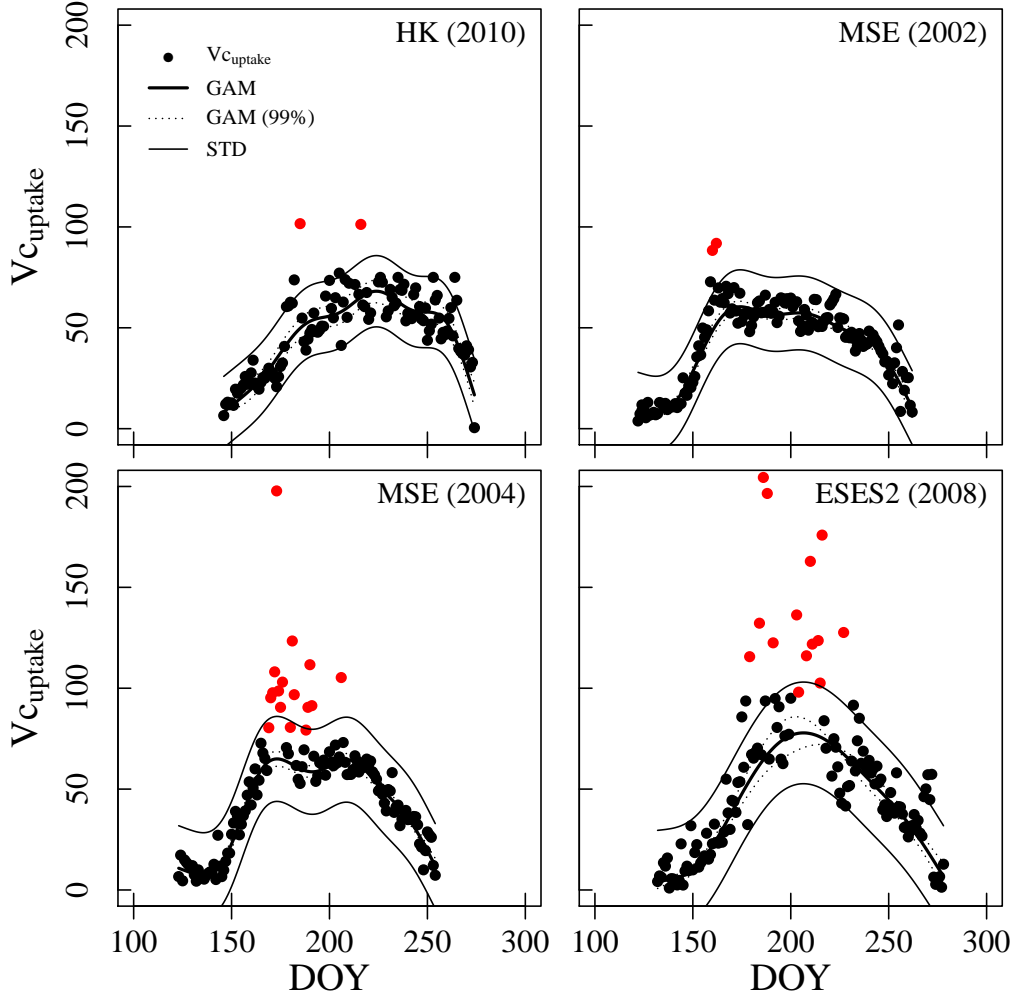


Fig. 3.1 Detection of the outliers by two statistical methods as described in the text, i.e., generalized additive model (GAM) and detecting extreme value methods. Black closed circle are  $V_{Cuptake}$ , red closed circle are the extreme values, thick solid line is GAM, dashed line is the 99% confidence intervals, and thin solid line is standard deviation line.

as their agreement and systematic deviation. ME is calculated as:

$$ME = 1 - \frac{\sum_{i=1}^N (y_i - \hat{y}_i)^2}{\sum_{i=1}^N (y_i - \bar{y})^2} \quad (3.13)$$

Although  $R^2$  is 1 as perfect agreement, the modeled and the observed are in disagreement when ME is less than 0 (Smith et al., 1996). Only positive values of ME, therefore, are considered to assess the model performance, and the model performance becomes better as ME approaches 1.

### 3.7.2 Sensitivity of variables

Estimation of GPP is determined by the compounding interaction of the meteorological, physiological, and phenological conditions. To assess the relative influence of controlling variables such as  $T_a$ , VPD,  $R_g$ , and LAI have on GPP, a one-way sensitivity analysis (SA) was conducted. One variable was changed in an incremental increase of 5% (ranging from 5 to 80%) while other variables were held constant. The results of SA arranged the variables by the significance of their impact on GPP estimation.



# Chapter 4

## Results: estimation of GPP for rice paddy sites

### 4.1 Meteorological conditions at the study sites

Weather conditions of 10-day intervals during the rice growth period are presented in Fig. 4.1. Weather data were obtained every half hour from the meteorological sensors installed on eddy covariance towers. Daily global radiation ( $R_g$ ) among the sites ranged from 7 to 30  $\text{MJm}^{-2}\text{d}^{-1}$ .  $R_g$  in Haean during 2010 increased rapidly with the start of growing season, reached the maximum value of 25.2  $\text{MJm}^{-2}\text{d}^{-1}$  and, decreased in June (DOY 152 – 181).  $R_g$  showed a fluctuation around 10  $\text{MJm}^{-2}\text{d}^{-1}$  with a large decrease (9  $\text{MJm}^{-2}\text{d}^{-1}$ ) in August (DOY 213 – 243). At Haean during 2011,  $R_g$  decreased continually to about 7  $\text{MJm}^{-2}\text{d}^{-1}$  in May, June, and July, fluctuated around 10  $\text{MJm}^{-2}\text{d}^{-1}$  in August, and decreased to about 1.3  $\text{MJm}^{-2}\text{d}^{-1}$  at the time of the harvest. At the Haenam site in 2008,  $R_g$  decreased (8.6  $\text{MJm}^{-2}\text{d}^{-1}$ ) in May and June, but increased rapidly to the maximum of about 20  $\text{MJm}^{-2}\text{d}^{-1}$  during July. In Mase,  $R_g$  showed similar seasonal change among the study years (2002 – 2005), decreasing with the start of the growing season and with large fluctuations during June to September (DOY 152 – 270); the maximum value of about 22  $\text{MJm}^{-2}\text{d}^{-1}$  occurred in June and July. During 2007 and 2008 at El Saler, the highest  $R_g$  compared to other rice paddy sites was recorded; it ranged from about 14 to 29  $\text{MJm}^{-2}\text{d}^{-1}$ . The maximum  $R_g$  between 24  $\text{MJm}^{-2}\text{d}^{-1}$  to 29  $\text{MJm}^{-2}\text{d}^{-1}$  occurred in May and June, followed by a gradual decline to about 14  $\text{MJm}^{-2}\text{d}^{-1}$  until the end of the growing season. The average air temperatures ( $T_a$ ) generally increased after the start of growing season and

decreased again at the time of senescence, ranging from 13 to 29 °C on average for the 10-day intervals (Fig. 4.1). Mean  $T_a$  of the growing season was about 20 °C at HK, about 25 °C at

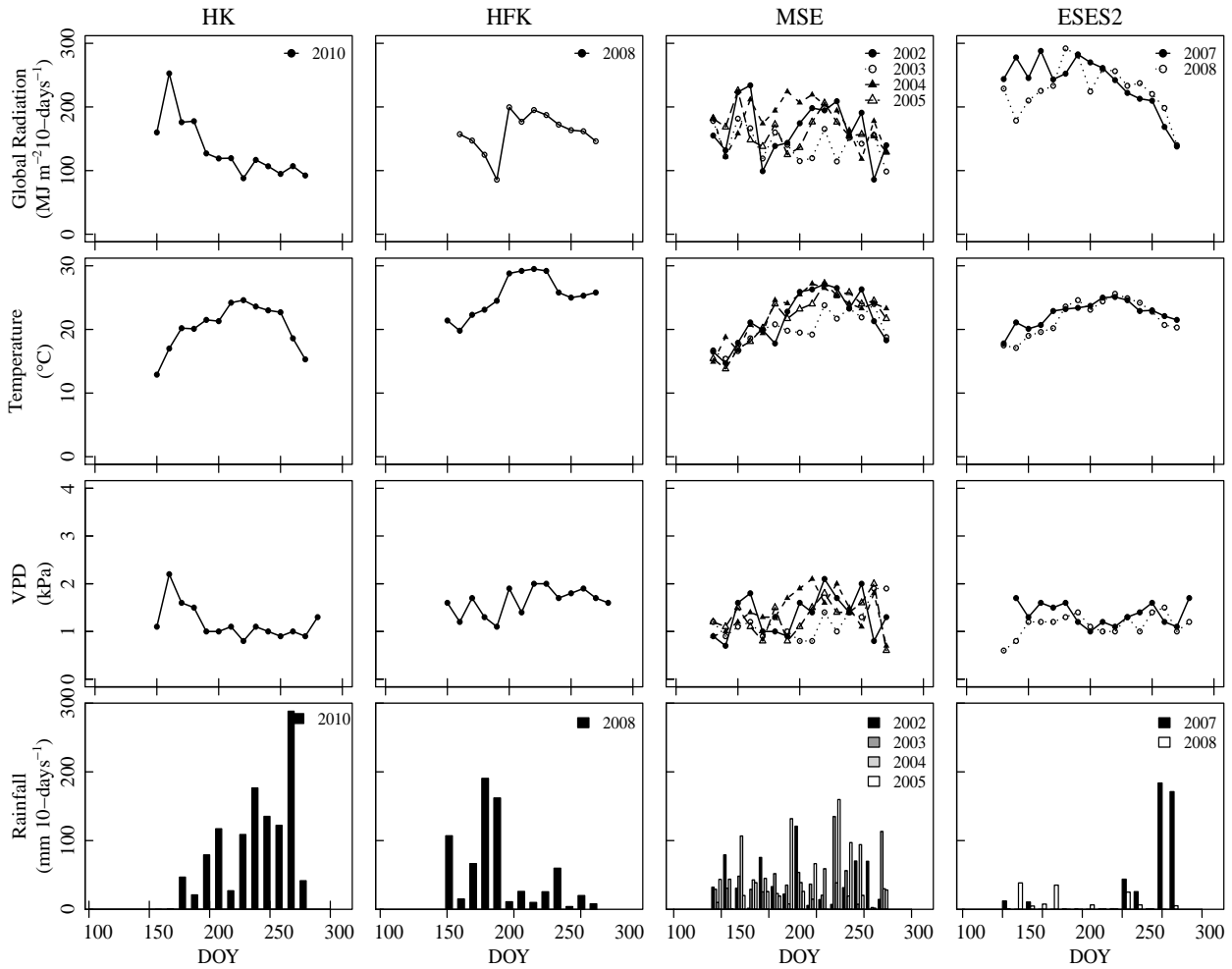


Fig. 4.1 Seasonal time courses for meteorological variables measured at rice paddy sites that potentially influence GPP, i.e., can be considered driver variables for plant response as it affects carbon uptake, crop growth and primary production. Total global radiation ( $R_g$ ), mean air temperature ( $T_a$ ), mean maximum vapor pressure deficit (VPD), and total rainfall are given for 10-day intervals during the growth period for all rice paddy study sites. General site characteristics are given in Table 3.1. HK = Haeon (S. Korea), HFK = Haenam (S.Korea), MSE = Mase (Japan), and ESES2 = El Saler-Sueca (Spain).

HFK, ca. 22 °C at MSE, and about 22 °C at ESES2.

The patterns and magnitudes of daily maximum VPD over the 10-day period were different among the sites. VPD of HK during 2010 reached a maximum of about 2.2 kPa in the early growing season, gradually declined until July around DOY 200, and remained constant (1 kPa) until the end of the growing season. VPD of HFK fluctuated during May, June, and July, increased to the maximum of 1.2 kPa in August, and decreased to 0.8 kPa at the end of the

measurement period. Unlike HK and HFK, VPD of MSE fluctuated during the growing season, ranging from 0.7 to 2.1 kPa. VPD of ESES2 during 2007 was large (about 1.7 kPa) at the beginning of the growing season, and decreased to about 1 kPa in July and remained relatively constant until the end of the growing season. VPD in ESES2 during 2008 rose from 0.6 to 1.2 in the early growing season in May and remained around 1.2 kPa throughout the measurement period. In the case of rice paddies, the sensitivity of GPP to VPD variation was not high due to the rice paddy fields maintaining relatively humid conditions. Water vapor deficit did not appear to be a limiting factor for gas exchange.

Total precipitation during the growing season varied from 121 to 1351 mm among the sites (Table 3.1, Fig. 4.1). The sites in Asia (HK, HFK, and MSE) recorded total precipitation from 545 mm up to 1351 mm associated with the summer monsoon, which was much greater precipitation than at the European site, ESES2 (121 – 437 mm). Especially, HK and HFK showed the largest total precipitation among the sites due to the intensive rainfall and typhoons associated with changma (see Kwon et al., 2010), i.e., 1165 mm of which 36% occurred in August (HK in 2010) and 706 mm of which 30% occurred in June (HFK in 2008). The total precipitation of MSE in 2002 – 2005 ranged from 545 to 647 mm during the growing season. The total precipitation at ESES2 was 437 mm in 2007 and 121 mm in 2008. The major portion of the total precipitation in 2007 was contributed by two precipitation events in September (DOY 260 – 273) which resulted in 184 mm and 171 mm of rainfall.

## 4.2 LAI development

Fig. 4.2 shows the seasonal change in LAI. LAI of rice paddies showed a similar seasonal change among all sites, i.e., increasing rapidly at the beginning of the growing season to a peak in mid-summer (DOY 200 – 224) and decreasing from the peak until the end of the growing season.

The maximum LAI observed at the rice paddies ranged from 4.4 to 6.1 in July and August (DOY 200 – 224). In the case of MSE, the magnitude of maximum LAI ranged from 4.4 to 5.5, but differences in the time of achieving maximum were apparent, i.e., the maximum LAI occurred on DOY 204 in 2002, 224 in 2003, 209 in 2004, and 207 in 2005. Canopy development as viewed from the changes in LAI of ESES2 during 2008 was about 10 days later than during 2007.

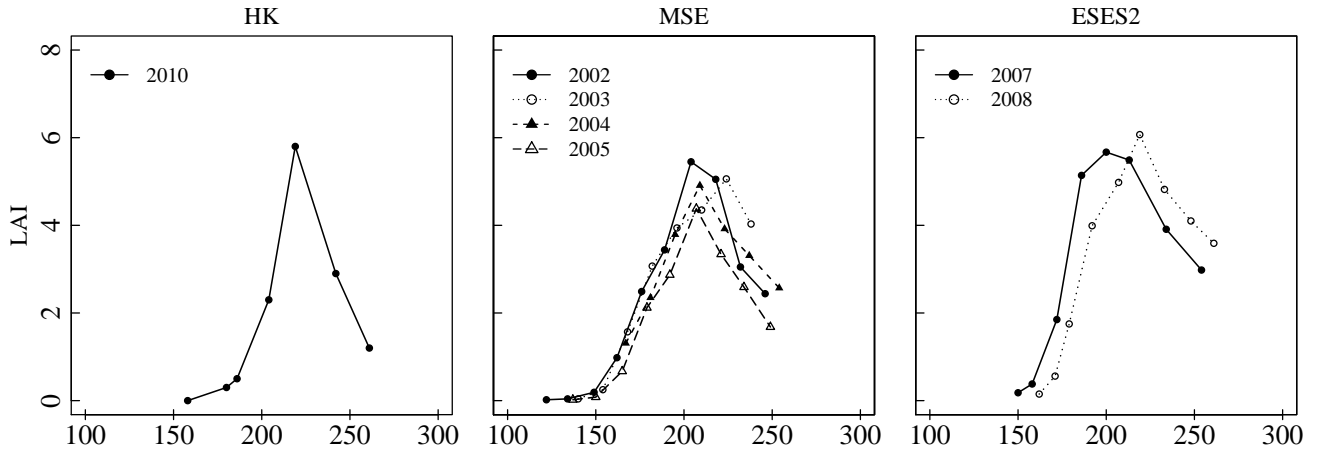


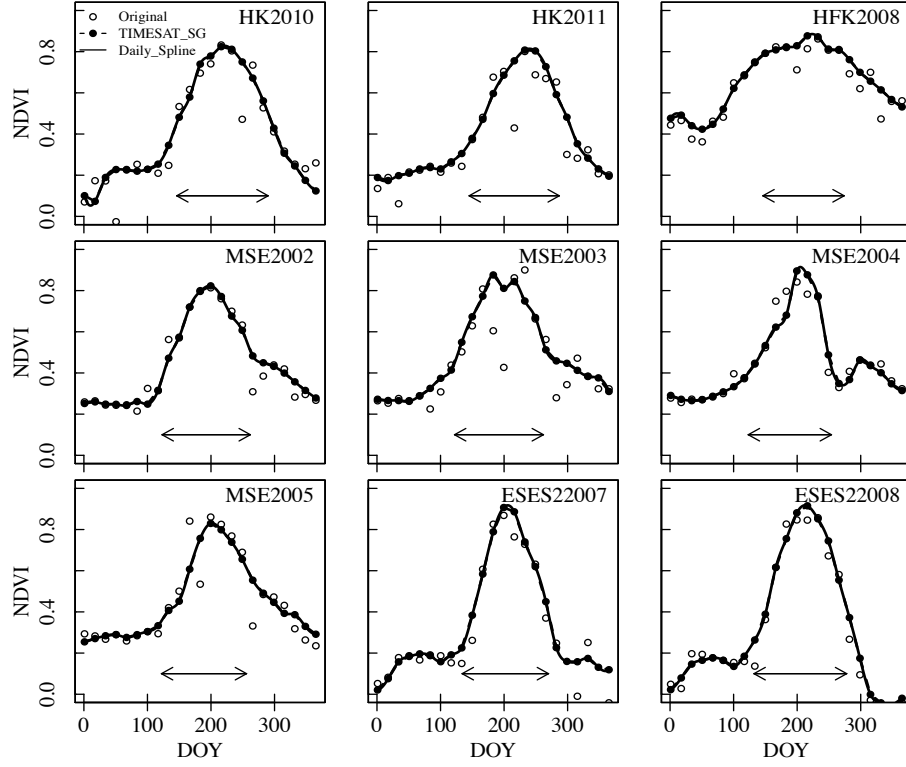
Fig. 4.2 Seasonal time courses in the years indicated for change in leaf area index (LAI) of the studied rice paddies. HK = Haeon (S. Korea), HFK = Haenam (S.Korea), MSE = Mase (Japan), and ESES2 = El Saler-Sueca (Spain).

Considering from Fig. 4.1 the factors possibly responsible for the observed variation in canopy development, the level of radiation input and temperature during the early growing season may be important in determining the time course of plant growth and canopy gas exchange.

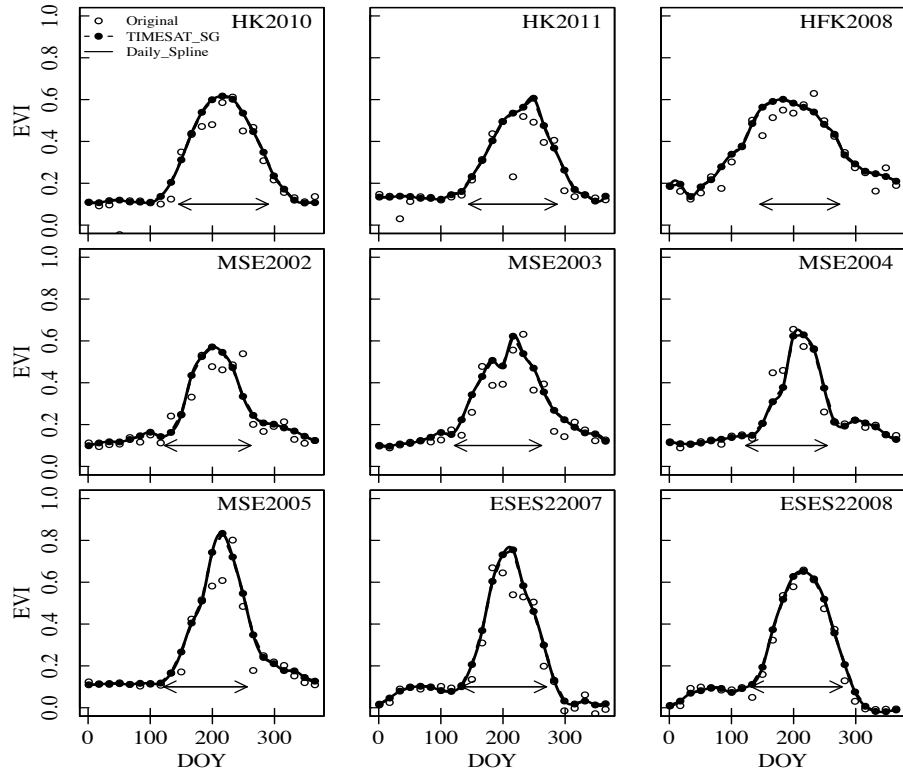
### 4.3 Dynamics of vegetation indices

Fig. 4.3 illustrates both the annual and the seasonal patterns from planting to harvest of rice paddy site downloaded VIs from the MODIS data base, the smoothed VIs (i.e., TIMESAT processed), and the interpolated daily VIs. The arrows in the figure identify the period from the planting to harvest time at the specific location where eddy covariance data were obtained. Nevertheless, it should be remembered that the footprint of the measured fluxes changes, and that field observations of growth can be at times be better or worse in terms of linkage with the fluxes. The VI values as well may vary with respect to their ability to accurately reflect changes at the eddy covariance sites (cf. section 3.1.1.1 for details with respect to measurements at Haeon).

Nevertheless, the growth period patterns in downloaded NDVI and EVI of rice paddy sites were similar, increased in April and May as growing season began, and decreased in September and October as senescence, maturation of the rice, and harvests occurred. An exception is found for HFK during 2008 where the VIs increased before rice planting and decreased primarily after harvest. As a result, NDVI during the growth period at this site was relatively constant, while EVI exhibited a slow decrease.



(a) NDVI, TIMESAT NDVI, and daily NDVI



(b) EVI, TIMESAT EVI, and daily EVI

Fig. 4.3 MODIS vegetation indices for (a) NDVI and (b) EVI for the years indicated. HK = Haeon (S. Korea), HFK = Haenam (S.Korea), MSE = Mase (Japan), and ESES2 = El Saler-Sueca (Spain). Symbols indicate original VI data downloaded from the database (open circles), VI smoothed by TIMESAT method (closed circle), and estimated daily VI (solid line) from spline interpolation. The arrows below the NDVI/EVI values indicate the period of rice growth at each site.

Due to this clear difference, the information obtained from HFK during 2008 must be treated with care or must be eliminated from the analysis. HFK is followed further here because it is important in terms of Korean national rice production, and similarities or differences in comparison to other EC sites are of interest.

The NDVI from Asia rice paddy sites (HK, HFK, and MSE) were more scattered than those of ESES2 during the summer monsoon season (DOY 152 – 243) due to the influence of frequent cloud cover and dense water vapor in the air. This scatter has an influence on subsequent analyses that define the smoothed curves and the estimated daily VIs. It must be kept in mind that the statistical methods to obtain the seasonal curves does not necessarily provide correct data for the crops and that processing of the scattered observations may negatively affect the sought after relationship between VIs and LAI or  $V_{c_{\text{uptake}}}$ . For example, the scattering of data for MSE during 2003 results in a double peak in mid-summer which is an artifact. Deviations occurred in the magnitude of VI change during the growth season. Similar values of VIs occurred early in the year (DOY 1 – 100) at all sites except HFK. NDVI at planting varied between 0.2 and 0.4, while EVI varied between 0.1 and 0.2. The maxima for NDVI varied between 0.8 and 0.9, while maxima for EVI were between 0.6 and 0.8.

## 4.4 LAI estimation

### 4.4.1 Estimating LAI from the seasonal course of VIs

#### 4.4.1.1 Relationship between ground-measured LAI and VIs

To link time dependent change in ground-based LAI measurements to VIs, linear and exponential relationships between the measured LAI and VIs were examined. The linear relationship is not included in the results presented, since the exponential model in general provided better explanation. The statistical results of both the linear and exponential relationships are provided in the Appendix A (Table A.1 and Table A.2). The utility of the exponential model was studied further, since it has been often used to describe time dependent change in LAI (e.g., Pontauiller et al., 2003; Lu et al., 2004 and 2005; Fan et al., 2008).

Leaf area development was considered with respect to two phases: the vegetative phase with increasing LAI from the beginning of the growing season (DOY 120 – 144) to the maximum leaf expansion in mid-summer (DOY 180 – 220) and the flowering and reproductive phase with decreasing LAI from midsummer to the harvest period (DOY 250 – 290). This was undertaken in order to adjust for the biochemical and physiological changes in leaf function during these phases (Muraoka and Koizumi, 2005 and 2007), and with the expectation that regulation of protein and pigment synthesis is most likely altered when the growth of rice grains compete for plant resources. In order to assess these changes, two analyses, i.e., one that considers data obtained over the entire growing season (E) and another one that considers partial data from the two seasonal periods, i.e., the increasing phase in LAI (B) and the decreasing phase for LAI (A).

Fig. 4.4 shows the relationships between measured LAI and VIs for the entire growing season (E) at the respective rice paddy sites, HK (in 2010), MSE (from 2002 to 2005), and ESES2 (from 2007 to 2008). In all cases, the measured LAI was exponentially and positively correlated with NDVI and EVI. Overall, the relationship between LAI and NDVI was stronger than EVI with  $R^2 > 0.6$  and  $RMSE < 1.63$ . At MSE and ESES2, where multiple years of data are included, greater scatter is found in the relationship than when individual years are analyzed (cf. HK for 2010). Additional factors influence the relationship between measured LAI and the VIs, reducing the goodness of fit and modifying the shape of the predicted relationship. One factor

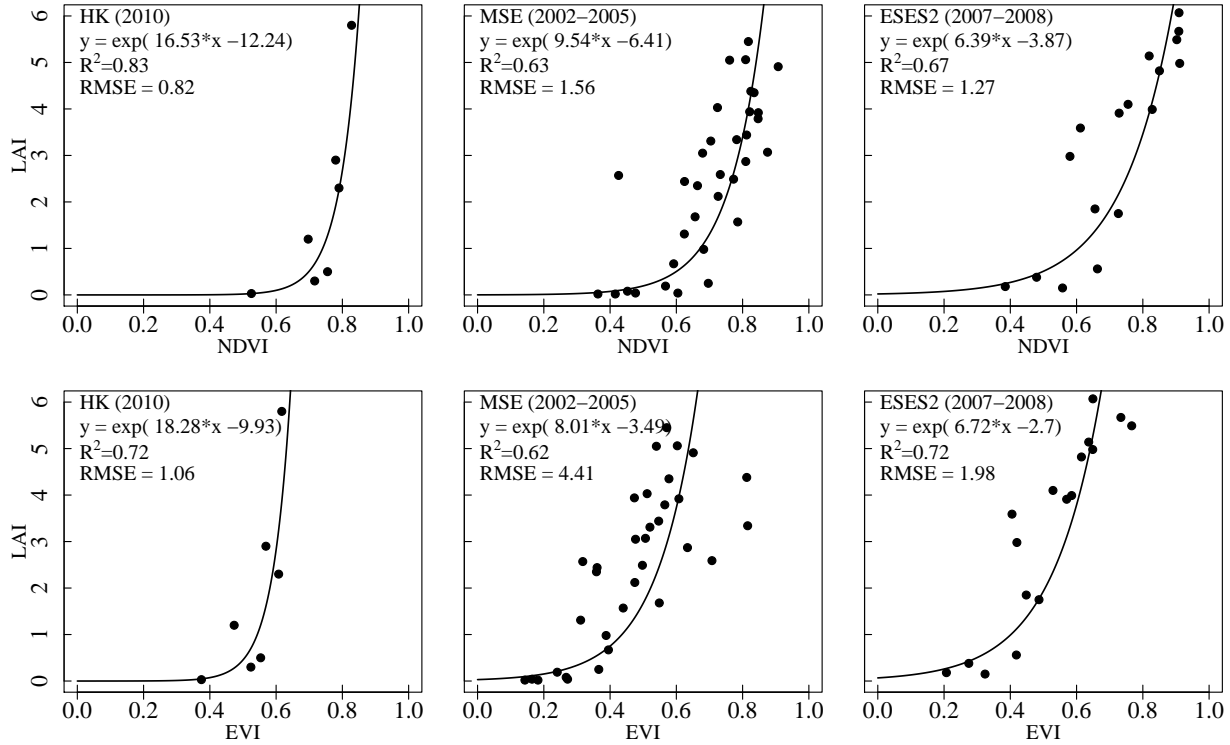


Fig. 4.4 The relationship between measured LAI and NDVI or EVI for the years indicated and utilizing data from the entire growing season. HK = Haeon (S. Korea), MSE = Mase (Japan), and ESES2 = El Saler-Sueca (Spain). The solid line indicates the exponential equation established for the relationship as described in the text. The coefficients,  $R^2$  of the regression, and root mean square error (RMSE) are given.

that possibly could play a role is the seasonal phenological development which could vary from year to year. This is tested by separating the season into two phases as described above.

Fig. 4.5 shows the relationship between LAI and NDVI for the two respective growth phases before (B, left panel) and after (A, right panel) maximum NDVI. It is quite apparent that a different correlation is found during the increasing versus the decreasing phase of LAI changes. The increasing phase represents the most active vegetative/growth period, which was associated with LAI increase from 0 to 6, and NDVI changes between 0.3 and 0.9. The decreasing phase describes the reproductive stage associated with panicle initiation and flowering (Xiao et al., 2002). During this phase, LAI changed from 6 to 2, while most of the points of NDVI ranged between 0.9 and 0.6. Among the sites, the relationship between LAI and NDVI in the increasing phase exhibited much higher  $R^2$  between 0.84 and 0.90 and lower RMSE between 0.84 and 1.21 in comparison to results with data over the entire season. In the decreasing phase, the few observations at the HK site do not support statistical analysis or further conclusions. However,

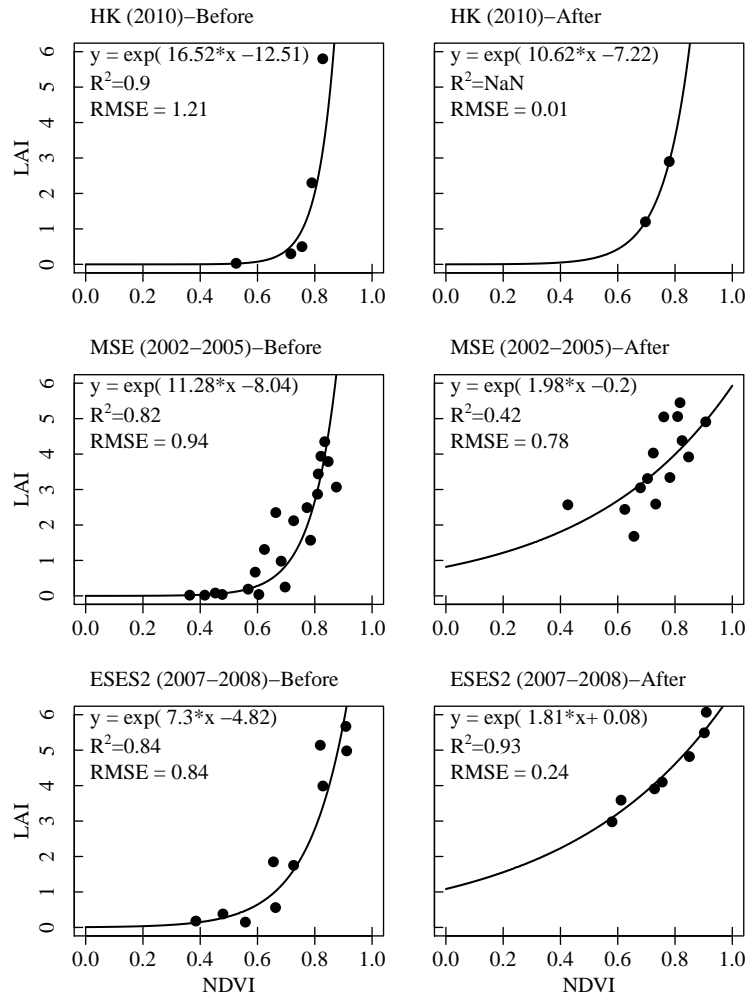


Fig. 4.5 The relationship between measured LAI and NDVI for the years indicated where the data are separated into two phases, e.g., until maximum VIs are reached (Before) and after maximum VIs are attained (After). HK = Haeon (S. Korea), MSE = Mase (Japan), and ESES2 = El Saler-Sueca (Spain). The solid line indicates the exponential equation established for the relationship as described in the text. The coefficients,  $R^2$  of the regression, and root mean square error (RMSE) are given.

the regression for MSE and ESES2 are quite similar and demonstrate how late season phenology influences the analyses shown in Fig. 4.4.

LAI and EVI relationships for the period before (B) and after (A) peak EVI are shown in Fig. 4.6. There was large data scatter in the relationship between measured LAI and EVI, hence weaker explanation than obtained with the LAI vs. NDVI relationship. LAI vs. EVI was a good predictor for the HK site, however, there was no significant improvement. Considering the late season relationship with NDVI or EVI, less exponential tendency was found than during the increasing phase and a linear relationship may even be acceptable. It is concluded that NDVI is a better predictor of season changes in rice LAI than EVI.

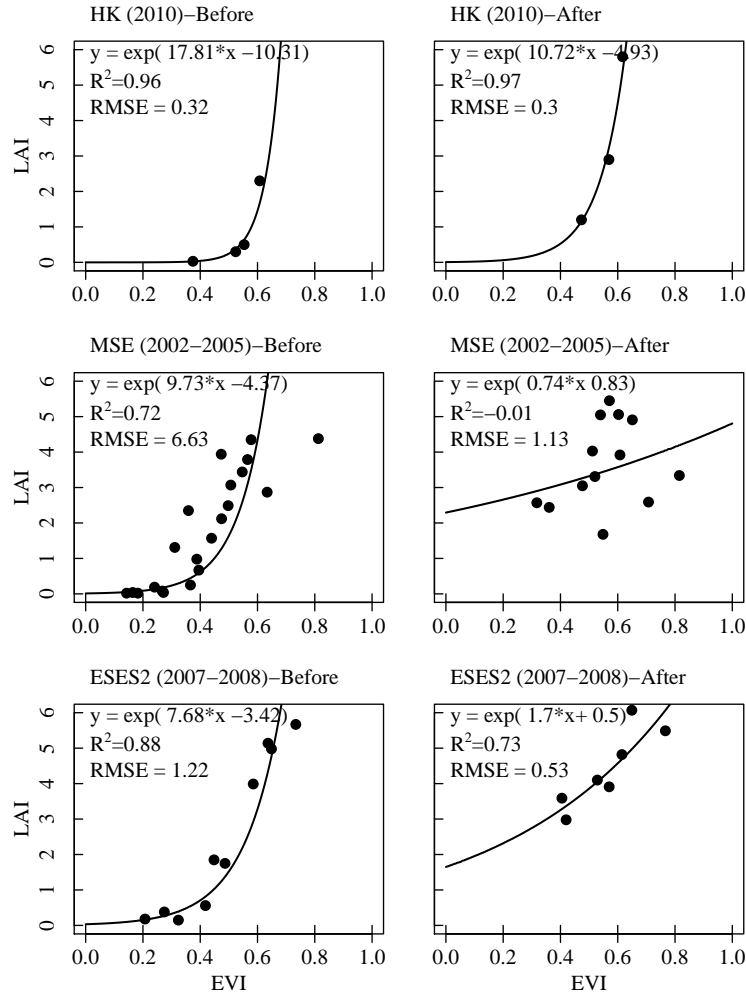


Fig. 4.6 The relationship between measured LAI and EVI for the years indicated where the data are separated into two phases, e.g., until maximum VIs are reached (Before) and after maximum VIs are attained (After). HK = Haeon (S. Korea), MSE = Mase (Japan), and ESES2 = El Saler-Sueca (Spain). The solid line indicates the exponential equation established for the relationship as described in the text. The coefficients,  $R^2$  of the regression, and root mean square error (RMSE) are given.

Since it is desirable to establish relationship between VIs and LAI that are generally applicable or “universal” rather than site specific, the conclusions reached above with respect to individual sites were examined further by pooling the data for Asian sites and all sites (including the Mediterranean site in Spain).

During the summer monsoon in the Asian region, the remotely sensed vegetation indices were influenced by frequent cloud cover and high water vapor density in the air. For this reason, Asian rice paddy sites were first treated separately. Fig. 4.7 shows the relationship between LAI and VIs for the Asian sites (HK and MSE) and for all rice paddy study sites combined (HK, MSE, and ESES2) and for years with data acquired over the entire growing season. The LAI –

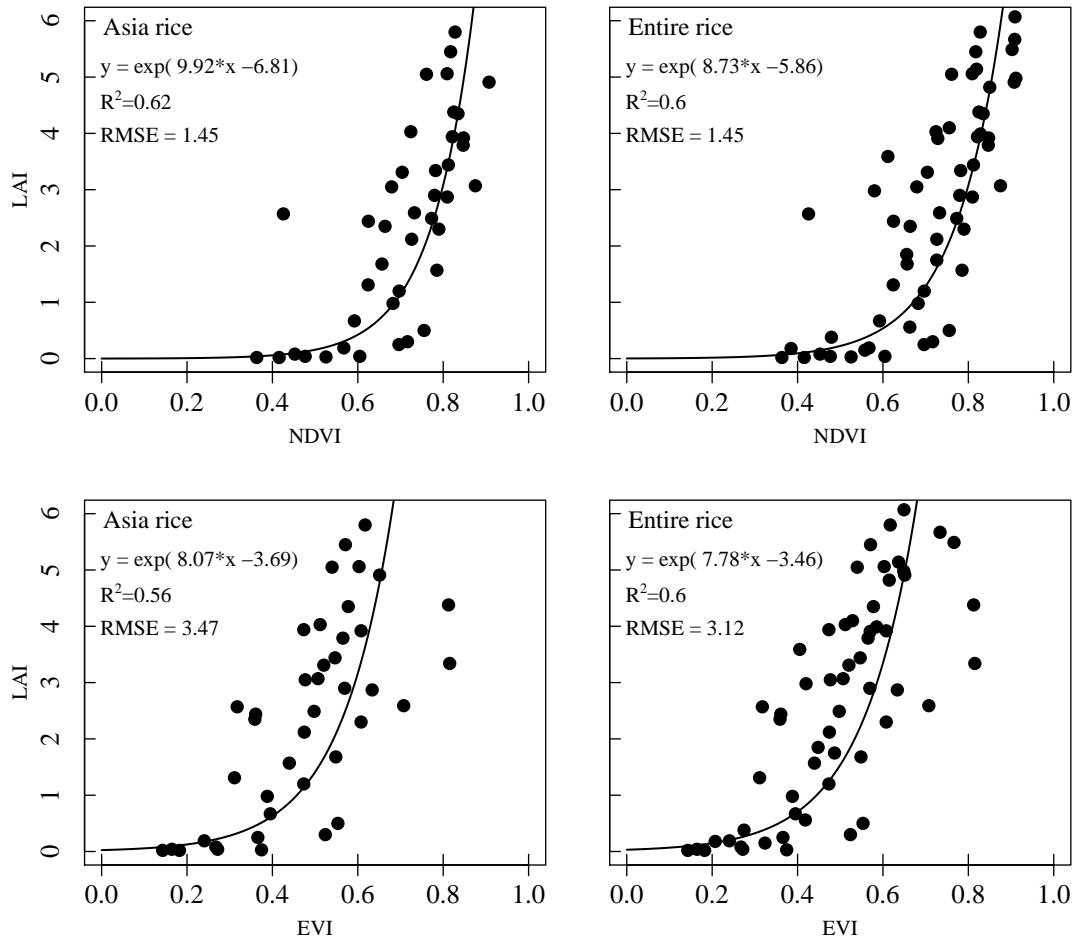


Fig. 4.7 The pooled relationships between measured LAI and NDVI or EVI utilizing data from the entire growing season. The regression for Asian sites includes the data from HK and MSE shown in previous figures, while the regression for the entire complement of sites adds in the observations from ESES2. The solid line indicates the exponential relationship established for the relationships as described in the text. The coefficients,  $R^2$  of the regression, and root mean square error (RMSE) are given.

NDVI relationship for the Asia rice paddies was very strong, with an  $R^2$  of 0.62 and RMSE of 1.45. The combined rice paddy sites also showed reasonably strong correlation, with  $R^2$  of 0.60 and RMSE of 1.45. The LAI-NDVI relationships exhibited better correlations than the LAI-EVI relationships. Fig. 4.8 shows the BA relationships for separate Asia and combined rice paddy study sites, respectively. The LAI-NDVI relationship showed good agreements in the increasing phase ( $R^2$  above 0.76 and RMSE below 1.03), but a relatively poor exponential tendency in the decreasing phase ( $R^2$  above 0.27 and RMSE below 0.93). The general conclusions are the same as for individual sites. Separating the seasonal phases provides a better explanation of LAI changes.

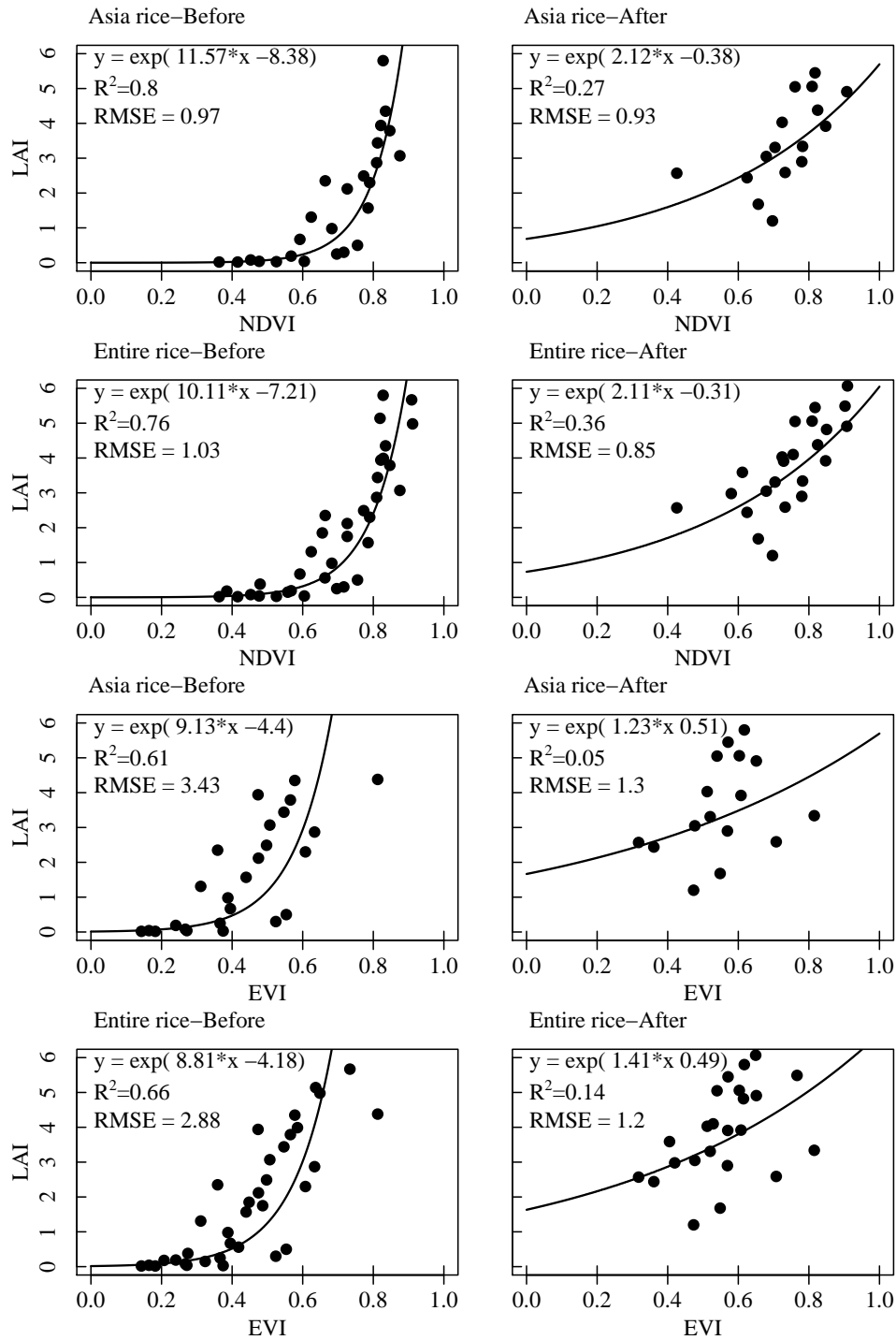


Fig. 4.8 The pooled relationships between measured LAI and NDVI or EVI where the data are separated into two phases, e.g., until maximum VIs are reached (Before) and after maximum VIs are attained (After). The regression for Asian sites includes the data from HK and MSE shown in previous figures, while the regression for the entire complement of sites adds in the observations from ESES2. The solid line indicates the exponential relationship established for the relationships as described in the text. The coefficients,  $R^2$  of the regression, and root mean square error (RMSE) are given.

The LAI-EVI relationship was relatively scattered, overall NDVI was a better and more accurate predictor for LAI than EVI. There was no convincing reason to consider results from

the Asian sites as different from the case where all available data were pooled.

#### 4.4.1.2 Estimation of seasonal LAI

The LAI-NDVI relationships from Figs. 4.7 and 4.8 were next tested to determine their utility in reproducing the measured seasonal changes in LAI. Separating the season into two phases, led to the result that abrupt changes in LAI occurred during the transition from B to A in mid-season. Additionally, the performance of these equations with respect to reproducing measured time courses was not better than obtained with the exponential relationship using data over the entire season (Fig. 4.7).

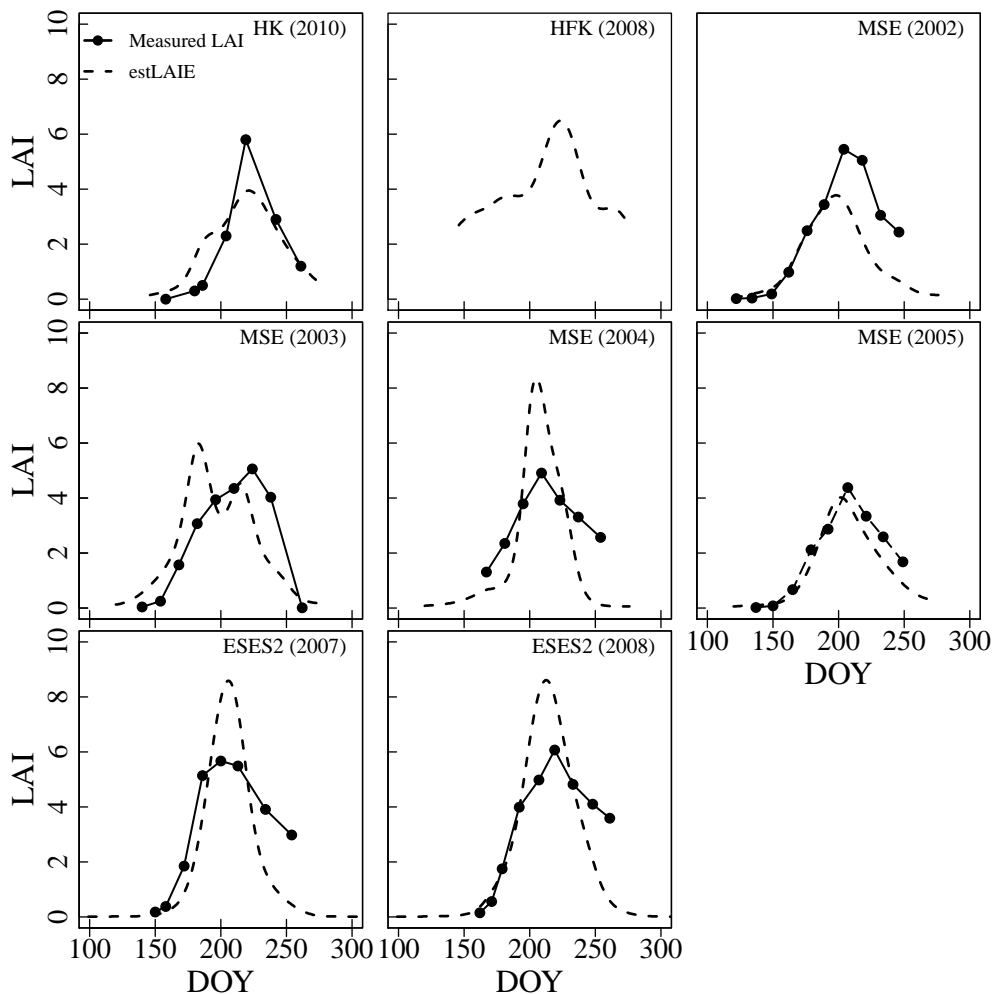


Fig. 4.9 Daily measured LAI (closed circle with solid line) and estimated LAI (dashed line) at rice paddies for the years indicated. HK = Haeon (S. Korea), MSE = Mase (Japan), and ESES2 = El Saler-Sueca (Spain). Estimates are calculated with an exponential fit to pooled data from all rice paddy sites, using observations over the entire season (upper right panel in Fig. 4.7)

Daily LAI over the growing season was best estimated by the exponential relationship between LAI and NDVI for the pooled rice paddy sites (hereafter referred to as LAI \_EN \_exp;

Fig. 4.9). There were no observation data for LAI in HFK during 2008, hence the data shown in Fig. 4.9 are only estimated LAI. Estimated LAI ranged from 0 to 8.6. As shown in the figure, LAI was underestimated for HK during 2010 and MSE during 2002, and overestimated for MSE during 2004, ESES2 during 2007 and 2008. LAI was overestimated at the beginning of the growing season and underestimated at the end of the growing season for MSE during 2003. LAI was accurately estimated for MSE during 2005. The timing of the peak in LAI was acceptable in comparison to the peak of the measured LAI (within  $\pm 3$  to 6 days). There were bi-annual peaks for MSE during 2003 (DOY 183 and 215), the second peak occurring 9 days after the peak of measured LAI.

The large deviations between measured and predicted LAI that occur over the season indicate that the scatter in data shown in Fig. 4.7 make it extremely difficult to use the seasonal exponential relationship to predict LAI across rice paddy sites. The different seasonal patterns in the deviations mean that further use of LAI values together with the PIXGRO model will lead to unpredictable influences in the estimation of GPP. According to Haboudane et al. (2002), Fan et al. (2008), Potitthep et al. (2010), the relationship between LAI and NDVI assumes an exponential tendency in most cases. However, most of these previous studies focus on single or more localized sites. In cases where the study locations are spread geographically in different climate regions and where year to year climate variation occurs such simple relationships may not apply. Therefore, an attempt to identify a better approach was undertaken that is based on similarities or consistencies in the developmental processes of the rice crop.

#### 4.4.2 Estimation of LAI according to consistent phenological development

A general growth curve for rice across the study sites was established with the general additive model (GAM: Hastie, T. J. and Tibshirani, R. J., 1990), which explains the LAI change in relation to the maximum LAI, as determined for the sites via the maximum in NDVI (Fig. 4.10). After determining NDVI maximum, observed LAI values were plotted on a time scale in terms of days before the maximum (negative values) or after maximum (positive values). The function is scaled from 0 to 1 by dividing all observation values for LAI by the maximum value measured.

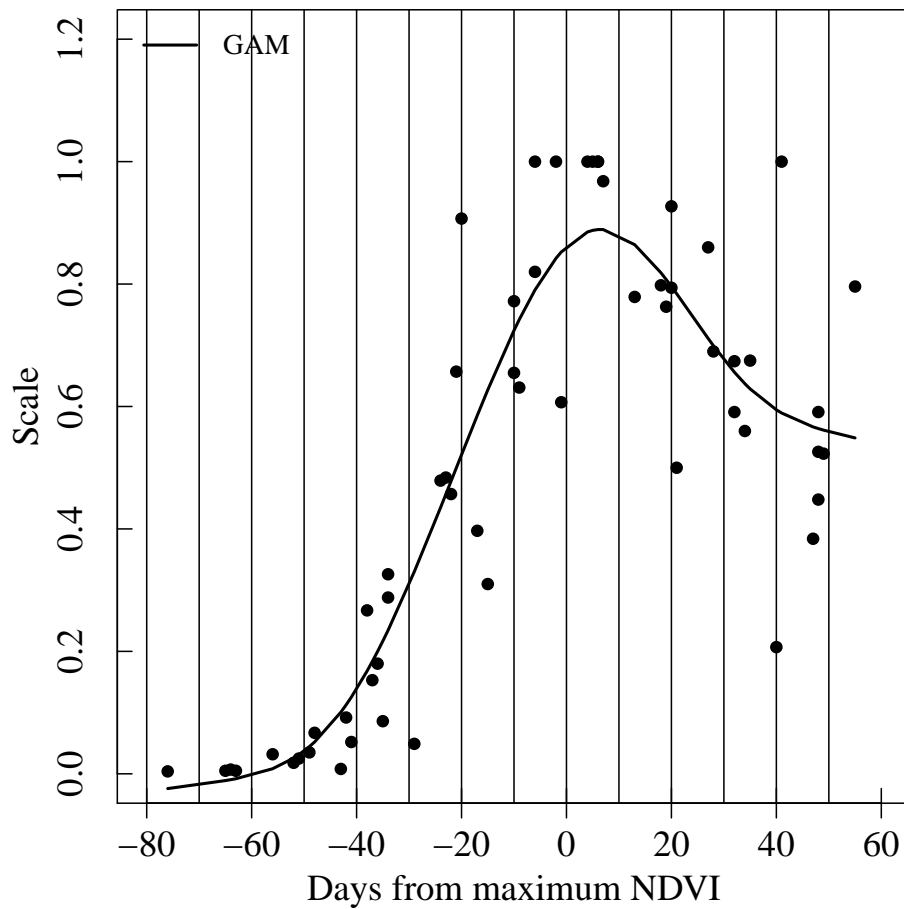


Fig. 4.10 A scaled general growth scale curve utilizing data from all rice paddy sites. The scaling results by dividing LAI observations by maximum LAI. The black closed circles indicate the relationship between the scaled LAI and DOY based on time shifts according to maximum NDVI. The solid line indicates the general growth curve determined with the generalized additive model (GAM).

As shown in Fig. 4.10, the rice LAI at all sites slowly increased about 80 days before the maximum NDVI (Day 0) and rose rapidly from 40 days before Day 0 to Day 0. The maximum in scaled of rice LAI occurred between Day 0 and 10 days after Day 0. A relatively slow decrease occurred after this peak. A general seasonal change in LAI may be estimated for each site by multiplying daily values of the curve in Fig. 4.10 by the average maximum LAI observed at all sites. The timing depends on planting and management of the rice crop. LAI development at specific sites is obtained by shifting the daily values according to DOY of the maximum NDVI at the site (Fig. 4.11). The estimated LAI obtained with this method ranged from 0 to 5.3 and the seasonal patterns in LAI were reproduced relatively well across all rice paddy sites.

The method using the LAI consistent development curve to estimate LAI has a limitation

Table 4.1. Statistics for the correlation between measured LAI and estimated LAI comparing the exponential model (Fig. 4.9) and the LAI consistent development curve method (Fig. 4.11).  $R^2$  is the determination of coefficient, RMSE is root mean square error, and CV is coefficient of variation.

Site	Year	LAI by consistent development curve			LAI by the exponential model		
		$R^2$	RMSE	CV (%)	$R^2$	RMSE	CV (%)
HK	2010	0.70	1.02	71.38	0.82	0.87	53.85
MSE	2002	0.90	0.29	30.01	0.73	1.09	60.79
MSE	2003	0.71	0.41	47.80	0.54	0.59	62.40
MSE	2004	0.87	0.17	31.25	0.71	0.50	70.37
MSE	2005	0.90	0.70	57.02	0.91	0.32	31.83
ESES2	2007	0.96	0.40	46.33	0.79	0.20	87.12
ESES2	2008	0.97	0.38	40.80	0.83	0.15	85.42

due to use of the average maximum LAI value. However, the estimated LAI was much better than obtained with the exponential model as shown in Table 4.1. Therefore, this method was used in further analysis of the eddy covariance flux data from the rice sites. Despite deviations from measurement, the curve in Fig. 4.10 and time courses in Fig. 4.11 were assumed applicable. This step is important in working toward a method for predicting GPP universally across the rice paddy sites.

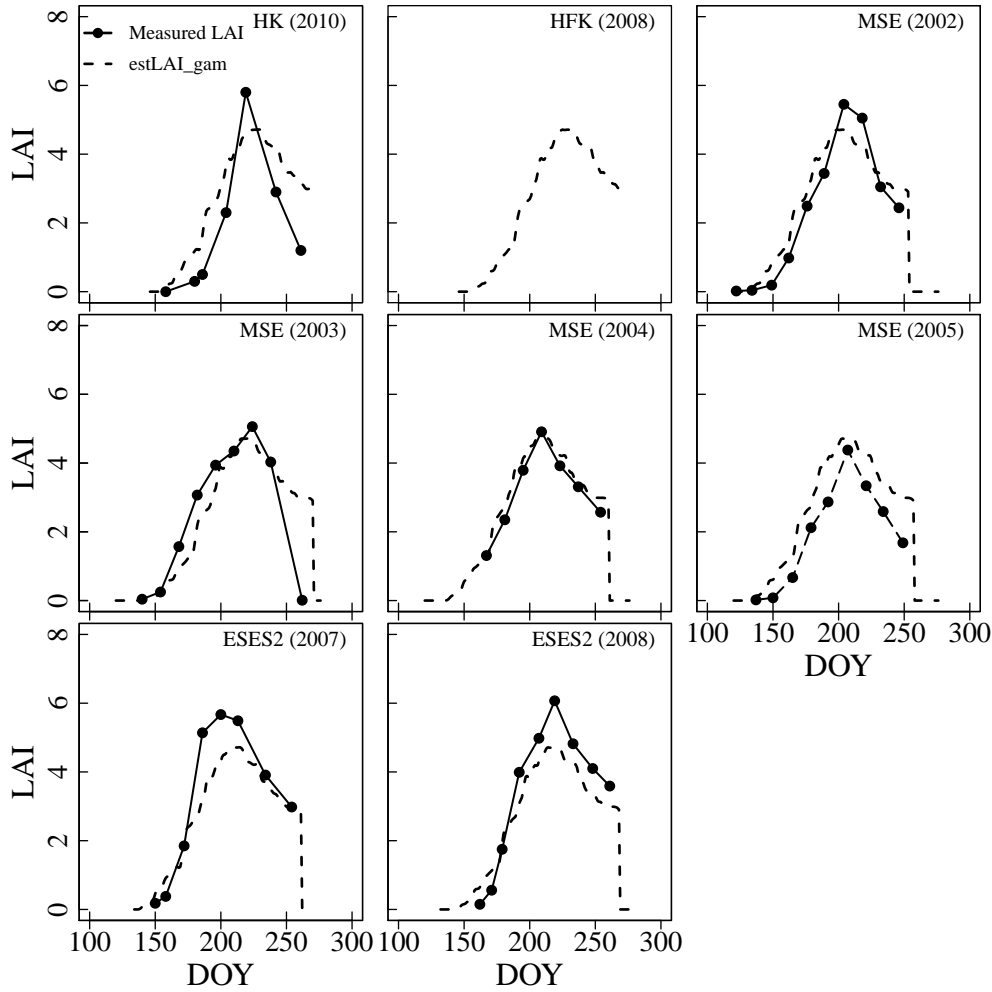


Fig. 4.11 Daily measured LAI (closed circle with solid line) and estimated LAI (dashed line) obtained with the consistent phenological development approach (see text for stepwise procedure) at rice paddy sites for the years indicated. HK = Haeon (S. Korea), HFK = Haenam (S. Korea), MSE = Mase (Japan), and ESES2 = El Saler-Sueca (Spain).

## 4.5 $V_{c_{\text{uptake}}}$ estimation by NDVI

Having established a reliable that allows estimation of the seasonal course of LAI across sites, the influence of differences between measured vs. predicted LAI on estimation of carboxylation capacity was tested. The seasonal change of carboxylation capacity ( $V_{c_{\text{uptake}}}$ ) is illustrated in Fig. 4.12 as determined by both the measured LAI ( $V_{c_{\text{uptake\_org}}}$ ) and the estimated LAI ( $V_{c_{\text{uptake}}}$ ). The seasonal pattern of  $V_{c_{\text{uptake\_org}}}$  increased rapidly and in a characteristic manner after planting, reached a maximum in most cases at ca. DOY 170 to 180 and then decreased slowly during further development and later senescence of the rice crop. It should be noted that the results apply only during the period where  $\text{LAI} > 1.0$  and where  $V_{c_{\text{uptake}}}$  can be determined with relatively high certainty as discussed under methods (Section 3.2).

Table 4.2. Statistics for the linear correlation between  $V_{c_{\text{uptake\_org}}}$  and  $V_{c_{\text{uptake}}}$ .  $a$  is a slope,  $b$  is a intercept,  $R^2$  is the coefficient of determination, RMSE is root mean square error, and CV is coefficient of variation.

Site	Year	$V_{c_{\text{uptake}}}$ by consistent phenological development					$V_{c_{\text{uptake}}}$ by the exponential model				
		a	b	$R^2$	RMSE	CV (%)	a	b	$R^2$	RMSE	CV (%)
HK	2010	0.87	-0.92	0.82	7.33	15.97	0.95	0.74	0.85	1.75	3.94
MSE	2002	0.96	0.74	0.95	1.24	2.93	1.08	0.85	0.89	4.58	10.82
MSE	2003	0.95	-0.06	0.86	2.14	5.63	0.90	2.83	0.83	2.20	5.40
MSE	2004	1.01	0.07	0.99	0.51	1.29	1.05	5.35	0.75	6.96	22.45
MSE	2005	0.87	0.74	0.94	5.83	13.18	1.14	0.37	0.93	6.41	17.06
ESES2	2007	1.30	-4.98	0.93	9.93	24.63	1.31	1.71	0.74	17.37	39.53
ESES2	2008	1.09	0.03	0.96	3.20	11.10	1.15	3.13	0.84	8.59	27.00

Approximate maximum values based on measured LAI was  $88 \mu\text{mol CO}_2 \text{ m}^{-2} \text{ leaf area s}^{-1}$  at HK during 2010; 78 in 2002, 70 in 2003, 83 in 2004, and 83 in 2005 at MSE; and difficult to determine for ESES2 due to the high degree of scatter in the data. These results are influenced by the consistency of measurements or homogeneity at the measurement sites. The most homogeneous results were obtained from MSE, where it appeared that carboxylation capacity in 2004 and 2005 was slightly higher than during 2002 and 2003. The values for  $V_{c_{\text{uptake\_org}}}$  also depend on the exact determination of LAI, e.g., the methods that each research group uses during their measurements. Since these influences are impossible to remove, one must conclude that the maximum for  $V_{c_{\text{uptake\_org}}}$  may be ca. 80 to  $85 \mu\text{mol CO}_2 \text{ m}^{-2} \text{ leaf area s}^{-1}$ . The consistent results at MSE demonstrate that  $V_{c_{\text{uptake\_org}}}$  after maximum may decrease differently depending on climate or other factors. Data from MSE in 2004 and 2005 exhibited a more rapid decrease than in 2002 and 2003 during the senescence period. The scattered data from ESES2 must occur due to day to day changes in the measured fluxes, since LAI changes from day to day were essentially zero. The cause of such changes is unclear.

Comparisons of  $V_{c_{\text{uptake}}}$  obtained with LAI from the consistent phenology development model as well as the commonly used exponential-curve based model are given in Table 4.3.  $V_{c_{\text{uptake}}}$

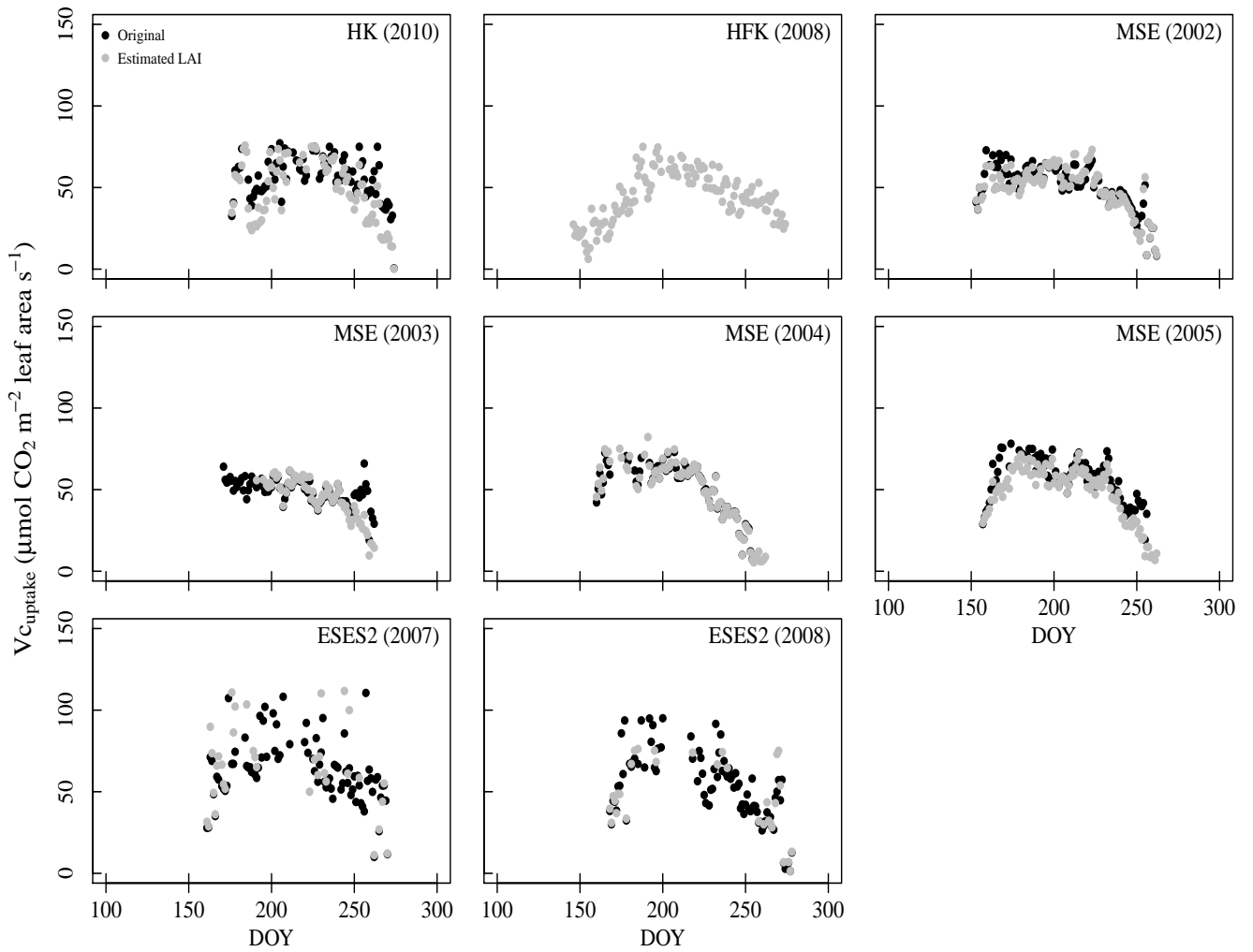


Fig. 4.12 Seasonal change of  $V_{c_{\text{uptake}}}$  obtained with measured LAI ('Original', black closed circle) and with the consistent development LAI-NDVI model, ('estimated LAI', gray closed circle) of rice paddy sites for years indicated. HK = Haean (S. Korea), HFK = Haenam (S.Korea), MSE = Mase (Japan), and ESES2 = El Saler-Sueca (Spain).

obtained with the consistent development model agreed better with the values obtained with measured LAI with respect to  $R^2$ , RMSE and the correspondence with the 1:1 relationship, except at the HK site. Results at HK were, however, also quite good with  $R^2$  of 0.82, RMSE of 7.33, and CV was 16%. The high values of  $R^2$  (above 0.82), low RMSE (below 9.93), and low CV (3-25%) reflect the agreement illustrated in Fig. 4.12 and further demonstrate that LAI obtained by the consistent development method is useful in the estimation of GPP at the study sites.

The remaining question is whether or how well estimated  $V_{c_{\text{uptake}}}$  can be determined from remote sensing in order to provide values along with LAI over the seasonal course of rice plant development to the PIXGRO model. As in the case of measured LAI, correlations of estimated

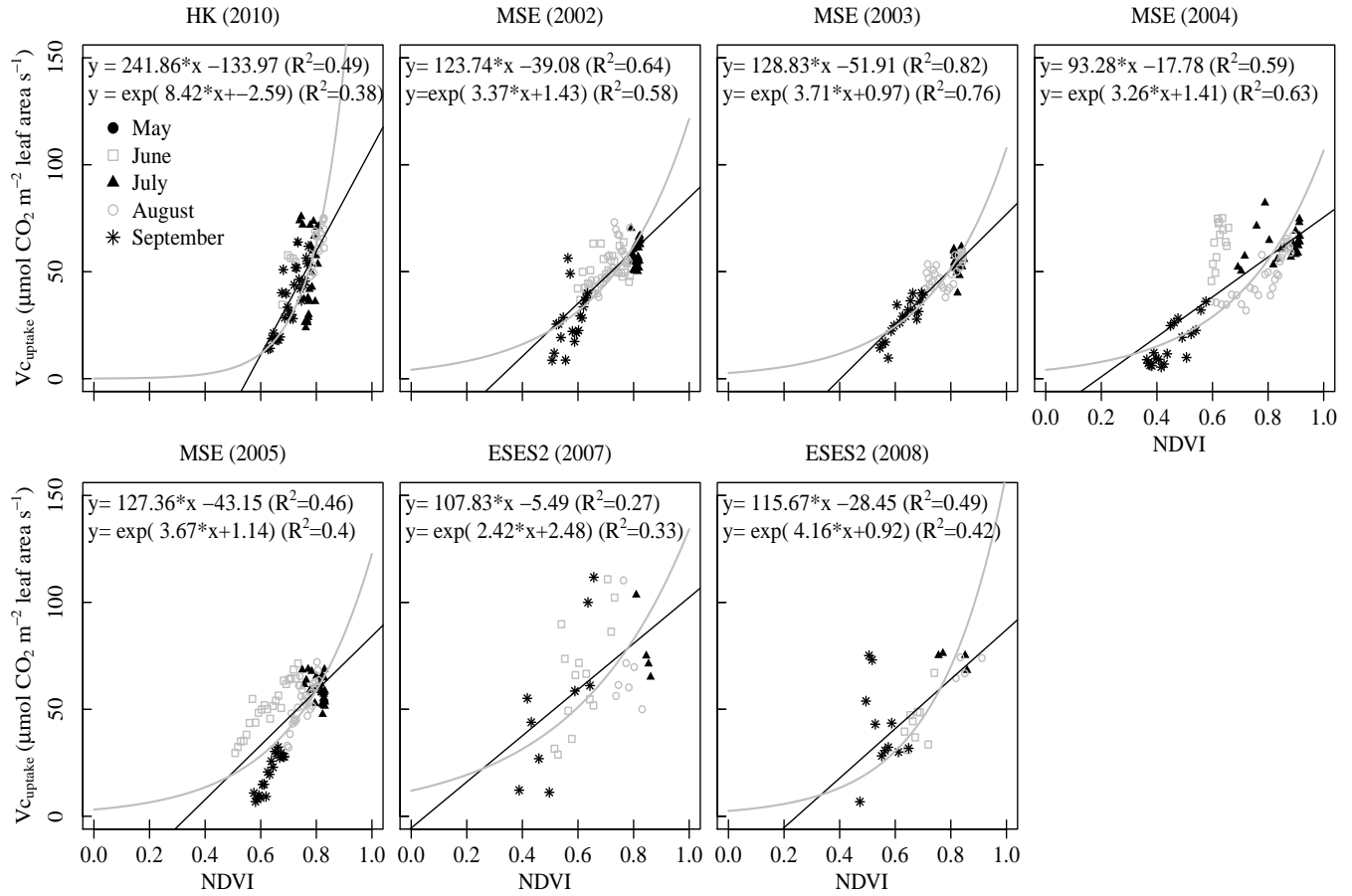


Fig. 4.13 The relationship between  $V_{c_{uptake}}$  and NDVI of rice paddies for the years indicated. HK = Haeon (S. Korea), MSE = Mase (Japan), and ESES2 = El Saler-Sueca (Spain). The correlations may be examined according to each month during the rice growing period, considering the order May (black closed circle), June (open square), July (closed triangle), August (open circle), and September (star). The coefficients and  $R^2$  of the regressions are given.

$V_{c_{uptake}}$  with NDVI and EVI were examined, considering individual sites, Asian sites, and all sites, and using data from entire season or before and after the VI maximum. The tabulated results of these correlations are presented in Appendix A3. It can be concluded that NDVI was in general a better predictor of  $V_{c_{uptake}}$  and, therefore, only there results are discussed here.

Correlation between  $V_{c_{uptake}}$  and NDVI found at individual sites are presented in Fig. 4.13, where different symbols indicate  $V_{c_{uptake}}$  determinations made during different months of the growing season. As seen from the figure, relatively good explanation of the variation was obtained for HK in 2010 and MSE in 2002 and 2003 with either a linear or exponential fit to the data. In the remaining cases, the exponential equation does not appear to approximate the overall scatter that is observed. In all cases (except ESES2 in 2007 where the values are essentially equal), the  $R^2$  values obtained with the linear model are much higher. Thus, a linear model is

Table 4.3. Statistics for the linear correlation between  $V_{c_{\text{uptake\_org}}}$  and  $V_{c_{\text{uptake}}}$  obtained with the best-fit linear model (Fig. 4.14) with the coefficient of determination ( $R^2$ ), root mean square error (RMSE), and coefficient of variation (CV).

Site	Year	$R^2$	RMSE	CV (%)
HK	2010	0.75	8.90	22.77
MSE	2002	0.81	7.17	22.24
MSE	2003	0.67	9.53	28.86
MSE	2004	0.72	5.63	27.98
MSE	2005	0.80	8.88	26.60
ESES2	2007	0.46	21.33	49.06
ESES2	2008	0.72	8.27	33.82

used below in determinations of GPP.

However, it is also apparent from Fig. 4.13 that hysteresis occurs. This is relatively small in HK during 2010 and MSE during 2002 and 2003, but it quite pronounced in the remaining years of MSE observation and at ESES2. Thus, the linear models for prediction of  $V_{c_{\text{uptake}}}$  may be expected overall to over- and under-estimate GPP during particular periods of the season, even through seasonal sums during the period with  $\text{LAI} > 1.0$  may agree well between observed and modeled data. Proceeding on the basis of a linear interpretation of the relationship between  $V_{c_{\text{uptake}}}$  and NDVI, the best-fit model for the pooled rice data is illustrated in Fig. 4.14 with  $R^2$  of 0.38 and RMSE of 14.47.

The predicted values of  $V_{c_{\text{uptake}}}$  using this linear model and seasonal changes in NDVI are shown in Fig. 4.15. Mid- and late season changes in observed and modeled  $V_{c_{\text{uptake}}}$  are in relatively good agreement. Rapid changes during the early season and the peak values for  $V_{c_{\text{uptake}}}$  are less well reproduced. From the overall comparison in Fig. 4.15, it can be hypothesized that seasonal GPP will be underestimated except for MSE during 2002 and 2003. The predicted time dependent changes at HFK are uncharacteristic when considering all other sites. This difference most likely results from the mosaic nature of the site, where the flux footprint and flux data are influenced by other crops or vegetation. This indicates that the results of the study must be applied where large relatively homogeneous locations with rice planting occur.

An alternative approach to describing  $V_{c_{\text{uptake}}}$  is illustrated in Fig. 4.16. As in the case of

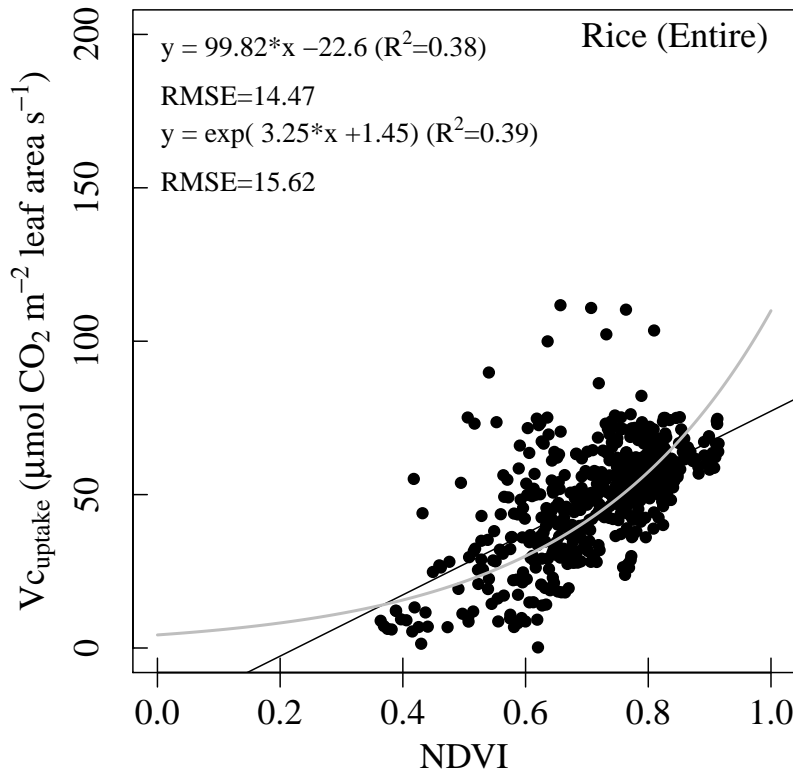


Fig. 4.14 Relationship between  $V_{c_{\text{uptake}}}$  and NDVI utilizing data from the entire growing season.  $V_{c_{\text{uptake}}}$  calculated using estimated LAI from the relationship shown in previous figures. The solid lines indicate the linear equation (black line) and exponential equation (gray line) established for the relationship as described in the text. The coefficients,  $R^2$  of the regression, and root mean square error (RMSE) are given.

LAI (Fig. 4.10), a seasonal development curve may be determined and adjusted for different planting time by shifting the curve according to the maximum in NDVI. Including data from all sites demonstrates that the seasonal change defined in the manner for  $V_{c_{\text{uptake}}}$  is in fact very consistent. Use of this method assumes that the NDVI maximum is more reliable than seasonal changes in NDVI which may be complicated by non-homogeneity within the relatively large 250 x 250 m best resolution MODIS pixels. In other words, the signal at maximum is clearly recognizable, and rice crop development is recognized at a characteristic stage despite disturbance effects from the surroundings. The GAM curve shown in Fig. 4.16 may have the potential to reproduce the early peak in  $V_{c_{\text{uptake}}}$  obtained from the measured eddy covariance data. However, the curve obtained with the GAM method may not be adequate, since the highest values for scaled  $V_{c_{\text{uptake}}}$  are only 0.8.

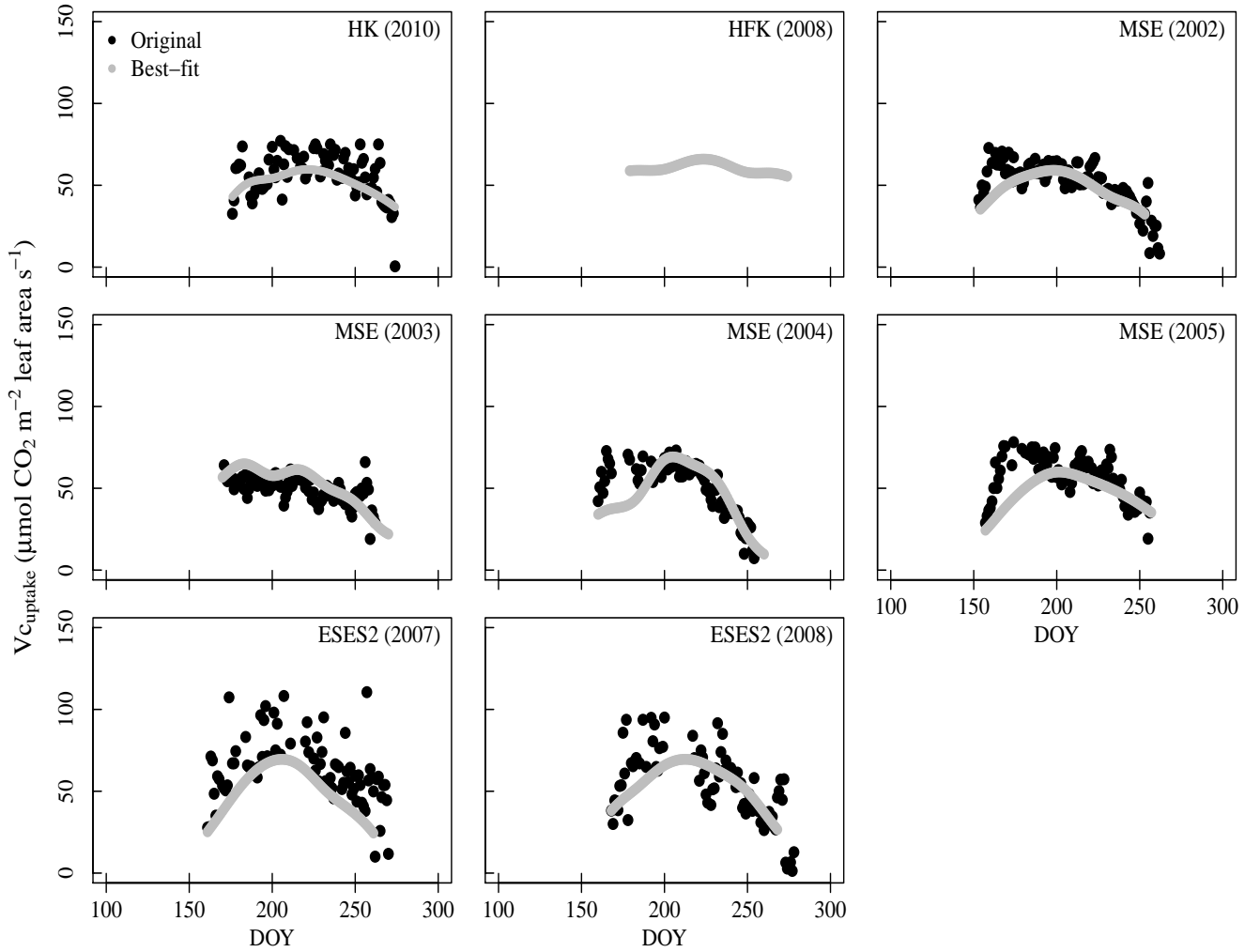


Fig. 4.15 Seasonal time courses in  $V_{c_{\text{uptake}}}$  estimated using the best-fit linear model (Fig. 4.14 - gray closed circle) and  $V_{c_{\text{uptake}}}$  estimated using observed data (black closed circle) for the years indicated. HK = Haean (S. Korea), HFK = Haenam (S.Korea), MSE = Mase (Japan), and ESES2 = El Saler-Sueca (Spain).

## 4.6 GPP estimation with the best-fit model

Daily GPP as reproduced by two models (LAI from the consistent development and  $V_{c_{\text{uptake}}}$  linearly dependent on NDVI; and LAI and  $V_{c_{\text{uptake}}}$  both dependent on consistent development curves) are compared to observation for all sites in Figs. 4.17 and 4.18. Accumulated observed GPP during the growing season varied from  $672 \text{ gC m}^{-2} \text{ d}^{-1}$  to  $1294 \text{ gC m}^{-2} \text{ d}^{-1}$ , although the period for comparison varied slightly (see Table 3.1). Carbon uptake appeared to increase from Korea, to Japan and to Spain due to different climate conditions. Modeled values ranged from  $670 \text{ gC m}^{-2} \text{ d}^{-1}$  to  $1020 \text{ gC m}^{-2} \text{ d}^{-1}$  with  $R^2$  above 0.79, RMSE below 3.48, CV above 38.02% and modeling efficiency (MF) between 0.92 and 0.72 (Table 4.4). There was little difference found between the two methods in determining the seasonal course of  $V_{c_{\text{uptake}}}$ . Simulated GPP was

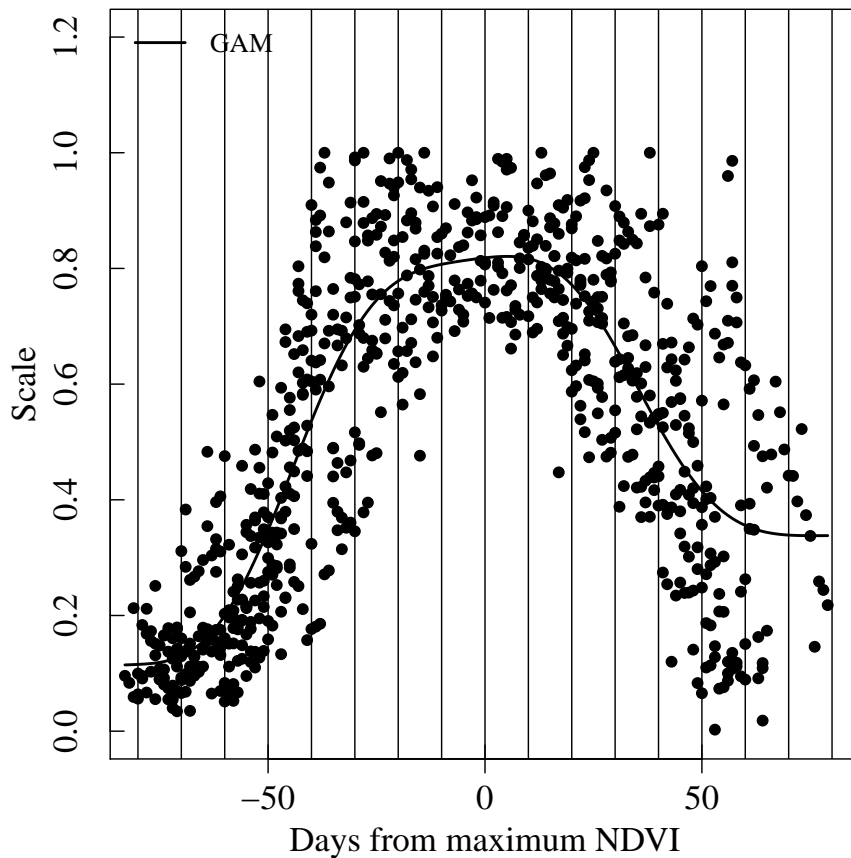


Fig. 4.16 A scaled general seasonal curve for  $V_{c_{\text{uptake}}}$  utilizing data from all rice paddy sites. The scaling results by dividing estimated  $V_{c_{\text{uptake}}}$  by maximum  $V_{c_{\text{uptake}}}$  for each site and year. The black closed circle indicates the relationship between the scaled  $V_{c_{\text{uptake}}}$  and DOY based on time shifts according to maximum NDVI. The solid line indicates the general seasonal curve determined by generalized additive model (GAM).

in general under-estimated as expected due to the remaining difficulties in estimating  $V_{c_{\text{uptake}}}$  in dependence on NDVI. Deviations from observation over the course of the season at each site reflect the differences found for observed and predicted  $V_{c_{\text{uptake}}}$  as represented in Fig. 4.18 or in Table 4.3. Although the alternative method based on consistent phenological development did not lead to an improvement in GPP prediction, further development of the response curve shown in Fig. 4.16 may lead to better success as discussed in Chapter 6.

Table 4.4. Summary of observed GPP and modeled GPP obtained with the linear regression model for  $V_{c_{\text{uptake}}}$  from NDVI at all rice paddy sites with mean, standard deviation (STD), accumulated GPP (acc.GPP), difference between simulated GPP and observed GPP (%), slope (a), intercept (b), determination coefficients ( $R^2$ ), root mean square error (RMSE), coefficient of variation (CV), and modeling efficiency (MF).

Summary of observed GPP and modeled GPP									
Site	Year	Observed GPP			Modeled GPP			Period (DOY)	Difference (%)
		Mean	STD	acc.GPP	Mean	STD	acc.GPP		
HK	2010	6.01	8.60	672	5.99	8.70	670	114	0
HFK	2008	7.11	9.15	780	7.84	10.41	860	96	10
MSE	2002	7.21	9.73	897	6.57	9.43	817	109	-9
MSE	2003	7.12	9.40	749	7.26	10.20	763	92	2
MSE	2004	9.19	11.82	987	7.94	11.18	852	94	-14
MSE	2005	8.03	10.50	908	7.31	10.08	826	99	-9
ESES2	2007	10.41	12.89	1294	7.81	11.32	971	109	-25
ESES2	2008	9.22	11.95	1157	8.12	11.40	1020	110	-12

Statistic for the correlation between observed GPP and modeled GPP							
Site	Year	a	b	$R^2$	RMSE	CV (%)	MF
HK	2010	0.91	0.54	0.80	0.77	65.40	0.79
HFK	2008	1.01	0.67	0.79	0.75	68.25	0.72
MSE	2002	0.93	-0.15	0.93	0.94	38.02	0.92
MSE	2003	1.03	-0.08	0.90	0.31	44.91	0.88
MSE	2004	0.87	-0.09	0.85	2.00	51.21	0.84
MSE	2005	0.91	-0.01	0.90	1.20	42.32	0.90
ESES2	2007	0.82	-0.72	0.87	3.48	51.48	0.83
ESES2	2008	0.88	-0.02	0.86	1.82	50.50	0.85

Table 4.5. Summary of observed GPP and modeled GPP with the general seasonal curve model for  $V_{c_{uptake}}$  from NDVI at all rice paddy sites with mean, standard deviation (STD), accumulated GPP (acc.GPP), difference between simulated GPP and observed GPP (%), slope (a), intercept (b), determination coefficients ( $R^2$ ), root mean square error (RMSE), coefficient of variation (CV), and modeling efficiency (MF).

Summary of observed GPP and modeled GPP									
Site	Year	Observed GPP			Modeled GPP			Period (DOY)	Difference (%)
		Mean	STD	acc.GPP	Mean	STD	acc.GPP		
HK	2010	6.01	8.60	672	6.20	9.28	694	114	3
HFK	2008	7.11	9.15	780	7.23	10.13	793	96	2
MSE	2002	7.21	9.73	897	7.30	10.63	908	109	1
MSE	2003	7.12	9.40	749	6.77	9.75	712	92	-5
MSE	2004	9.19	11.82	987	8.61	11.57	925	94	-6
MSE	2005	8.03	10.50	908	8.08	11.18	913	99	1
ESES2	2007	10.41	12.89	1294	8.12	11.37	1010	109	-22
ESES2	2008	9.22	11.95	1157	7.93	11.03	995	110	-14

Statistic for the correlation between observed GPP and modeled GPP							
Site	Year	a	b	$R^2$	RMSE	CV (%)	MF
HK	2010	0.97	0.36	0.81	0.31	66.93	0.78
HFK	2008	0.96	0.38	0.76	0.38	70.31	0.70
MSE	2002	1.05	-0.25	0.92	0.50	42.54	0.90
MSE	2003	0.98	-0.21	0.89	0.40	44.97	0.88
MSE	2004	0.89	0.44	0.82	1.42	54.96	0.82
MSE	2005	1.01	-0.01	0.90	0.13	45.04	0.88
ESES2	2007	0.81	-0.31	0.84	3.35	53.96	0.81
ESES2	2008	0.83	0.24	0.82	2.43	57.42	0.80

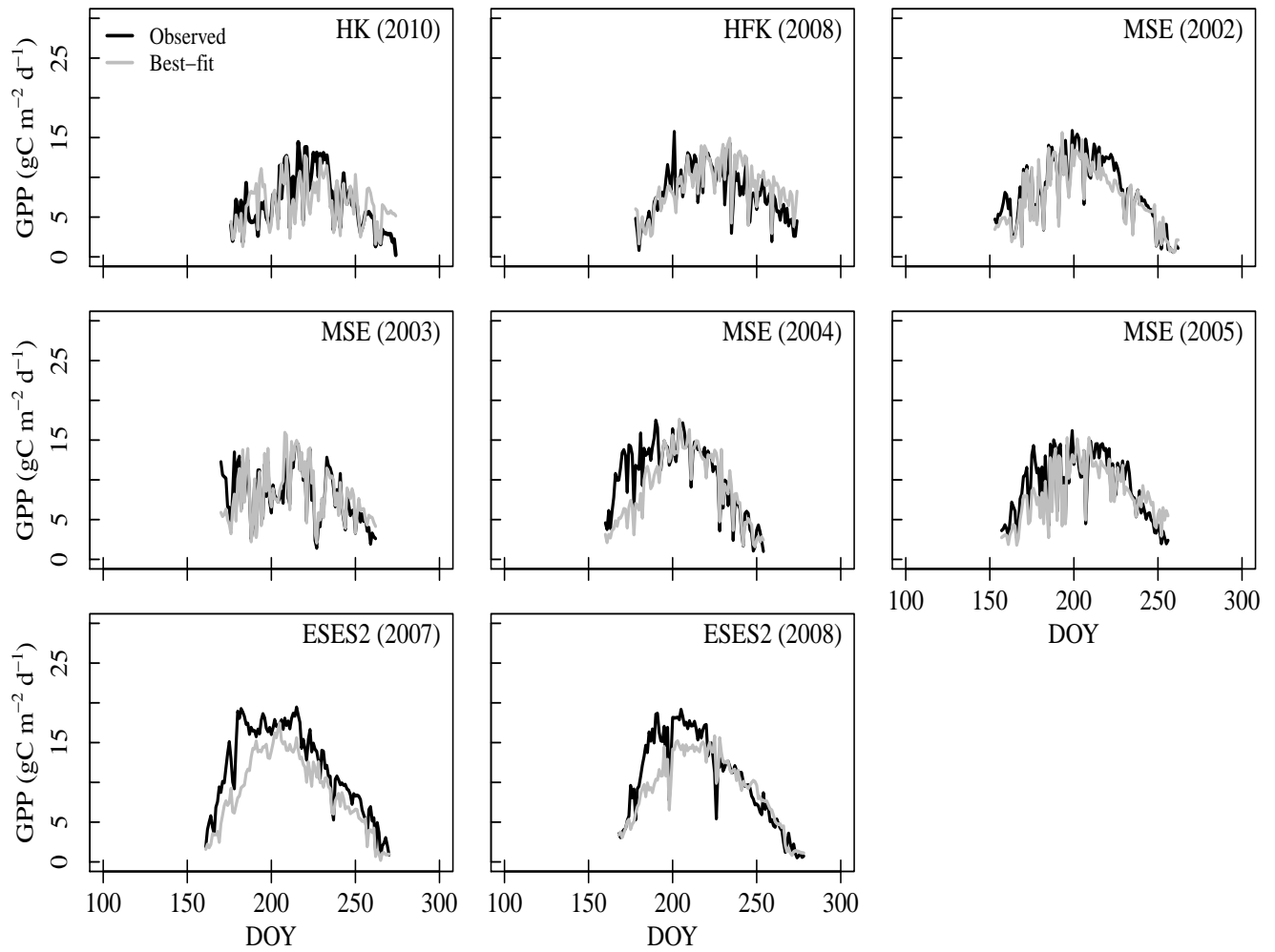


Fig. 4.17 Daily GPP estimation obtained with the linear regression model for  $V_{c_{\text{uptake}}}$  (gray solid line) and observed GPP (black solid line) of rice paddy sites for the years indicated. HK = Haeon (S. Korea), HFK = Haenam (S.Korea), MSE = Mase (Japan), and ESES2 = El Saler-Sueca (Spain).

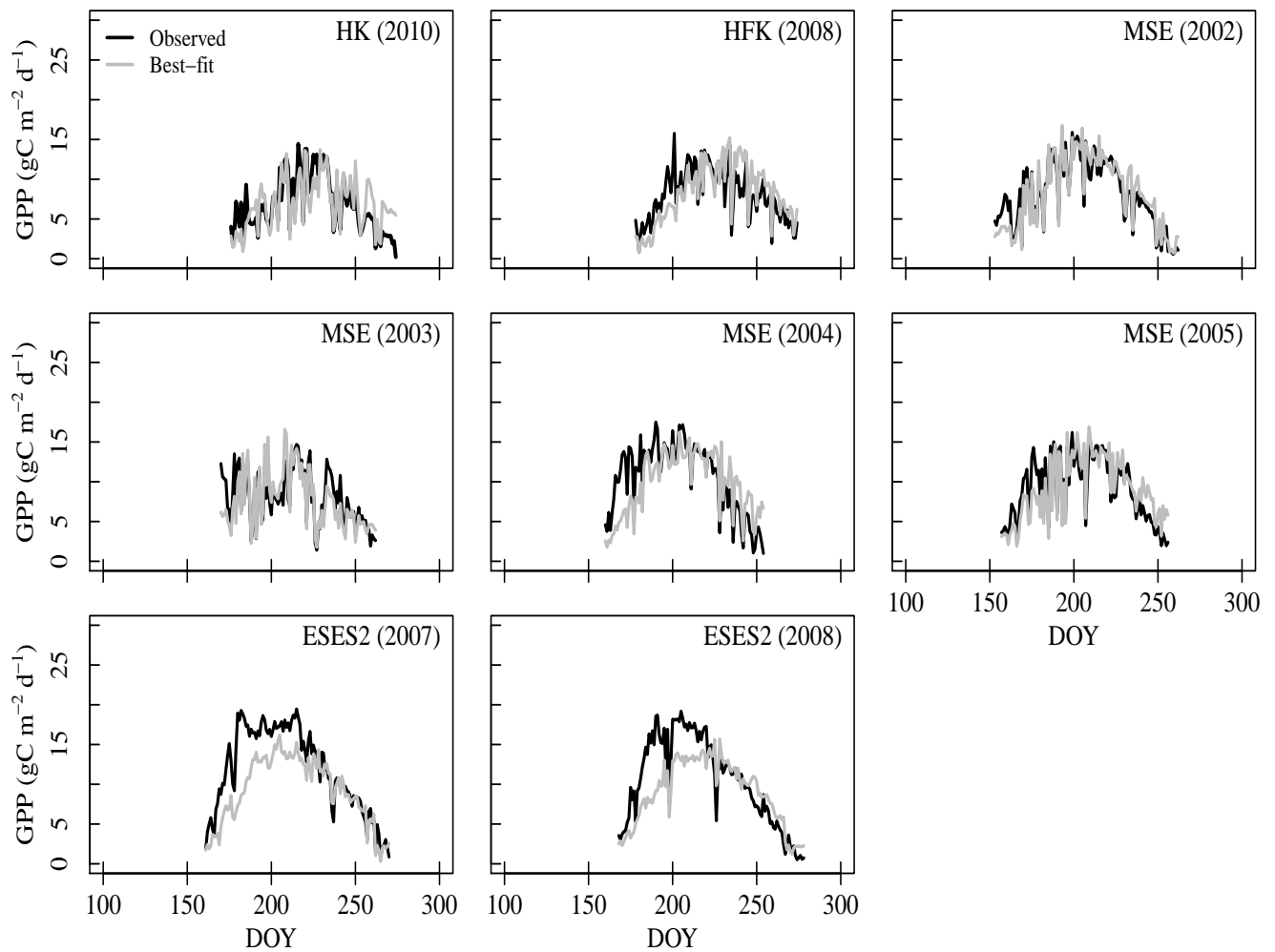


Fig. 4.18 Daily GPP estimation with the general seasonal curve model for  $V_{c_{\text{uptake}}}$  (gray solid line) and observed GPP (black solid line) of rice paddy sites for the years indicated. HK = Haeon (S. Korea), HFK = Haenam (S.Korea), MSE = Mase (Japan), and ESES2 = El Saler-Sueca (Spain).

# Chapter 5

## Results: GPP from dry-land crops

### 5.1 Meteorological condition

Meteorological conditions of 10-day intervals are illustrated in Fig 5.1 for the dry-land crops soybean, maize, potato, and sugar beet indicating the growth period in study years. Weather data were obtained every half hour from the meteorological sensors installed on eddy covariance towers. A data gap occurred for maize at US-Ne3 in 2003 from DOY 250 to the harvest.

Global radiation ( $R_g$ ) among the dry-land crop sites ranged from about 10 to 30 MJ m<sup>-2</sup>d<sup>-1</sup>. At the potato field in Haeon in 2010 (HK 2010), a rapid early increase of  $R_g$  to ca. 26 MJ m<sup>-2</sup>d<sup>-1</sup> was followed by a rapid decrease to ca. 18 MJ m<sup>-2</sup>d<sup>-1</sup> in June (DOY 152 – 170).  $R_g$  at HK during 2010 decreased with fluctuations from late June to August when the aboveground plant parts died.  $R_g$  at Lonzee in 2004 (BE-Lon 2004) with sugar beet increased to the maximum of about 23 MJ m<sup>-2</sup>d<sup>-1</sup> in late May and early June (DOY 140 – 155), and a sudden decrease occurred (14 MJ m<sup>-2</sup>d<sup>-1</sup>) in July (DOY 190 – 200).  $R_g$  at BE-Lon in 2004 decreased rapidly in July when precipitation was increasing. In Nebraska-Mead (US-Ne3), soybean was planted in 2002 and 2004.  $R_g$  reached the maximum of about 26 MJ m<sup>-2</sup>d<sup>-1</sup> in 2002 (US-Ne3 2002) and about 22 MJ m<sup>-2</sup>d<sup>-1</sup> in 2004 (US-Ne3 2004) in June around DOY 160.  $R_g$  from US-Ne3 in 2002 was somewhat higher than during 2004.  $R_g$  at US-Ne3 in 2002 decreased in June and August, while the decrease occurred in July in 2004. Maize was grown at US-Ne3 in 2003 and 2005 (US-Ne3 2003 and US-Ne3 2005).  $R_g$  at US-Ne3 in 2003 and 2005 fluctuated throughout the growing season at ca. 20 MJ m<sup>-2</sup>d<sup>-1</sup>.  $R_g$  at the maize field achieved a maximum of about 27 MJ m<sup>-2</sup>d<sup>-1</sup> in July around DOY 195 during both study years. At Klingenberg in 2007 (DE-Kli 2007)

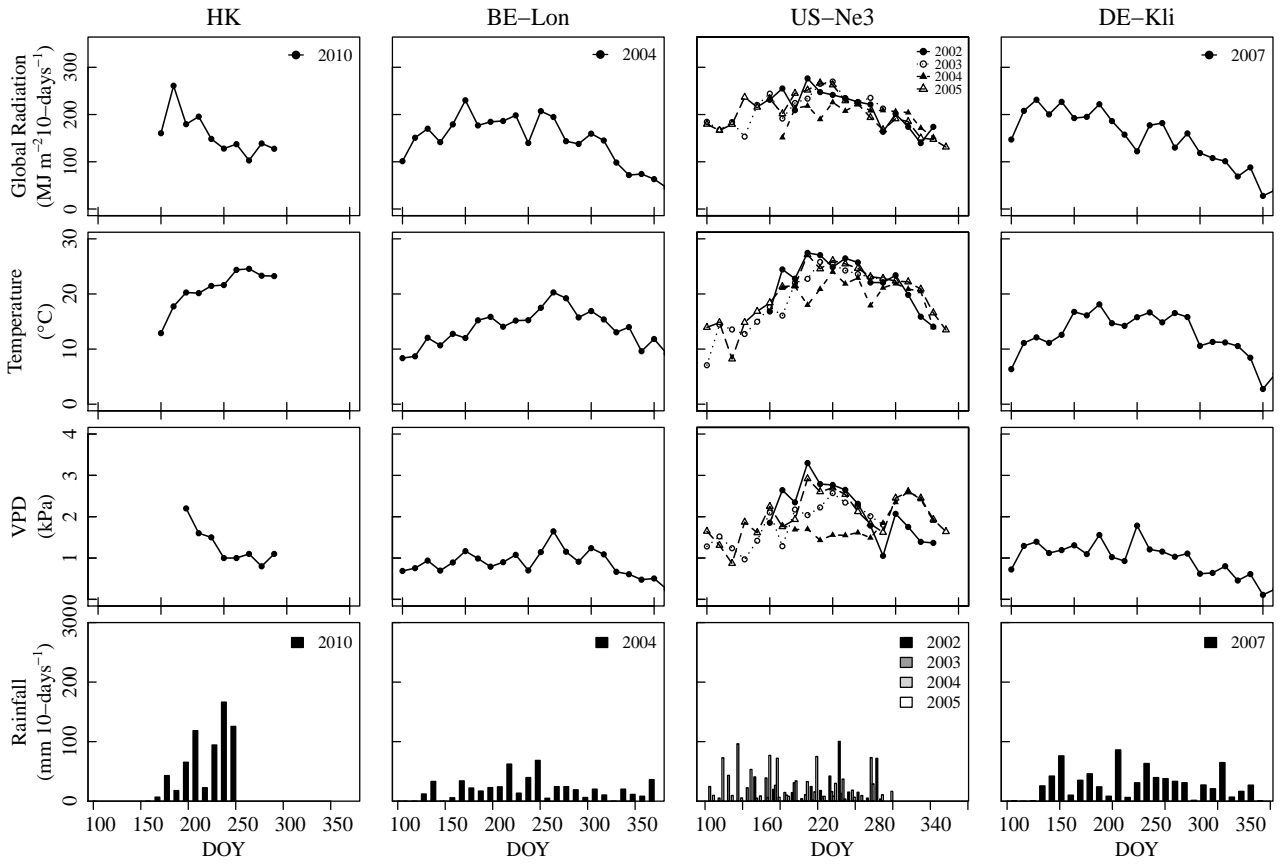


Fig. 5.1 Seasonal time courses for meteorological variables at dry-land crop sites that influence GPP, e.g., can be considered driver variables for plant response as it affects carbon uptake, crop growth, and primary production. Total global radiation ( $R_g$ ), mean air temperature ( $T_a$ ), mean maximum vapor pressure deficit (VPD), and total rainfall are given for 10-day intervals during the growth period. General site characteristics are given in Table 3.1. HK = Haeon (S. Korea) for potato, BE-Lon = Lonze (Belgium) for sugar beet (2004), DE-Kli = Klingenberg (Germany) for maize, and US-Ne3 = Nebraska-Mead (USA) for soybean (2002 and 2004) and maize (2003 and 2005).

with maize,  $R_g$  reached the maximum of about  $23 \text{ MJ m}^{-2} \text{ d}^{-1}$  in May (around DOY 140) and then gradually decreased to  $10 \text{ MJ m}^{-2} \text{ d}^{-1}$  until the end of the growing season. Overall, the seasonal patterns and range of fluctuation in  $R_g$  was similar at all sites. Due to the monsoon season, the period (DOY 150 – 190) with high radiation input was very short at Haeon Catchment (HK). The 10-day average air temperature ( $T_a$ ) during the plant growth period ranged from 10 to  $27^\circ \text{C}$  among the sites. Similar seasonal patterns were reported to those that occurred with global radiation except at HK.  $T_a$  at HK during 2010 increased while  $R_g$  was decreasing due to monsoon weather conditions. The 10-day average  $T_a$  at HK during 2010 increased to 24

°C and maintained constant (23 °C) until the end of the growing season.  $T_a$  at DE-Kli during 2007 increased to a peak of 18.1 °C in the early growing season in June (around DOY 170) and then slowly decreased until the end of the growing season. In general, temperature was higher at HK and US-Ne3 which may have an effect on canopy development and GPP. The 10-day averaged daily maximum vapor pressure deficit (VPD) was ranged from 0.3 to 3.3 kPa among the dry-land crop sites. At HK in 2010, the seasonal VPD pattern was the same as shown for HK paddy rice (Fig. 4.1). In case of dry-land crops, only HK was subjected to Asian monsoon climate that is generally characterized by hot and humid condition and low radiation input (Jung et al., 2013). VPD at BE-Lon during 2004 with sugar beet was also relatively low (0.7-1.6 kPa). Daily maximum VPD averaged over 10-day intervals from about 1 to 2.8 kPa at US-Ne3 during 2002, which was planted with soybean. VPD at US-Ne3 during 2002 showed a large decrease in late August (1 kPa). VPD at US-Ne3 during 2004 was relatively constant (0.6 – 0.8 kPa) until late summer (around DOY 250) and increased until the harvest (1.1 kPa). Maize was planted in 2003 and 2005 at the US-Ne3 site. Maximum average VPD values were recorded from 1 to 2.9 kPa. VPD gradually increased and decreased over the course of the growing season in US-Ne3 during 2003 and 2005. VPD was relatively low from 0.4 to 0.8 and constant during the growing season at DE-Kli during 2007. VPD at DE-Kli during 2007 showed a decreasing tendency over the whole growing season. The variation of VPD was relatively large among the dry-land crop sites. The driest sites from the standpoint of atmospheric humidity were HK during early season, DE-Geb, and US-Ne3. While the influences on GPP of these differences may not be dramatic, it may be that they cannot be neglected. The total precipitation during the growth period ranged at the observation sites from 178 mm (US-Ne3 during 2003) to 660 mm of (HK during 2010) (Table 3.1). The 10-day period total precipitation pattern is presented in Fig 5.1 (lowest panel). HK during 2010 showed the highest precipitation of 660 mm during the growing season which was ca. 40 % higher than at the other sites due to intensive rainfall during the summer monsoon. At BE-Lon in 2004 with sugar beet, 411 mm of total precipitation was recorded during the growing season, while low precipitation occurred in April and September. The total precipitation with soybean at US-Ne3 during 2002 and 2004 was 372 and 311 mm, respectively. US-Ne3 during 2003 recorded the lowest total precipitation of 178 mm during the growing period. Except at HK during 2010, DE-Geb in 2006, and US-Ne3 in 2003, the total

measured precipitation was similar among the dry-land crop sites (from 311 mm to 411 mm). At all sites, precipitation events were frequent. Thus, initially we hypothesize that drought stress influences on plant development and GPP did not occur, however this must be re-examined later in review of the overall results.

## 5.2 LAI development

The observed seasonal change in LAI of dry-land crops is illustrated in Fig. 5.2. Different

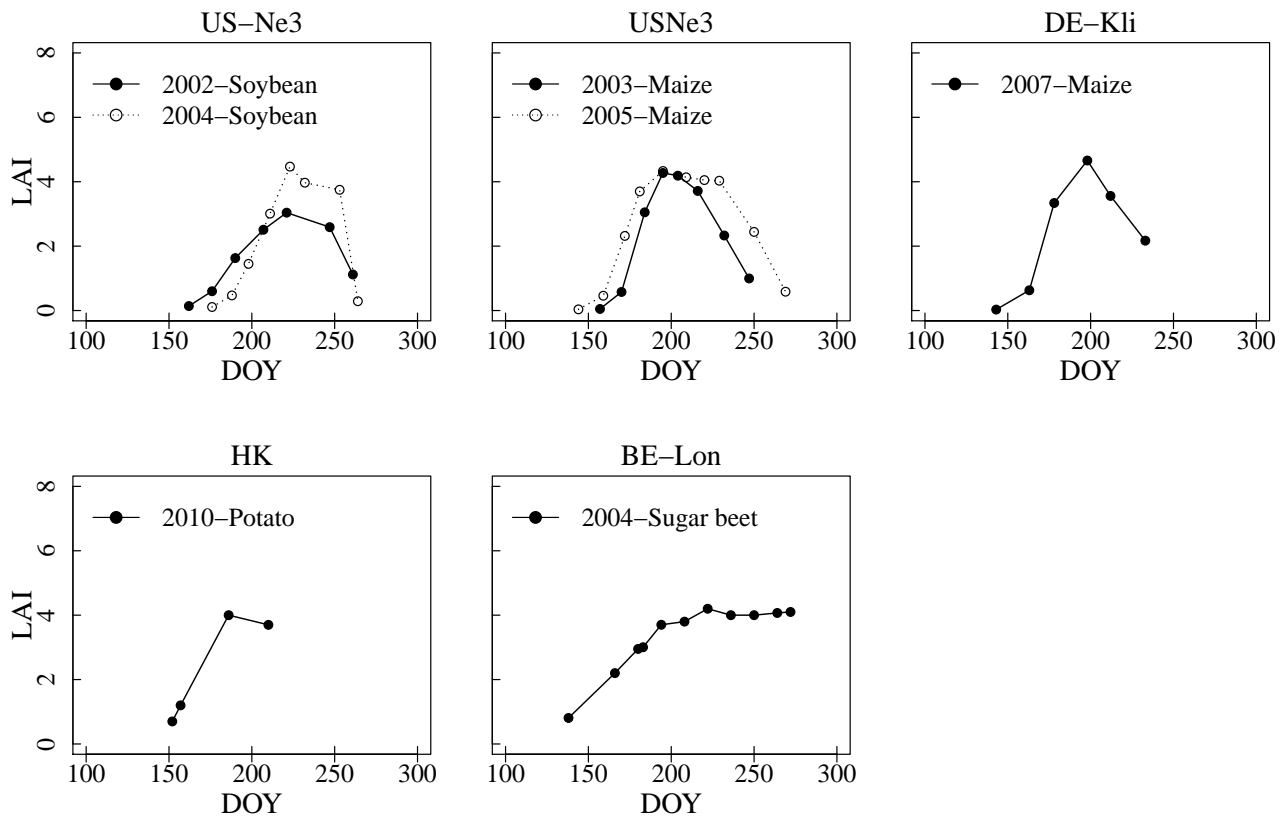


Fig. 5.2 Seasonal time courses in the years indicated for change in leaf area index (LAI) of the studied dry-land crop sites. US-Ne3 = Nebraska (USA) for soybean (2002 and 2004) and maize (2003 and 2005), DE-Kli = Klingenberg (Germany) for maize, HK = Haeon (S. Korea) for potato, BE-Lon = Lonze (Belgium) for sugar beet (2004).

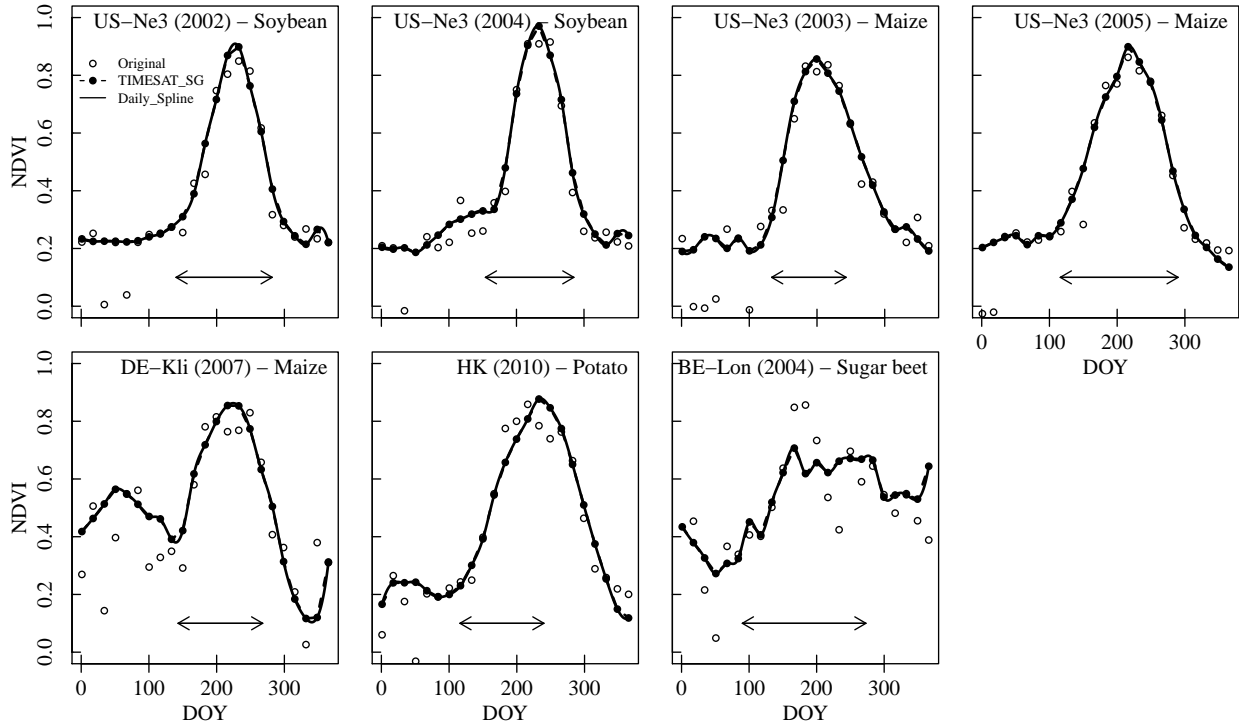
planting dates for soybean at US-Ne3 in 2002 and 2004 resulted in different rates of development of LAI, although the overall seasonal pattern was quite similar. Maximum LAI of 3.0 and 4.5 occurred on almost same day during both years (DOY 221 and DOY 223, respectively). LAI for maize developed with a similar seasonal pattern at all sites. LAI increased slowly until ca. 20

days after planting, followed by a rapid increase until the peak LAI was reached. Subsequently LAI decreased until harvest at the maize sites. Only maize LAI from US-Ne3 in 2005 exhibited a longer period with relatively constant LAI during summer (DOY 195 – 229). Maximum LAI was 4.3 on DOY 195 for US-Ne3 in 2003 and 2005, and 4.7 at DE-Kli in 2007 on DOY 198.

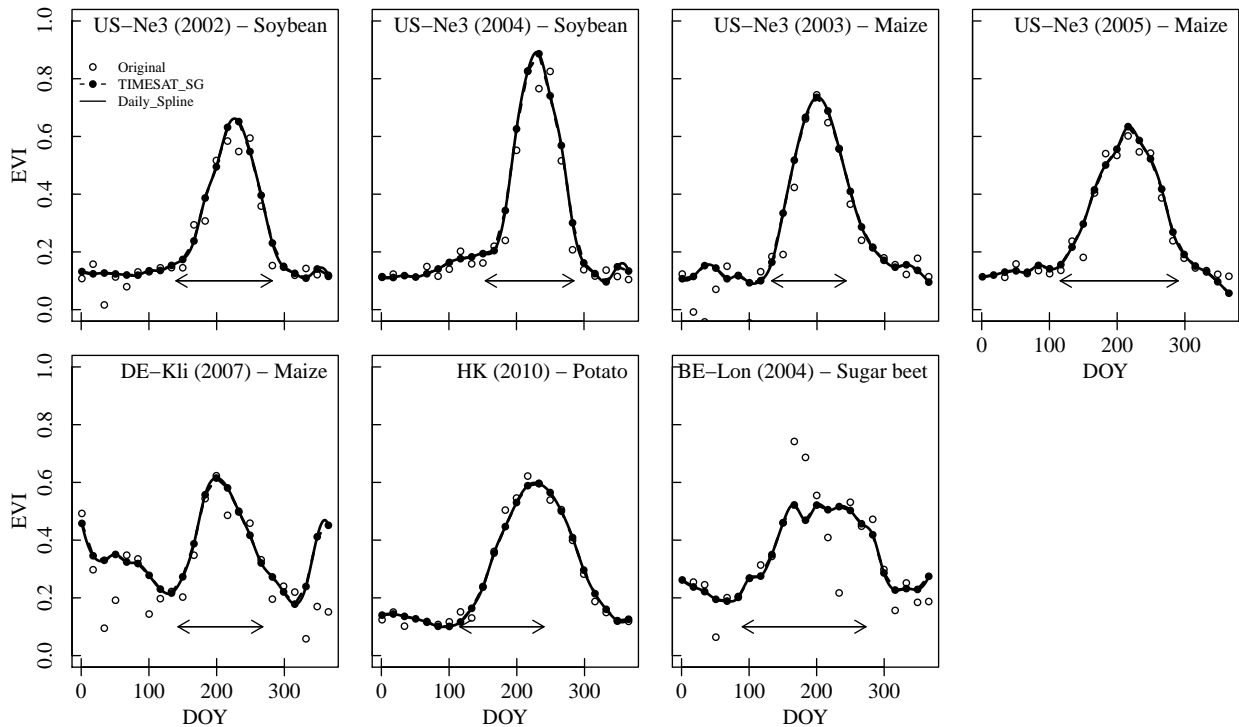
LAI development in potato exhibited a rapid increase to maturity after which the above-ground plant parts rapidly died before the potato harvest. The growing period was relatively short, although LAI was not measured after DOY 209, making it difficult to define the decreasing phase. Maximum LAI of 4.0 occurred on DOY 186 at HK in 2010, which is in reasonable agreement with other maximum values published in the literature (indicating for potato maximum LAI of ca. 3 to 3.5). LAI of sugar beet at BE-Lon in 2004 increased as the sugar beets grew during June and July. When LAI of sugar beet reached the maximum of 4.0 (DOY 222), LAI remained constant until the harvest. The measured LAI from dry-land crops was interpolated by spline to estimate a daily value, which could be used together with daily observations of GPP and carboxylation capacity.

### 5.3 Dynamics of vegetation indices

Fig. 5.3 shows both the annual and the seasonal patterns from planting to harvest of dry-land crop site downloaded VIs from the MODIS data base, the smoothed VIs using TIMESAT processing, and interpolated daily VIs. The arrows in the figure identify the period between planting and harvest time at the specific location where eddy covariance data were obtained. The growth period patterns in downloaded NDVI and EVI of dry-land crops varied according to the crop examined. Furthermore, NDVI and EVI from dry-land crops were more scattered than from rice paddy sites. This scatter has influence on the subsequent analyses of smoothing and estimating daily VIs. It should be kept in mind that this influence may negatively affect the relationships determined between VIs and LAI or  $V_{c_{\text{uptake}}}$ . For example, at HK during 2010 VIs increased in April and decreased in September while the aboveground parts of the potato plants died in August before NDVI decreased. The irregularities in the seasonal pattern shift or modify the established relationship between VIs and LAI or  $V_{c_{\text{uptake}}}$  for potato. As an initial explanation, we can assume that the added scatter is due to the much less homogeneous and smaller areas covered by



(a) NDVI, TIMESAT NDVI, and daily NDVI



(b) EVI, TIMESAT EVI, and daily EVI

Fig. 5.3 MODIS vegetation indices for (a) NDVI and (b) EVI for the years indicated. US-Ne3 = Nebraska (USA) for soybean (2002 and 2004) and maize (2003 and 2005), DE-Kli = Klingenberg (Germany) for maize, HK = Haeen (S. Korea) for potato, BE-Lon = Lonzee (Belgium) for sugar beet (2004). Symbols indicate original VI data downloaded from the database (open circles), VI smoothed by TIMESAT method (closed circle), and estimated daily VI (solid line) from spline interpolation. The arrows below the NDVI/EVI values indicate the period of crop growth at each site.

the fields as compared to rice paddies and greater interference by reflection from surrounding landscape elements.

The interpolated daily VIs were derived from the smoothed VIs which removed unreasonable values (i.e., due to clouds, snow, shadows, bidirectional effects, high solar or scan angles and transmission errors). TIMESAT procedures compensate for the absence of data and allow determination of a continual seasonal course in VIs. Daily VIs increased with the onset of the dry-land crops growing season, however, decreases began and continued during different growth phases for each crop site. For example, daily NDVI of potato at the HK site during 2010 continued to decreased after harvest until the pre-planting NDVI of 0.2 was reached. Sugar beet for BE-Lon during 2004 remained relatively constant after NDVI reached a peak and until the harvest. Daily NDVI for US-Ne3 during 2002 and 2004 followed the same pattern as soybean growth. Daily NDVI of maize for DE-Kli during 2007, and US-Ne3 during 2003 and 2005 increased with onset of the growing season, and decreased with senescence and harvest. However, DE-Kli during 2007 fluctuated strongly both before planting and after harvest. The seasonal patterns in NDVI and EVI were in general similar, although the relative levels at different times of the season differed (Fig. 5.3). The maxima for NDVI varied between 0.8 and 0.9, while maxima for EVI varied between 0.6 and 0.9.

## 5.4 GPP estimation of individual crop types

As a result of eddy covariance data being available from multiple sites and multiple years for rice, as well as the relatively high homogeneity of the crop over large paddy areas, the results obtained with rice provide guidelines that can be further used in the analysis of dry-land crop CO<sub>2</sub> uptake. For the four dry-land crops focused on here as important landscape elements in Haeian Catchment in Korea, limited data are available, especially with respect to site providing both flux data and seasonal determinations of LAI development. Thus, for each of the crops, soybean, maize, potato, and sugar beet, the following analysis steps were carried out: 1) establishment of a consistent development curve for LAI, 2) testing of potential of the curve to reproduce LAI observations, 3) examination of the predicted  $V_{c_{\text{uptake}}}$  curve obtained with predicted versus observed LAI, 4) determination of the best linear relationship obtained between NDVI or EVI and predicted  $V_{c_{\text{uptake}}}$ , 5) determination of a consistent development

Table 5.1. Statistics for the correlation between measured LAI and estimated LAI, where the LAI estimates are obtained with a general growth curve,  $R^2$  is the coefficient of determination, RMSE is root mean square error, and CV is coefficient of variation.

Site	Year	$R^2$	RMSE	CV (%)
US-NE3	2002	0.98	0.06	33.27
US-NE3	2004	0.96	0.30	57.68
US-NE3	2003	0.82	0.28	107.56
US-NE3	2005	0.96	0.18	36.06
DE-Kli	2007	0.87	0.15	71.30
HK	2010	0.94	0.72	27.86
BE-Lon	2004	0.98	0.10	22.82

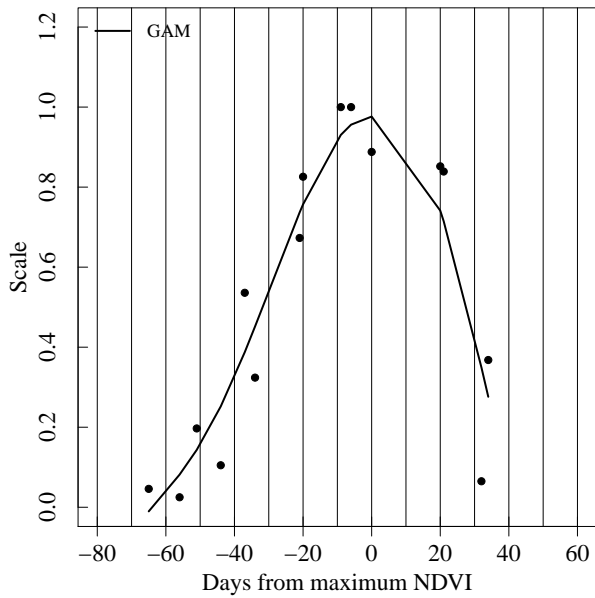
curve for  $V_{c_{\text{uptake}}}$ , 6) estimation of GPP using LAI from the consistent development and  $V_{c_{\text{uptake}}}$  linearly dependent on vegetation index, and 7) estimation of GPP using LAI and  $V_{c_{\text{uptake}}}$  both dependent on consistent development curves.

### 5.4.1 LAI estimation

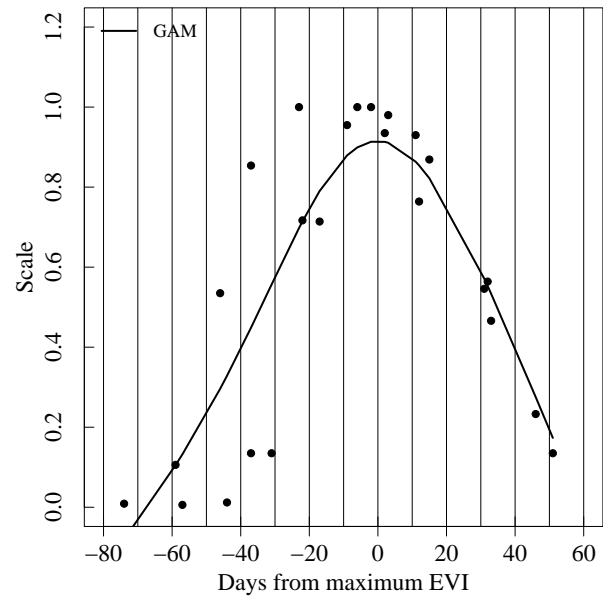
General growth curve for the four crops were established with GAM as described previously for the LAI estimation of the rice paddy sites. As shown in Fig. 5.4, the scaled maximum for both soybean and maize LAI is on Day from maximum = 0, e.g., coincided with maximum in VI as also used in the case of rice. For soybean, NDVI was again applicable as predictor of LAI, but in the case of maize, NDVI provided poor results, whereas EVI was useful. The statistical results of NDVI versus EVI are provided in Appendix B (Table B.4). The general growth curves obtained for the root crops potato and sugar beet differed greatly from those of soybean and maize. In the case of potato, the maximum in NDVI occurred much later than maximum LAI, which was achieved very rapidly. With sugar beet from Lonze, maximum NDVI occurred when LAI was only 50% of maximum. It remains unclear whether these patterns have been strongly influenced by disturbance of the NDVI signal by surrounding vegetation. Nevertheless, since data were only available from single sites, the relationships shown can be used to estimate LAI over the course of the growing season.

The general seasonal change in LAI for each crop may be estimated for each site and year

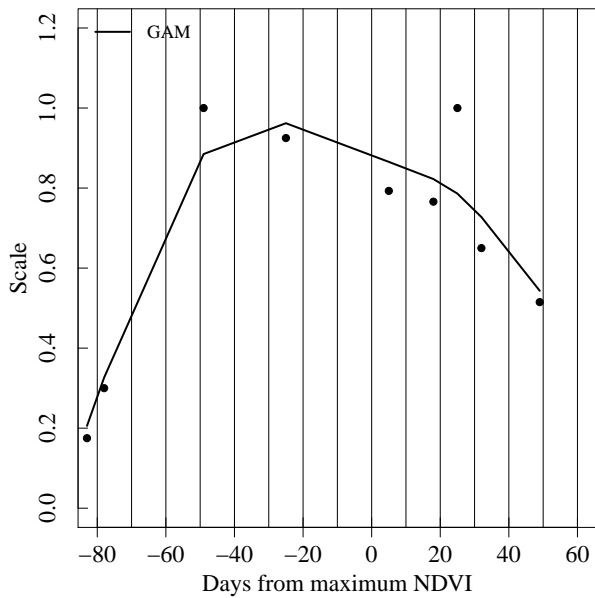
by multiplying daily values of the curve in Fig. 5.4 by the average maximum LAI observed at the crop sites. For soybean and maize, the maximum is obtained from multiple years,



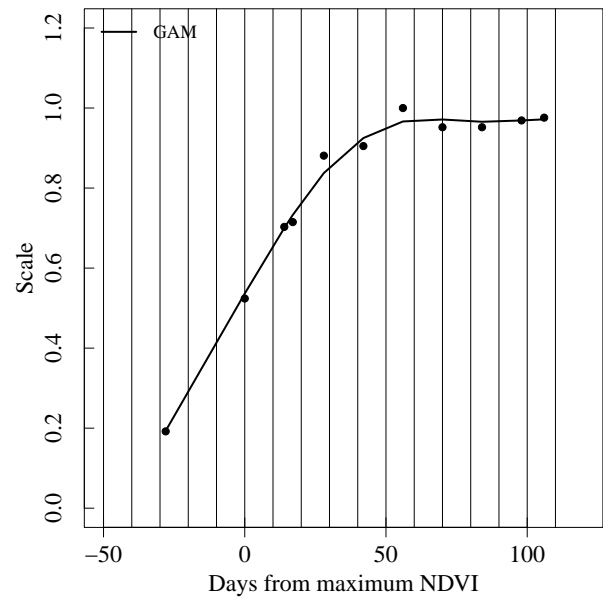
(a) Soybean



(b) Maize



(c) Potato



(d) Sugar beet

Fig. 5.4 General growth curves scaled from 0 to 1, utilizing data from each crop site and dividing by maximum observed LAI (black closed circle). The black closed circles indicate the relationship between the scaled LAI and DOY based on time shifts according to maximum VIs. The solid line indicates the general growth curve determined with the generalized additive model (GAM).

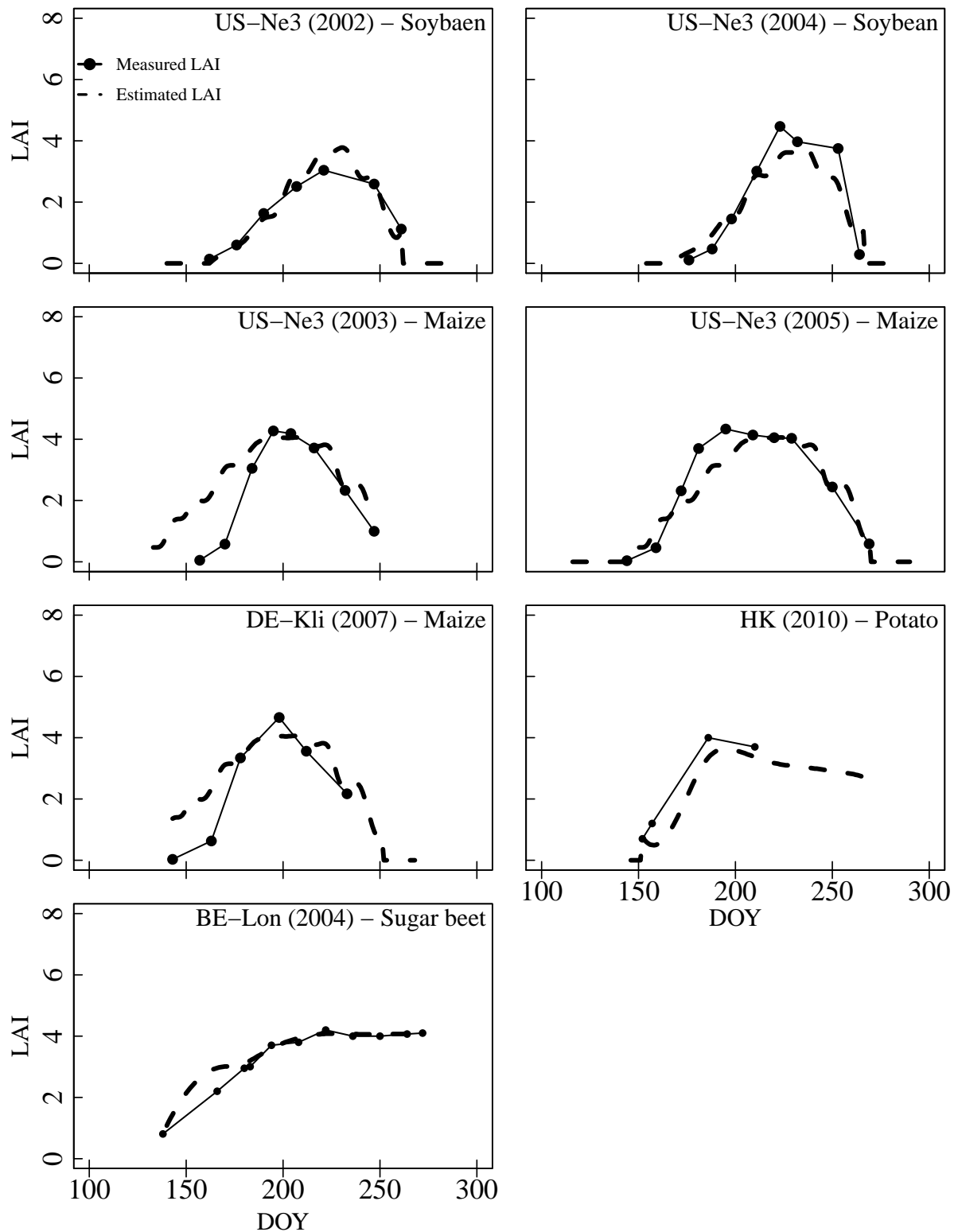


Fig. 5.5 Measured LAI (closed circle with solid line) and estimated daily LAI (dashed line) obtained with the consistent phenological development approach (see text for stepwise procedure) at dry-land crop sites for the years indicated. US-Ne3 = Nebraska (USA) for soybean (2002 and 2004) and maize (2003 and 2005), DE-Kli = Klingenberg (Germany) for maize, HK = Haeon (S. Korea) for potato, BE-Lon = Lonze (Belgium) for sugar beet (2004).

but in the case of potato and sugar beet LAI maximum is from one year of observation. The

specific LAI seasonal course depends on the time at which the maximum in the appropriate vegetation index occurs. Thus, the predicted LAI change is obtained according to DOY of the maximum VI at the site and in a particular year (Fig. 5.5). The estimated LAI for soybean ranged from 0 to 3.78. LAI for US-Ne3 during 2002 was overestimated at the middle of the growing season but still with a high  $R^2$  of 0.98 and low RMSE of 0.06. The seasonal pattern during 2004 was well reproduced with  $R^2$  of 0.96 and RMSE of 0.30 (Table 5.1). The estimated LAI for maize ranged from 0 to 4.06. LAI for KL during 2007 was overestimated at the beginning of the growing season and underestimated at peak LAI development with  $R^2$  of 0.87 and RMSE of 0.15. LAI for US-Ne3 during 2003 was overestimated during the early growing season with  $R^2$  of 0.82 and RMSE of 0.28. The seasonal pattern for US-Ne3 during 2005 was underestimated from ca. DOY 170 to 200 and accurately estimated after DOY 200 with  $R^2$  of 0.96 and RMSE of 0.18. The estimated LAI for potato ranged from 0 to 3.64. LAI for HK during 2010 was slightly underestimated during the growing season with  $R^2$  of 0.94 and RMSE of 0.72. LAI estimation of sugar beet for BE-Lon during 2004 ranged from 0 to 4.08. Estimated LAI for BE-Lon during 2004 was overestimated during the early growing season and then followed well the observed with  $R^2$  of 0.98 and RMSE of 0.10 (Table 5.1).

## 5.4.2 $V_{c_{\text{uptake}}}$ estimation

### 5.4.2.1 Seasonal changes of $V_{c_{\text{uptake}}}$

The seasonal change of  $V_{c_{\text{uptake}}}$  is illustrated in Fig. 5.6 as determined by both the measured LAI ( $V_{c_{\text{uptake\_org}}}$ ) and the estimated LAI ( $V_{c_{\text{uptake}}}$ ). The seasonal patterns of  $V_{c_{\text{uptake\_org}}}$  for dry-land crops changed seasonally in a characteristic manner for each crop. In the case of soybean, both study years are similar with increase after planting and a decline occurring with senescence.  $V_{c_{\text{uptake\_org}}}$  reached a maximum of ca. 90  $\mu\text{mol CO}_2 \text{ m}^{-2} \text{ leaf area s}^{-1}$  at DOY 190 during 2002, remained around 75  $\mu\text{mol CO}_2 \text{ m}^{-2} \text{ leaf area s}^{-1}$  during summer (- DOY 243), and decreased until the harvest. Approximate maximum values based on measured LAI was 100  $\mu\text{mol CO}_2 \text{ m}^{-2} \text{ leaf area s}^{-1}$  at DOY 199 in 2004, fluctuated between ca. 100 and 60  $\mu\text{mol CO}_2 \text{ m}^{-2} \text{ leaf area s}^{-1}$  during the summer time (DOY 246), and decreased until the harvest. The seasonal pattern of  $V_{c_{\text{uptake\_org}}}$  for maize at US-Ne3 during 2003 and 2005 increased from 20 to 30 days after planting until ca. DOY 180 to 190 and then remained constant at ca. 80  $\mu\text{mol}$

Table 5.2. Statistics for the linear relationship between  $V_{c_{\text{uptake\_org}}}$  and  $V_{c_{\text{uptake}}}$  obtained with the linear model from VIs (Fig. 5.7).  $a$  is a slope,  $b$  is a intercept,  $R^2$  is the determination of coefficient, RMSE is root mean square error.

Site	Year	$a$	$b$	$R^2$	RMSE	CV (%)
US-NE3	2002	0.69	22.81	0.39	2.17	7.57
US-NE3	2004	1.07	-0.64	0.81	4.26	14.52
US-NE3	2003	0.81	-2.18	0.85	9.16	43.44
US-NE3	2005	1.37	-17.10	0.90	5.02	14.29
DE-Kli	2007	1.15	-10.90	0.81	3.80	16.49
HK	2010	1.31	-18.40	0.62	5.14	27.24
BE-Lon	2004	1.16	-18.38	0.73	8.72	20.30

$\text{CO}_2 \text{ m}^{-2} \text{ leaf area s}^{-1}$  during mid-season and then decreased in late season. There was no eddy covariance data available after DOY 243 in US-Ne3 during 2003. Therefore the further steps in analysis in following sections are carried out only until DOY 243. The seasonal  $V_{c_{\text{uptake\_org}}}$  of maize for DE-Kli during 2007 increased slowly from the beginning of the growing season to a peak around DOY 220, and then remained relatively constant until the harvest. The maximum values of  $V_{c_{\text{uptake\_org}}}$  were  $80 \mu\text{mol CO}_2 \text{ m}^{-2} \text{ leaf area s}^{-1}$  at DE-Kli during 2007; 78 in 2003 and 75 in 2005 at US-Ne3.

$V_{c_{\text{uptake\_org}}}$  for HK during 2010 increased rapidly after the planting, reached a peak of  $67 \mu\text{mol CO}_2 \text{ m}^{-2} \text{ leaf area s}^{-1}$  and declined in July (- DOY 206). A second increase in  $V_{c_{\text{uptake\_org}}}$  was also obtained for HK in 2010 from ca. 39 to  $55 \mu\text{mol CO}_2 \text{ m}^{-2} \text{ leaf area s}^{-1}$  in late July and August thereafter decreased until the above ground biomass died. Seasonal  $V_{c_{\text{uptake\_org}}}$  for sugar beet at BE-Lon during 2004 increased to a peak of about  $80 \mu\text{mol CO}_2 \text{ m}^{-2} \text{ leaf area s}^{-1}$  in June (DOY 157) and remained subsequently near  $70 \mu\text{mol CO}_2 \text{ m}^{-2} \text{ leaf area s}^{-1}$  until the harvest.  $V_{c_{\text{uptake}}}$  obtained with estimated LAI from the consistent phenological development curves showed a good agreement with  $V_{c_{\text{uptake\_org}}}$ . In the case of soybean,  $R^2$  was above 0.97 and RMSE below 1.95 (Table 5.2).  $V_{c_{\text{uptake}}}$  of maize also showed a good agreement with  $V_{c_{\text{uptake\_org}}}$ , with  $R^2$  above 0.82 and RMSE below 7.44 (Table 5.2). In the case of US-Ne3 during 2003 and KL during 2007, underestimation occurred during the early growing season, whereas  $V_{c_{\text{uptake}}}$  agreed well during mid- to late growing season. However, there is some scatter during the middle

of the season for all maize sites.  $V_{c\text{uptake}}$  for HK during 2010 followed a similar seasonal pattern

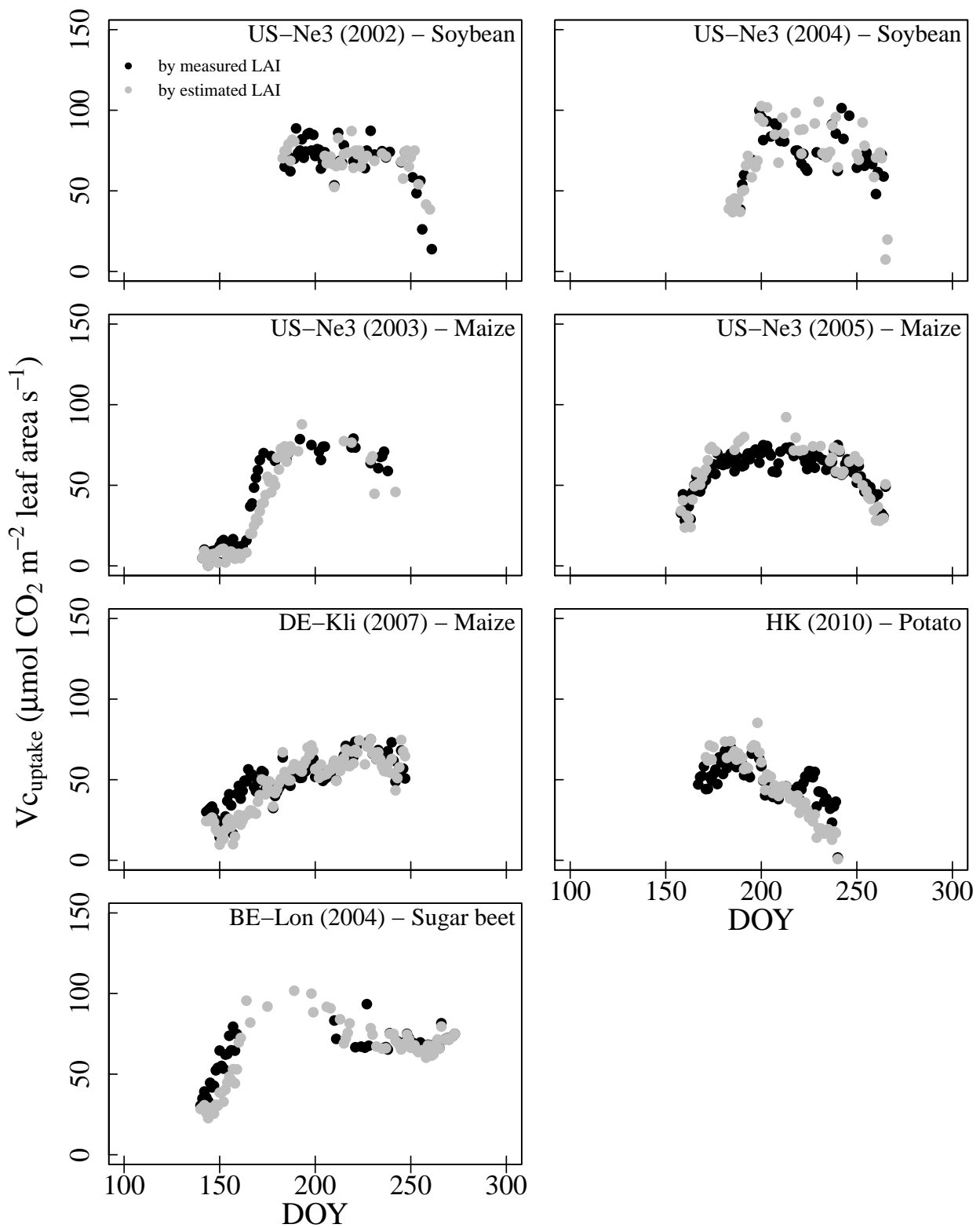


Fig. 5.6 Seasonal change of  $V_{c\text{uptake}}$  obtained with measured LAI ('Original', black closed circles) and with the consistent development LAI-NDVI model ('estimated LAI', gray closed circle) of dry-land crop sites for the years indicated. US-Ne3 = Nebraska (USA), DE-Kli = Klingenberg (Germany), HK = Haeon (S. Korea), BE-Lon = Lonzee (Belgium).

Table 5.3. Statistics for the linear correlation between  $V_{c_{\text{uptake\_org}}}$  and  $V_{c_{\text{uptake}}}$  obtained with the seasonal development curve from VIs (Fig. 5.8).  $a$  is a slope,  $b$  is a intercept,  $R^2$  is the determination of coefficient, RMSE is root mean square error.

Site	Year	$a$	$b$	$R^2$	RMSE	CV (%)
US-Ne3	2002	0.89	3.32	0.69	3.43	42.72
US-Ne3	2004	0.95	4.32	0.81	2.70	34.53
US-Ne3	2003	0.51	15.65	0.55	14.44	53.58
US-Ne3	2005	0.80	10.62	0.77	5.41	28.51
DE-Kli	2007	1.08	-1.81	0.58	2.62	24.79
HK	2010	0.92	0.13	0.29	3.80	35.39
BE-Lon	2004	1.04	-18.80	0.82	17.09	48.08

to  $V_{c_{\text{uptake\_org}}}$  from spring to midsummer (- DOY 206) with  $R^2$  of 0.49 and RMSE of 2.77. However,  $V_{c_{\text{uptake}}}$  for HK did not capture the fluctuations that occurred in August.  $V_{c_{\text{uptake}}}$  for BE-Lon during 2004 estimated in general a similar seasonal pattern as  $V_{c_{\text{uptake\_org}}}$  with the  $R^2$  above 0.90.  $V_{c_{\text{uptake}}}$  was slightly underestimated during the increasing phase in May and early June (DOY 135 – 157). During mid-season, unrealistic values were obtained (eliminated outliers) for  $V_{c_{\text{uptake\_org}}}$  whereas on a small number of days, reasonable values for  $V_{c_{\text{uptake}}}$  were estimated.

#### 5.4.2.2 $V_{c_{\text{uptake}}}$ by two approaches

As described in Chapter 4, an important question is whether the  $V_{c_{\text{uptake}}}$  values described in Fig. 5.6 can be determined from remote sensing over the seasonal course for use with the PIXGRO model. Thus, correlations of estimated  $V_{c_{\text{uptake}}}$  were examined in relation to NDVI and EVI, considering linear, exponential, and logarithm relationships, using data from the entire season or before (B) and after (A) the VI maxima. The tabulated results of these correlations are presented in Appendix B1. It can be concluded that the relationship from the entire season was in general a better predictor of  $V_{c_{\text{uptake}}}$  and, therefore, only these results are presented here. Based on the analysis with rice (section 4.5) as well as the statistical data in Appendix B, only linear relationships are considered (although the exponential regressions are also illustrated for comparison in Fig. 5.7). For soybean, potato, and sugar beet, useful correlations were obtained

with NDVI (as also found with rice), but for maize only EVI provided useful results. Additionally, as has been shown for rice, an alternative approach to describing  $V_{c_{\text{uptake}}}$  with a seasonal curve

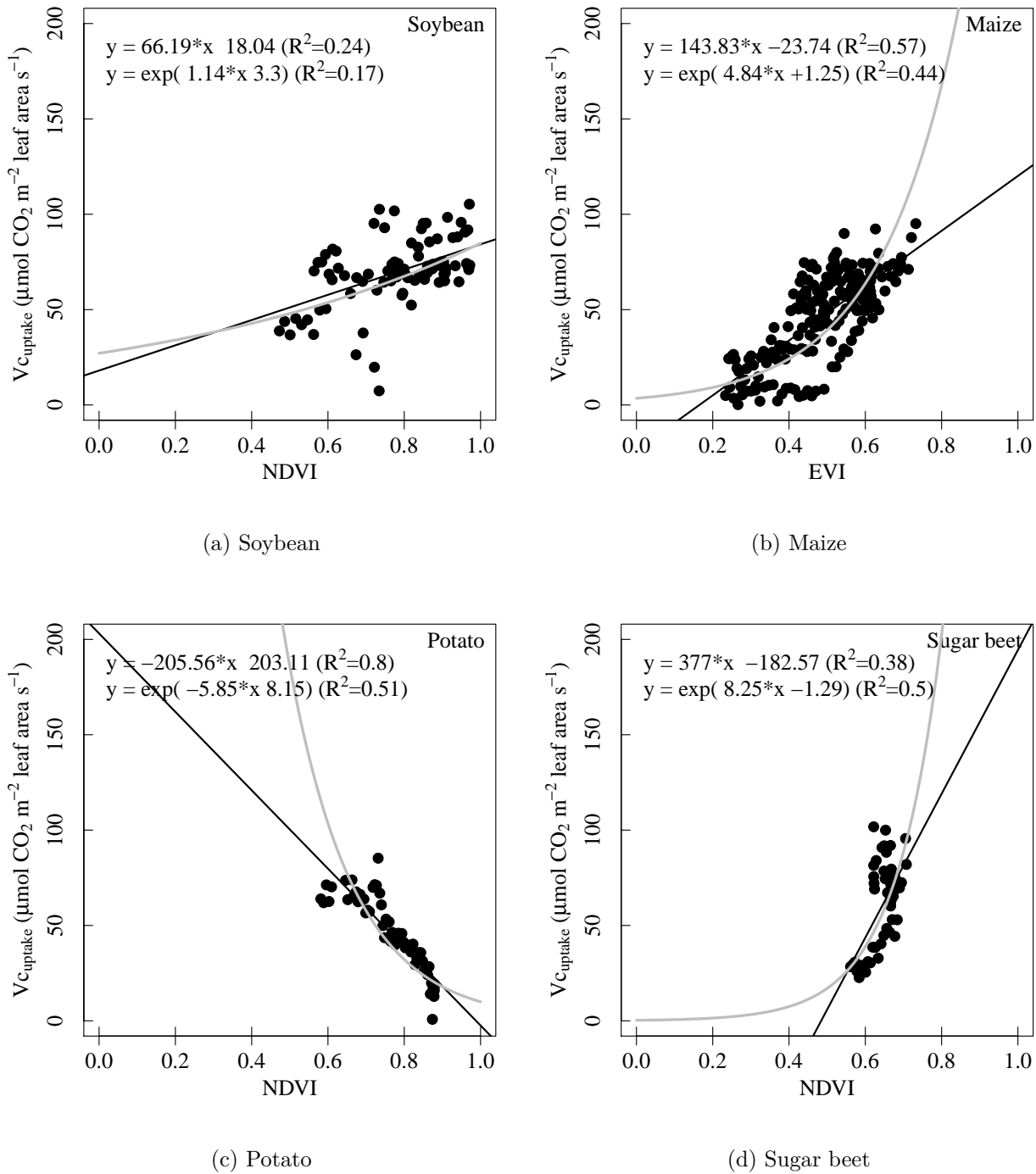


Fig. 5.7 Relationships obtained between  $V_{c_{\text{uptake}}}$  and VIs for the years indicated and where the data are from the entire growing season. The lines indicate the linear equation (black line) and exponential equation (gray line) established for the relationship as described in the text. The coefficients and  $R^2$  of the regressions are shown.

relative to the maximum in VIs is discussed below. The relationship between  $V_{c_{\text{uptake}}}$  and VIs examines only the period with LAI greater than 1 (see method section 3.2). Therefore, the

values of  $V_{c_{\text{uptake}}}$  coincide with NDVI values between 0.4 and 1.0, or in the case of maize, EVI values between 0.2 and 0.8. Fig. 5.7 shows the linear and exponential relationships between  $V_{c_{\text{uptake}}}$  and VIs for the four dry-land crops. The relationship for soybean between  $V_{c_{\text{uptake}}}$  and NDVI showed a weak linear relationship with  $R^2$  of 0.24. In the case of maize, the relationship obtained with EVI from the entire growing season provided a stronger linear relationship than exponential with  $R^2$  of 0.57.  $V_{c_{\text{uptake}}}$  and NDVI for potato showed strong linear correlation with  $R^2$  of 0.80, although with a negative slope. In the case of sugar beet, the exponential correlation ( $R^2=0.50$ ) was slightly better than the linear relationships ( $R^2=0.38$ ). However, the exponential relationships in general amplify  $V_{c_{\text{uptake}}}$  during the middle of the season, e.g. small increases in NDVI lead to high and totally unrealistic values for  $V_{c_{\text{uptake}}}$  and underestimate  $V_{c_{\text{uptake}}}$  during the early and late growing season. Therefore, the linear relationships shown were considered further to estimate  $V_{c_{\text{uptake}}}$  in the descriptions of GPP (section 5.4.3). An alternative approach to describing  $V_{c_{\text{uptake}}}$  is with a seasonal development curve as in the case of LAI (cf. Fig. 5.5). The seasonal development curve is based on the determinations of  $V_{c_{\text{uptake}}}$  in Fig. 5.6 shifted in time (i.e., adjusted for different planting time) according to the maximum in VIs as illustrated in Fig. 5.8. In the case of dry-land crops, the  $V_{c_{\text{uptake}}}$  data are unfortunately limited in quantity due to the limited number of study years for replication. The results in Fig. 5.8 illustrate the best seasonal development  $V_{c_{\text{uptake}}}$  curve obtainable for each crop. The seasonal development curve has been characterized for daily application with GAM (solid line in Fig. 5.8). However, initial testing of the GAM function resulted in many cases where GPP was underestimated (see section 5.4.3) The initial curve obtained with the GAM method may not be adequate, since the highest values for scaled  $V_{c_{\text{uptake}}}$  are only 0.8 (Fig. 5.8, solid line). Therefore, the curve was rescaled with a multiplier in order that maximum values for  $V_{c_{\text{uptake}}}$  were reproduced (Fig. 5.8, dashed line). In the case of rice, this rescaling was not carried out, but it should be remembered that the rice curve is based on many more year of observation and represents the average values for  $V_{c_{\text{uptake}}}$  across sites.

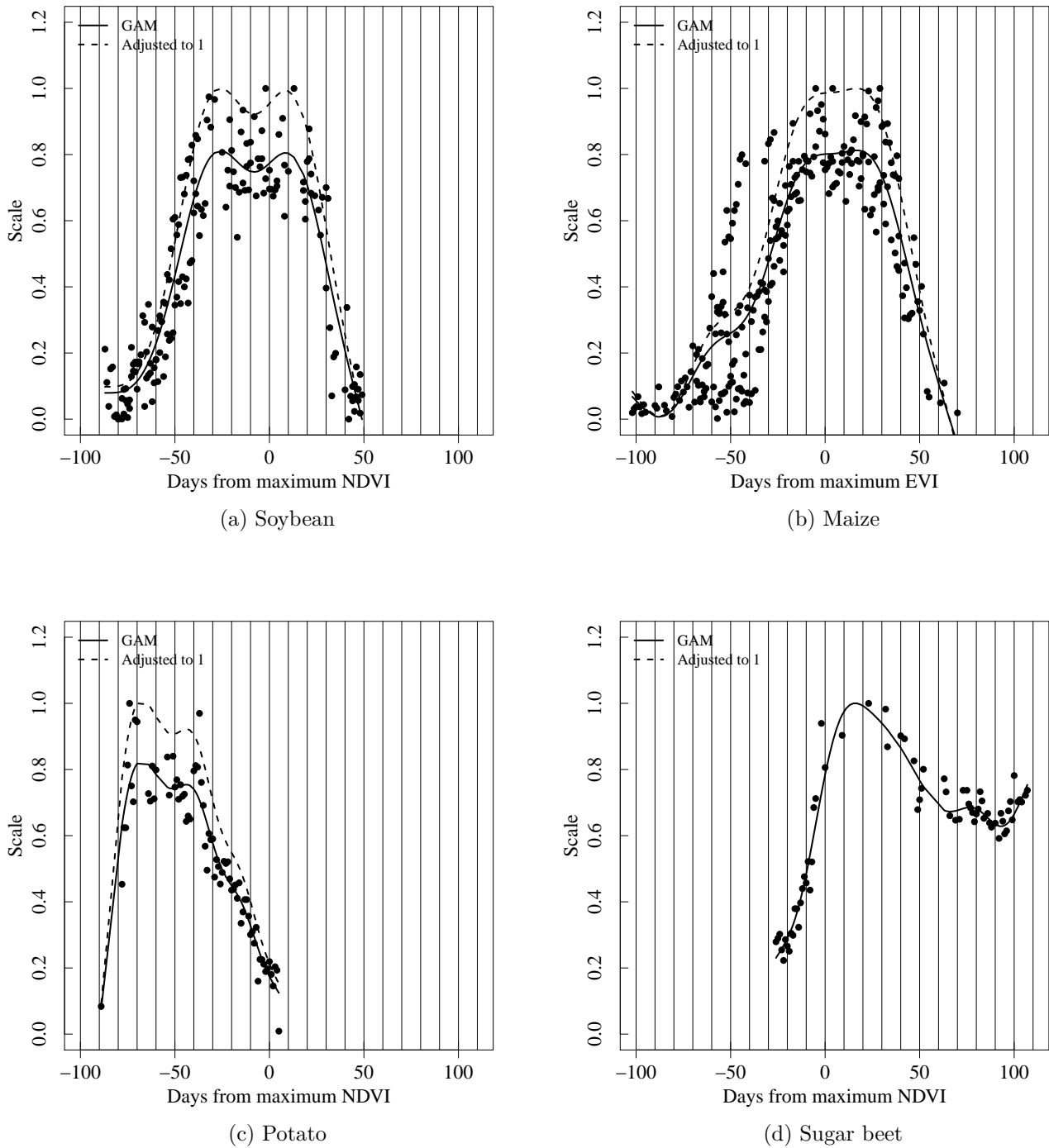


Fig. 5.8 Seasonal development curves for  $V_{c_{\text{uptake}}}$  scaled from 0 to 1 by dividing daily values by the maximum in  $V_{c_{\text{uptake}}}$  and utilizing data from each dry-land crop sites. The time of each observation is shown in relation to maximum in recorded VI. The solid line indicates the general growth curve determined by generalized additive model (GAM). The dashed line indicates an upward adjustment to reproduce the observed maxima in  $V_{c_{\text{uptake}}}$ .

### 5.4.3 GPP estimation with two models

Daily GPP as reproduced by two models (LAI from the consistent development and  $V_{c_{\text{uptake}}}$  linearly dependent on VIs; and LAI and  $V_{c_{\text{uptake}}}$  both dependent on consistent development curves) are compared to observations for all dry-land crop sites in Fig. 5.9, Fig. 5.10 and 5.11.

Table 5.4. Summary of observed GPP and modeled GPP with the best-fit linear model for  $V_{c_{\text{uptake}}}$  from VIs for dry-land crop sites with mean, standard deviation (STD), accumulated GPP (acc.GPP), difference between simulated GPP and observed GPP (%), slope (a), intercept (b), determination coefficients ( $R^2$ ), root mean square error (RMSE), coefficient of variation (CV), and modeling efficiency (MF).

Summary of observed GPP and modeled GPP									
Site	Year	Observed GPP			Modeled GPP			Period (DOY)	Difference (%)
		Mean	STD	acc.GPP	Mean	STD	acc.GPP		
US-Ne3	2002	10.30	3.63	813	8.81	3.56	696	78	-14
US-Ne3	2004	11.25	4.09	889	10.73	4.12	847	78	-5
US-Ne3	2003	12.84	9.01	1323	12.80	6.74	1319	107	0
US-Ne3	2005	14.72	6.30	1575	10.49	4.19	1122	107	-29
DE-Kli	2007	8.98	4.63	970	7.22	4.41	780	107	-20
HK	2010	6.56	3.81	486	5.72	3.06	423	73	-13
BE-Lon	2004	12.03	4.73	1612	8.35	2.44	1119	133	-31

Statistic for the correlation between observed GPP and modeled GPP							
Site	Year	a	b	$R^2$	RMSE	CV (%)	MF
US-Ne3	2002	0.87	-0.14	0.78	1.55	22.00	0.60
US-Ne3	2004	0.95	0.00	0.90	0.60	12.60	0.88
US-Ne3	2003	0.72	3.56	0.93	2.51	24.15	0.88
US-Ne3	2005	0.58	1.90	0.77	5.03	36.40	0.27
DE-Kli	2007	0.91	-0.95	0.91	1.81	24.62	0.77
HK	2010	0.77	0.67	0.92	1.21	22.82	0.84
BE-Lon	2004	0.40	3.52	0.61	4.66	40.54	-0.07

Accumulated observed GPP during the growing season varied from 486 gC m<sup>-2</sup> d<sup>-1</sup> to 1612 gC m<sup>-2</sup> d<sup>-1</sup> according to the crop type; from 846 to 909 gC m<sup>-2</sup> d<sup>-1</sup> for soybean, 972 to 1582 gC m<sup>-2</sup>

$\text{d}^{-1}$  for maize,  $486 \text{ gC m}^{-2} \text{ d}^{-1}$  for potato, and  $1612 \text{ gC m}^{-2} \text{ d}^{-1}$  for sugar beet. Modeled values by LAI from the consistent development and  $V_{\text{c}_{\text{uptake}}}$  linearly dependent on VIs ranged from  $423 \text{ gC m}^{-2} \text{ d}^{-1}$  to  $1319 \text{ gC m}^{-2} \text{ d}^{-1}$  with  $R^2$  above 0.61, RMSE below 5.03, CV above 12.60% and modeling efficiency (MF) between -0.06 and 0.88 (Table 5.4). Modeled values for GPP with LAI and  $V_{\text{c}_{\text{uptake}}}$  both dependent on consistent development curves ranged from  $296 \text{ gC m}^{-2} \text{ d}^{-1}$  to  $1184 \text{ gC m}^{-2} \text{ d}^{-1}$  with  $R^2$  above 0.60, RMSE below 8.17, CV above 27.96% and modeling efficiency (MF) between -0.15 and 0.52 (Table 5.5). Significant differences were found between the two methods in determining the seasonal course of  $V_{\text{c}_{\text{uptake}}}$ . Simulated GPP from  $V_{\text{c}_{\text{uptake}}}$  linearly dependent on VIs was largely under-estimated at US-Ne3 during 2005 and BE-Lon during 2004, little underestimated during the early growing season for US-Ne3 in 2002, and overestimated during the early growing season at the US-Ne3 in 2003. Limited study years may currently influence our ability to determine adequately the phenological curves as discussed in Chapter 6. However, modeled values for GPP with LAI and  $V_{\text{c}_{\text{uptake}}}$  both dependent on consistent development re-scaled curves ranged from  $362 \text{ gC m}^{-2} \text{ d}^{-1}$  to  $1196 \text{ gC m}^{-2} \text{ d}^{-1}$  with  $R^2$  above 0.60, RMSE below 6.54, CV above 22.10% and modeling efficiency (MF) between -0.28 and 0.82 (Table 5.6). GPP simulated with  $V_{\text{c}_{\text{uptake}}}$  considered consistent development re-scaled curves was better at the US-Ne3 in 2002 and 2005, DE-Kli in 2007, and BE-Lon in 2004 than  $V_{\text{c}_{\text{uptake}}}$  dependent on linear model. Simulated GPP from both LAI and  $V_{\text{c}_{\text{uptake}}}$  dependent on the development curves was in general underestimated, however, this method improved GPP estimation during the late growing season. Deviations from observation over the course of the season at each site reflect the differences found for observed and predicted  $V_{\text{c}_{\text{uptake}}}$  as represented in Table 5.3. Although the alternative method based on consistent phenological development led to an improvement in GPP prediction at the half of the study sites, the possibilities using this alternative method discussed in Chapter 6.

Table 5.5. Summary of observed GPP and modeled GPP with the general seasonal curve model  $V_{c_{\text{uptake}}}$  for dry-land crop sites with mean, standard deviation (STD), accumulated GPP (acc.GPP), difference between simulated GPP and observed GPP (%), slope (a), intercept (b), determination coefficients ( $R^2$ ), root mean square error (RMSE), coefficient of variation (CV), and modeling efficiency (MF).

Summary of observed GPP and modeled GPP									
Site	Year	Observed GPP			Modeled GPP			Period (DOY)	Difference (%)
		Mean	STD	acc.GPP	Mean	STD	acc.GPP		
US-Ne3	2002	10.30	3.63	813	8.16	3.48	644	78	-21
US-Ne3	2004	11.25	4.09	889	7.91	3.35	625	78	-30
US-Ne3	2003	12.84	9.01	1323	7.24	3.97	746	107	-44
US-Ne3	2005	14.72	6.30	1575	9.12	4.04	976	107	-38
DE-Kli	2007	8.98	4.63	970	6.33	3.49	684	107	-29
HK	2010	6.56	3.81	486	4.00	2.34	296	73	-39
BE-Lon	2004	12.03	4.73	1612	8.84	3.87	1184	133	-27

Statistic for the correlation between observed GPP and modeled GPP							
Site	Year	a	b	$R^2$	RMSE	CV (%)	MF
US-Ne3	2002	0.82	-0.26	0.72	2.21	27.96	0.36
US-Ne3	2004	0.75	-0.49	0.83	3.46	33.37	0.15
US-Ne3	2003	0.34	2.84	0.60	8.17	66.20	0.10
US-Ne3	2005	0.53	1.32	0.68	6.33	45.62	-0.15
DE-Kli	2007	0.71	-0.03	0.88	2.95	35.60	0.52
HK	2010	0.59	0.16	0.91	2.97	46.90	0.34
BE-Lon	2004	0.71	0.25	0.76	3.52	32.81	0.30

Table 5.6. Summary of observed GPP and modeled GPP with the general seasonal re-scaled curve model for  $V_{c_{\text{uptake}}}$  for dry-land crop sites with mean, standard deviation (STD), accumulated GPP (acc.GPP), difference between simulated GPP and observed GPP (%), slope (a), intercept (b), determination coefficients ( $R^2$ ), root mean square error (RMSE), coefficient of variation (CV), and modeling efficiency (MF).

Summary of observed GPP and modeled GPP									
Site	Year	Observed GPP			Modeled GPP			Period (DOY)	Difference (%)
		Mean	STD	acc.GPP	Mean	STD	acc.GPP		
US-Ne3	2002	10.30	3.63	813	9.10	3.7	719	78	-12
US-Ne3	2004	11.25	4.09	889	8.89	3.59	702	78	-21
US-Ne3	2003	12.84	9.01	1323	8.89	4.87	916	107	-31
US-Ne3	2005	14.72	6.3	1575	11.18	4.94	1196	107	-24
DE-Kli	2007	8.98	4.63	970	7.77	4.28	839	107	-14
HK	2010	6.56	3.81	486	4.89	2.85	362	73	-26
BE-Lon	2004	12.03	4.73	1612	8.76	3.85	1174	133	-27

Statistic for the correlation between observed GPP and modeled GPP							
Site	Year	a	b	$R^2$	RMSE	CV (%)	MF
US-Ne3	2002	0.87	0.10	0.73	1.32	22.10	0.60
US-Ne3	2004	0.81	-0.27	0.86	2.53	25.03	0.52
US-Ne3	2003	0.42	3.48	0.60	6.54	56.05	0.36
US-Ne3	2005	0.65	1.62	0.68	4.16	33.94	0.37
DE-Kli	2007	0.87	-0.03	0.88	1.34	22.05	0.82
HK	2010	0.72	0.20	0.91	1.95	32.85	0.68
BE-Lon	2004	0.71	0.21	0.76	3.55	33.29	0.28

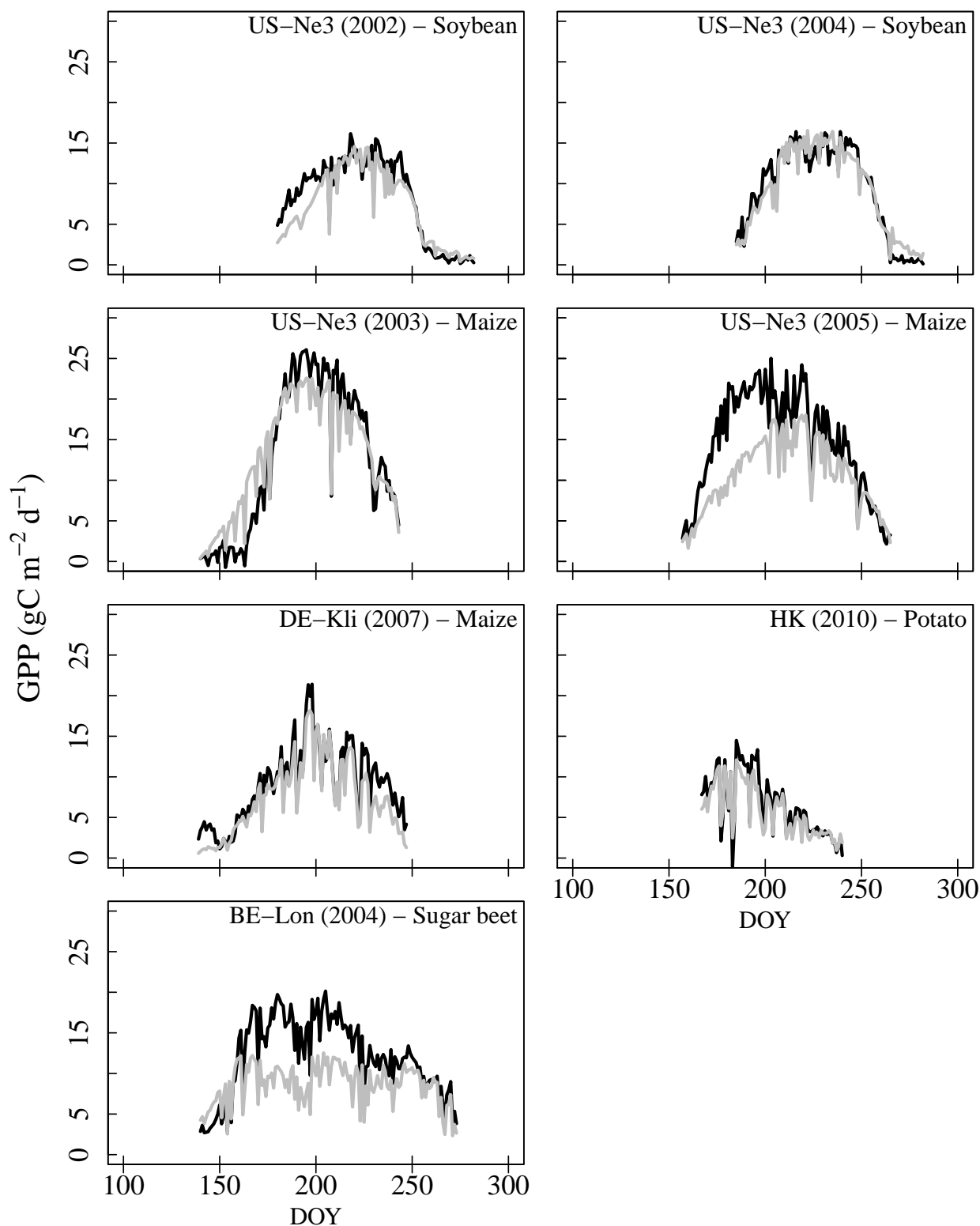


Fig. 5.9 Daily GPP estimation obtained with the linear regression model for  $V_{c_{uptake}}$  (gray solid line) and observed GPP (black solid line) of dry-land crop sites for the years indicated. US-Ne3 = Nebraska (USA), DE-Kli = Klingenberg (Germany), HK = Haeon (S. Korea), BE-Lon = Lonzeel (Belgium).

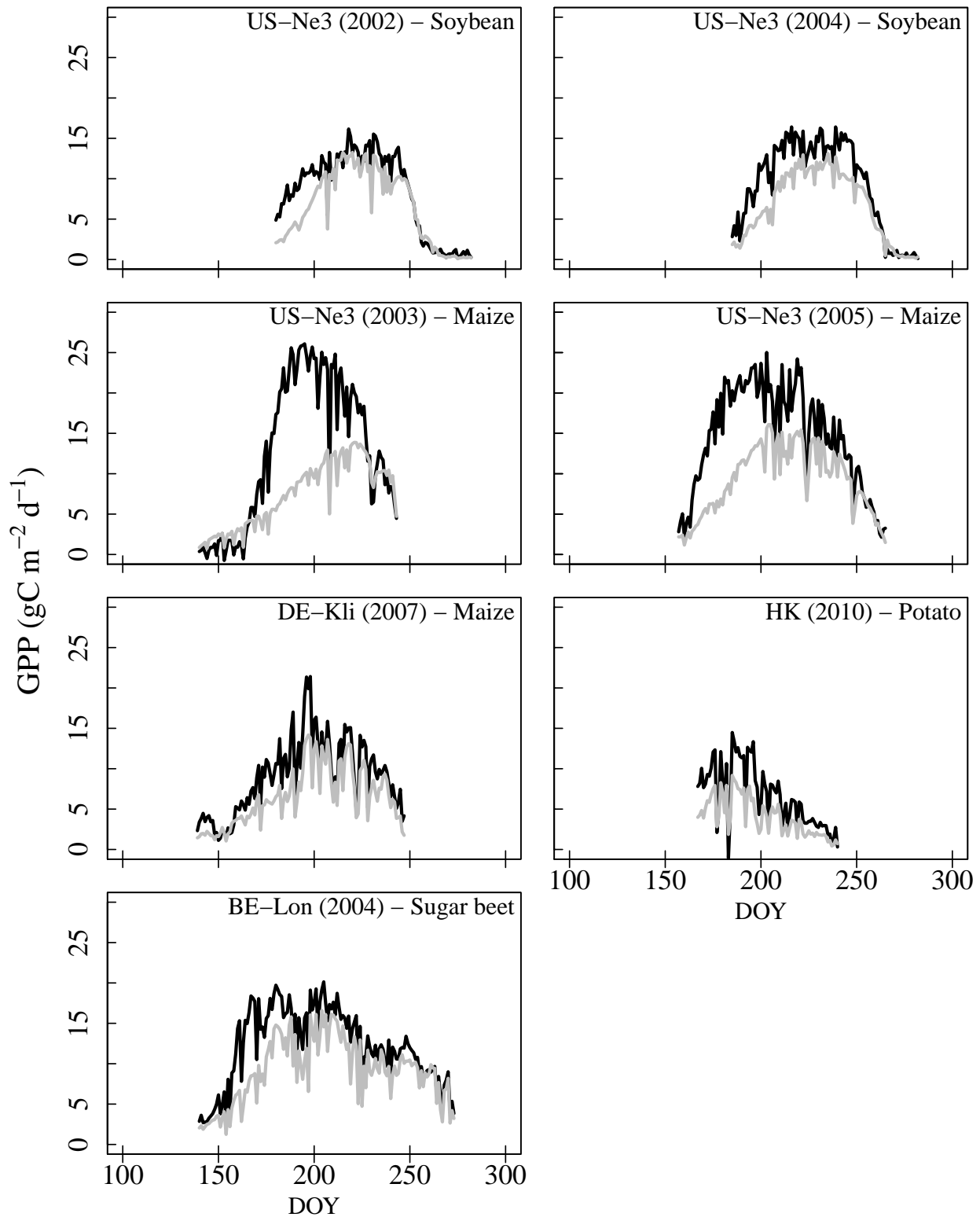


Fig. 5.10 Daily GPP estimation with the general seasonal curve model for  $V_{c_{uptake}}$  (gray solid line) and observed GPP (black solid line) of dry-land crop sites for the years indicated. US-Ne3 = Nebraska (USA), DE-Kli = Klingenberg (Germany), HK = Haeon (S. Korea), BE-Lon = Lonzeel (Belgium).

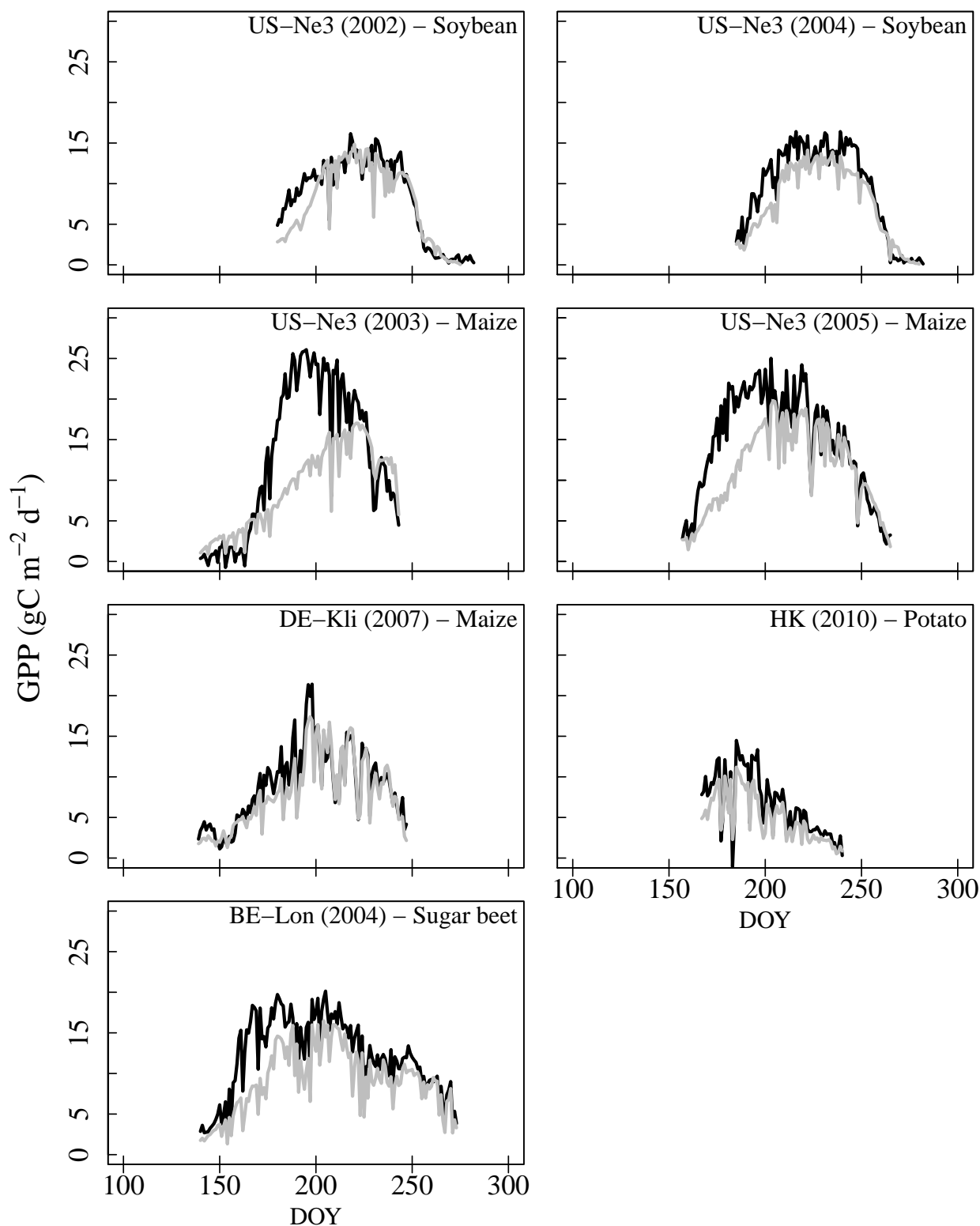


Fig. 5.11 Daily GPP estimation with the general seasonal re-scaled curve model for  $V_{C_{\text{uptake}}}$  (gray solid line) and observed GPP (black solid line) of dry-land crop sites for the years indicated. US-Ne3 = Nebraska (USA), DE-Kli = Klingenberg (Germany), HK = Haeon (S. Korea), BE-Lon = Lonzeel (Belgium).

# Chapter 6

## Discussion

In order to estimate GPP at large scales, inputting remotely sensed information to vegetation canopy models offers the required methodology. However, the reflectance observed by remote sensing is influenced by both physiological parameters and vegetation phenological development, i.e., changing canopy structure. The relative importance of these in determining vegetation indices is largely unknown. While in this study separation of these effects is not attempted, an approach is used to relate VIs stepwise both to LAI change and to physiological change over the course of the season. Seasonal changes in LAI and in the key physiological model parameter,  $V_{\text{C}_{\text{uptake}}}$  which reflects canopy carboxylation capacity at a given LAI are described in dependence on the vegetation indices NDVI and/or EVI. The relative successes and failures in the effort are discussed below.

### **6.1 Use of vegetation indices to estimate LAI of five crops**

In the case of rice paddy sites, LAI showed a good correlation with NDVI. The reflectance of rice paddies is influenced little by varying background effects, since the fields are flooded for long time periods (Xiao et al., 2002). Furthermore, the vegetation is not extremely dense and LAI has been shown to correlate with NDVI (Xiao et al., 2002; Pontauiller et al., 2003; Lu et al., 2005; Fan et al., 2008). In this sense, rice which grows with predominant vertical leaf orientation provides a good reference case for the work conducted here with other crops.

It was hypothesized in Chapter 1 that the physiological features of crops at the beginning of

the growing season are different than during senescence period, e.g., that LAI would show two different phases in relation to NDVI: 1) from the time of planting to the time of maturation of the canopy, and 2) from maturation throughout senescence and until harvest. While hysteresis effects of this type were apparent at some sites and during some years, the exponential relationship between NDVI and LAI over the entire season avoided over- and under-estimation at the beginning and end of the season as well as a major discontinuity in mid-season. However, the relationship between NDVI and LAI differed greatly between the various climate regions and across the study sites. Therefore, a general formulation for LAI exponentially correlated with NDVI resulted in very unsatisfactory predictions of the seasonal courses in LAI. The high sensitivity of LAI to small changes in LAI produce large deviations between predictions and measurements in mid-season.

An alternative approach was developed to identify the seasonal course of LAI for rice where the study locations are spread geographically in different climate regions and where year to year climate variation occurs. A consistent development curve for rice in the sense of LAI changes over time was described with GAM in relation to the maximum in NDVI, assuming that despite interference from surrounding features, the maximum in LAI and NDVI correspond. The consistent development curve resulted in significant improvements in prediction of the seasonal course for LAI. It allowed a generalized method to obtain estimates of rice paddy LAI across the study sites. The seasonal course of LAI followed the measured patterns in LAI much better than that obtained with an exponential model.

For the dry-land crops soybean, maize, potato, and sugar beet, LAI was also correlated with NDVI, although in the case of maize, EVI was a much better predictor. Yan et al. (2009) carried out estimations of GPP with a remote-sensing-based model for a double cropping system with winter wheat and maize, EVI was also found in their study to provide more accuracy. NDVI exhibited no sensitivity (the response was saturated) during the period of mature vegetation, whereas EVI remained more responsive to small changes. LAI of maize shows relatively rapid increase and decrease during the growth period (Fig. 5.2). EVI seems better suited to following these changes, resulting in a better correlation with EVI than NDVI in the case of maize. The linear and exponential relationships at the dry-land crops were compared from the entire season and by separating the season before and after maximum VIs. Overall, the linear relationships

using BV combinations (separation of the season into two time periods) were stronger, but the results still were inadequate for explaining or predicting the seasonal course of LAI.

As in the case of rice, consistent development curves were established for LAI with each crop. However, it was not possible to evaluate whether the seasonal courses are generally valid, since the years available for study were extremely limited. In the case of soybean and maize, there were multiple years upon which to base the development curve. For potato and sugar beet, the single years evaluated may lead to a highly biased and unsatisfying growth curve. It seems reasonable to suggest (hypothesize) that the consistent development curve will be improved with multiple years of data for the various crop types in further studies. We can conclude, however, that for the data sets under study this new approach worked as well as more traditional regression approaches. Further testing will demonstrate whether this “biologically-based” approach, as in the case of rice, is potentially better in estimation of the critical values for LAI needed in spatial models for GPP.

## 6.2 Use of vegetation indices to estimate $V_{c_{\text{uptake}}}$ for five crops

The eddy covariance methodology (EC) applied at rice paddy sites quantifies seasonal changes in GPP in relation to prevailing meteorological conditions (Kwon et al., 2010). By fitting the PIXGRO canopy model routine to flux data and with known LAI and meteorological conditions on a daily basis, an estimated seasonal time course for the key physiological parameter  $V_{c_{\text{uptake}}}$ , i.e., canopy carboxylation capacity, is obtained. Owen et al. (2007) obtained such estimates for many EC monitoring sites by assuming a constant LAI at the level of the maximum observed. They carried out their analysis with constant LAI, because measured time courses for LAI (periodic measurements) did not exist from many of the study sites. While assumption of a constant LAI at maximum level may allow a more complete use of data from EC study sites, and in the way lead to reasonable spatial models for GPP, the objective of the current study is to use remote sensing first to determine structural change (the seasonal course of LAI) and, therefore, to compare patterns for changes in canopy physiology for different crops, i.e., accurate seasonal patterns for  $V_{c_{\text{uptake}}}$ . At the beginning of this study (results is not shown) use of constant LAI

was also examined, but seasonal LAI gave significantly better predictions for GPP. A further consideration is that  $V_{c_{\text{uptake}}}$  patterns should be related to seasonal change in leaf carboxylation capacity as determined by other methods such as with leaf cuvette experimentation. The use of a seasonal course in LAI should help to bring information from EC and leaf level ecophysiological studies together.

Wang et al. (2008) and Muraoka et al. (2012) have demonstrated from cuvette experiments that leaf level carboxylation capacity is correlated with NDVI and/or EVI. Similarly, NDVI correlated with  $V_{c_{\text{uptake}}}$  in linear regression at rice paddy sites (Fig. 4.13 and Fig. 4.14). The HK site in 2010 and the ESES2 site in 2008 exhibited strong linear relationships. MSE also exhibited linear correlation during 2002 2003, 2004, and 2005, although as yet unexplained hysteresis phenomena were also observed. Similar hysteresis phenomena with respect to vegetation indices and photosynthetic capacity (i.e., LAI, maximum carboxylation rate) were demonstrated in previous studies by Muraoka et al. (2012) in deciduous forest at Takayama, Japan. Leaf photosynthetic capacity during leaf expansion, with mature leaves in mid-season, and during senescence shifted with respect to reflectance properties, causing hysteresis. The hysteresis phenomenon observed here for agricultural crops was not strong as found for forest, however, it remains a problem with respect to the use of remote sensing for determination of GPP.

$V_{c_{\text{uptake}}}$  of dry-land crops was examined with respect to possible linear, exponential, logarithmic, and logistic curve dependency in relation to NDVI and EVI, because of the difficulties to establish a general relationship among all of the crops, partly due to the limited data. Overall, a linear relationship provided the best prediction of  $V_{c_{\text{uptake}}}$  (Fig. 5.7) for soybean, maize, and potato.  $V_{c_{\text{uptake}}}$  of sugar beet was better described statistically with an exponential relationship, but the exponential model amplified  $V_{c_{\text{uptake}}}$  during the middle of the growing season. Therefore, seasonal development of  $V_{c_{\text{uptake}}}$  was again based on the linear relationship. However,  $V_{c_{\text{uptake}}}$  estimated by a linear relationship resulted in underestimation of GPP. An alternative approach attempted to calculate the seasonal course of  $V_{c_{\text{uptake}}}$  based on a development curve. The development curve of  $V_{c_{\text{uptake}}}$  predicted GPP with no significant improvement (only at HK and HFK were there a slightly better statistical result). Since the chosen method for defining the development curve did not allow the maximum in  $V_{c_{\text{uptake}}}$  to be reached, underestimation of GPP occurred. The methods used by GAM to obtain the desired development curve do not

allow maximum values to be achieved due to the smoothing algorithm employed. Generalized additive models (GAMs) have been used to understand non-linear ecological responses to a wide range of environmental variables (Hastie et al., 1990; Yee et al., 1991; Liu, 2008). GAMs are an extension of generalized linear models (GLMs), a linear function of GLMs (Eq. 6.1,  $\sum_{j=1}^p \beta_j X_j$ ) replaces to an unspecified smooth functions (Eq. 6.2,  $\sum_{j=1}^p f_j(X_j)$ , Hastie et al., 1986; Yee et al., 1991; Liu, 2008).

$$g(\mu) = \beta_0 + \sum_{j=1}^p \beta_j X_j \quad (6.1)$$

$$g(\mu) = f_0 + \sum_{j=1}^p f_j(X_j) \quad (6.2)$$

where the  $f_j$  are unspecified smooth function or non-parametric function. In this non-parametric function, there are many different types of smoothers, e.g., running lines, running means, cubic splines, etc., using the algorithms called back fitting, local scoring, likelihood, and etc. Therefore, GAMs can be more general and flexible to allow a wide range of response curves to the non-linear relationships. GAMs were proposed to provide the alternative approach for limitation of linear function, since it is an appropriate tool for data with complex dependencies. However, GAMs are based on assumption that all variables are independent and without error, and they never provide the exact regression values of the fitting curve (Hastie et al., 1986). The smoothing routines are not able to analyze the real physiological or phenological phenomenon, so the seasonal development curve from GAM did not reach the maximum estimated for each crop.

In the case of dry-land crops, the development curve for  $V_{c_{\text{uptake}}}$  was rescaled with a multiplier in order to reproduce the maximum values of  $V_{c_{\text{uptake}}}$  (Fig. 5.8). Predicted GPP for sugar beet was then significantly improved, but with the other crop sites showed underestimation of GPP still occurred over entire growing season (Fig. 5.10). On the other hand, rescaled development curve did lead to improvements at US-Ne3 during 2002 for soybean and 2005 for maize, DE-Kli during 2007 for maize, and BE-Lon during 2004 for sugar beet. Further research is required in order to established and validate seasonal curves for photosynthetic capacity across different location and the different climate conditions for the various crop types.

### 6.3 Limitations due to the remotely sensed vegetation indices

A number of shortcomings in the use of satellite vegetation indices to estimate GPP still remain. First, the uncertainties in VIs may be caused by missing or bad data or systemic error in obtaining the daily smoothed VIs. Secondly, VIs are not sensitive enough to capture rapid changes in the crop development during initial growth period (Wang et al., 2005). Similar results were found in this study for HK in 2010, MSE in 2003, and 2004, BE-Lon in 2004, and US-Ne3 in 2003 and 2005. Thirdly, VIs are relatively insensitive when LAI is over 4 (Brantley et al., 2011) leading to large predicted changes in LAI in derived regressions when VIs change during mid-season. Most of the rice sites, DE-Kli in 2007, and US-Ne3 in 2005 exhibited over- and/or underestimation of LAI predicted with the VIs regression. Since accurate LAI estimation is a key factor to calculate GPP (Bantley et al., 2010), continued research focus on improving such estimates is essential in future studies, and the consistent development approach must be explored further. Fourth, the patch sizes between MODIS satellite reflectance data and field size remains to date unmatched in many regions of the world. This is certainly the case at the Asian sites studied. Therefore, VIs could not capture the specific signal of crops studies. While rice paddy and soybean from US-Ne3 have more than 80% homogeneity, potato from HK and sugar beet from BE-Lon occupied much less of the MODIS patch size. For example, the resolution of MODIS is ca. 250 m by 250 m whereas the potato field size was ca. 158 m by 158 m, which also included the field margins. Homogeneity between the potato field and MODIS pixel was only ca. 60%. Although also influenced by the frequency and time of harvests and the smoothing routine, the estimated maximum in LAI occurred on DOY 186, while the maximum NDVI occurred around DOY 230 at the HK potato site (Fig. 6.1). It is possible that influences from the surrounding vegetation are responsible for this difference, whereas it may also be case that NDVI continues to change as a result of leaf properties and arrangement. Clarification requires detailed ground level studies of crop growth and remote sensing of VIs. Finally, LAI measurements were carried out every 2 or 3 weeks at eddy covariance sites. This infrequent sampling of LAI results in the tendency to miss important phenological events during the early growing season, which is critical to predicting the total growth season GPP.

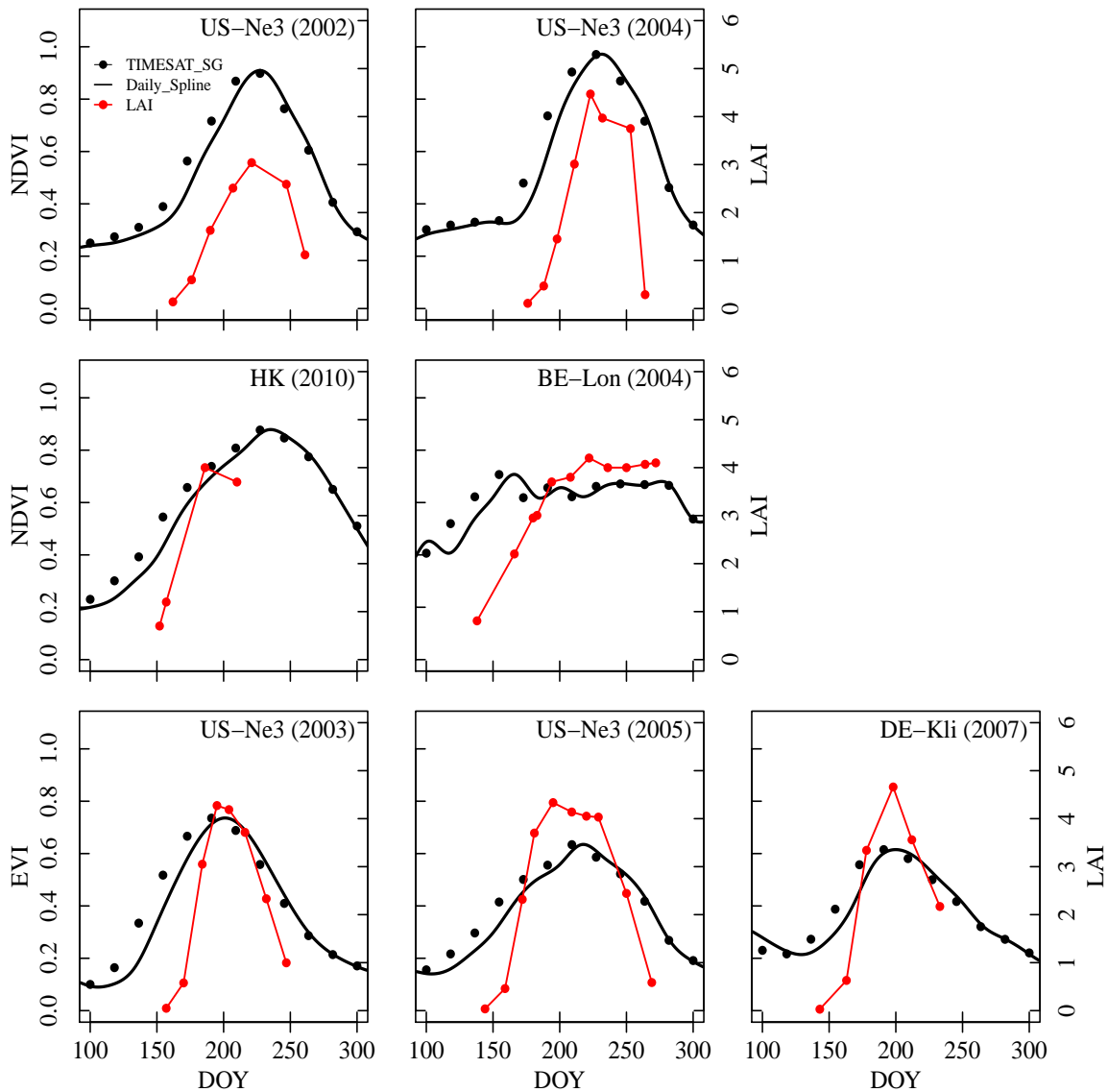


Fig. 6.1 NDVI and EVI by TIMESAT (closed circle), daily NDVI by spline (solid line), and measured LAI (closed red circle with solid line) at dry-land crop sites for the years indicated. US-Ne3 = Nebraska (USA), DE-Kli = Klingenberg (Germany), HK = Haeon (S. Korea), BE-Lon = Lonze (Belgium).

Further studies are required in more detail and with accurately sampled spatial data in agricultural ecosystems with various crop types in order to calibrate LAI and physiological parameters such as  $V_{c_{\text{uptake}}}$  for use in models for GPP. With such studies, the restriction here that eddy covariance data, GPP and  $V_{c_{\text{uptake}}}$  could only be evaluated for situations with  $\text{LAI} > 1.0$  can be improved.

## 6.4 GPP estimation for agricultural ecosystems

Despite the obvious importance of such studies, most EC measurements carried out to characterize agricultural ecosystem started only during the last decade. As a result, only few method have been applied to date to estimate or model GPP. These can be put into several categories: 1) GPP is estimated directly by eddy covariance measurement and interpreted with respect to the supplemental field data (Moureaux et al., 2008; Aubinet et al., 2009; Suyker et al., 2005; Suyker et al., 2010); 2) parameters are estimated to directly relate GPP to remote-sensing-based vegetation indices (Zhang et al., 2008; Yan et al., 2009; Wang et al., 2010); 3) observations have been used to estimate a key parameter of light use efficiency and GPP is evaluated by MODIS algorithm (Li et al., 2007; Chen et al., 2011), and 4) empirical approaches have attempted to use VIs and PAR estimates to calculate the seasonal course of GPP (Wu et al., 2009; Xiao et al., 2010; Gitelson et al., 2012; Peng et al., 2011; Peng et al., 2012). The current study differs from these first by focusing on the efficient gas exchange parameter  $V_{c_{uptake}}$  as first defined by Owen et al. (2007) and secondly by attempting to define consistent development curves for LAI and  $V_{c_{uptake}}$  and to reference these to the maximum observed VIs.

Previous studies reported the relationship between modeled GPP and observed GPP with  $R^2$  from 0.68 to 0.95 on and 8-day or daily interval at the soybean and maize sites (Yan et al., 2009; Wang et al., 2010; Gitelson et al., 2012; Peng et al., 2011; Peng et al., 2012),  $R^2$  of 0.86 at the crop sites in U.S.A. (Xiao et al., 2010). Harazono et al. (2009) reported an empirically estimated GPP using the remote sensed greenery ratio (GR) and PAR. Overall GPP was underestimation at MSE during 2003. In this study, the relationship between observed GPP and modeled GPP based on the consistent development curve for LAI shows remarkably improved results over regression based values with  $R^2$  from 0.79 to 0.93. Modeled GPP based on the consistent development curve for both LAI and  $V_{c_{uptake}}$  agreed with  $R^2$  from 0.76 to 0.92 (within the 95% confidence interval) at the rice paddy sites. In the case of dry-land crops, the relationship between modeled GPP based on the consistent development curve for LAI showed significantly improved results with  $R^2$  from 0.61 to 0.93 (within the 95% confidence interval), while modeled GPP based on the consistent development curve for both LAI and  $V_{c_{uptake}}$  exhibited an  $R^2$  from 0.60 to 0.91 (within the 95% confidence interval). Further study is in order because the development curve based approach seems to have potential to predict GPP

better than simple linear models or other statistical models to estimate the critical parameters in agricultural ecosystems (Fig. 5.10 and 5.11, Table 5.5 and 5.6). The modeled GPP at dry-land sites obtained with re-scaled curves for  $V_{c_{\text{uptake}}}$  showed a 1.4% improvement in  $R^2$ , 40% in RMSE, and 13% in total GPP.

Previous studies have been limited to only a few different crop types, and the results are not yet generalized adequately. Clearly, larger spatial and longer time series of data, e.g., longer time scales, must be investigated. From this study, it is suggested that remote sensing can be applied with consistent development curve for two major components of GPP modeling, i.e., LAI and carboxylation capacity. The method is sensitive to differences in management and adjustments can be made for differences in planting time at differences locations. Of course, it is critical to know what crop is being planted in the landscapes that are viewed.



# Chapter 7

## Conclusion

This study provides insight with respect to achieving improved methods for assessing GPP in agricultural ecosystems through the use of process-based models and remote sensing. The MODIS product provided by NASA underestimates and poorly represents GPP, especially in croplands (Zhang et al., 2008; Yan et al., 2009; Gilteson et al., 2012). By following a different methodology, MODIS vegetation indices are shown to be effective in estimating crop phenology, LAI, and the simplified physiological parameter  $V_{c_{\text{uptake}}}$  at local site-specific scale. In the case of paddy rice, a generalized model was developed to estimate GPP under various climate conditions and at geographically widely separated locations. Dry-land crops, since they differ genetically in terms of developmental controls, require multiple parameterizations of PIXGRO model in order to obtain GPP for various crop types. However, it is currently difficult to complete the evaluation of characteristic parameters for dry-land crops, due to lack of data from multiple sites and geographical locations for each, i.e., there is not adequate replicative studies as with the case of rice.

The study suggests methods for development of a “best-fit model” to estimate GPP by bridging satellite information on VIs and ground observations. The best-fit model constructed here, which used VIs to estimate phenology (LAI) and physiological parameter ( $V_{c_{\text{uptake}}}$ ) based on consistent development curves, provided accurate seasonal values for GPP with acceptable statistical values (Table 4.4 and Table 4.5), although limited so far to the period where LAI > 1.0. Photosynthetic capacity in relation to VIs changes over the course of growing season together with the carbon to nitrogen ratio of leaves in the plant canopy. Nitrogen in foliage determines investments in chlorophyll and rubisco (Bonan, 2002), i.e., the machinery for the

photosynthetic process. This may decrease over the course of the season with little influence on reflectance properties. Where data was available, this study found that carbon to nitrogen ratio did accompany in some cases change in vegetation indices. There types of physiological changes (reflecting the relationship between  $V_{C_{\text{uptake}}}$  and VIs) may account for the hysteresis effects that were observed in particular data sets (section 4.5).

Improvements in the modeling approach require that more detailed biological supplementary information should accompany EC studies in the future, e.g., frequent and spatial sampling of crop canopy structure, local on the ground measurements of VIs, monitoring of physiological characteristics such as C/N ratio, chlorophyll content, etc. On the one hand, there detailed studies must be designed to support an extension of the approach describe here, moving away from empiricism and linking remote sensing to the biological processes being observed. Ultimately, however, the estimation of the crop GPP should be possible and should be undertaken without the need for additional field surveys, since these cannot be conducted at large scales.

# Appendices



# Appendix A: A case study of rice paddy

Table A.1 Statistics for the linear and exponential relationship between estimated LAI and NDVI with slope ( $a$ ), intercept ( $b$ ), determination coefficients ( $R^2$ ), and root mean square error (RMSE).

Site	Year	Linear model				Exponential model			
		a	b	$R^2$	RMSE	a	b	$R^2$	RMSE
HK	2010	14.27	-8.52	0.38	2.15	16.53	-12.24	0.83	0.83
MSE	2002-2005	9.38	-4.06	0.59	2.36	10.26	-7.01	0.60	1.63
ESES2	2007-2008	11.27	-4.87	0.76	3.16	6.39	-3.87	0.67	1.27
HK-before	2010	13.86	-8.24	0.28	2.34	16.52	-12.51	0.90	1.21
HK-after	2010	20.47	-13.06	NA	1.54	10.62	-7.22	NA	0.01
MSE-before	2002-2005	7.43	-3.45	0.72	1.39	11.18	-7.99	0.80	0.93
MSE-after	2002-2005	8.59	-2.78	0.53	3.07	6.37	-3.75	0.23	1.30
ESES2-before	2007-2008	11.36	-5.41	0.8	2.66	7.30	-4.82	0.84	0.84
ESES2-after	2007-2008	7.87	-1.58	0.9	3.77	1.81	0.08	0.93	0.24
Asia		9.52	-4.31	0.53	2.33	10.57	-7.34	0.61	1.50
Entire		10.3	-4.66	0.6	2.6	9.21	-6.25	0.59	1.52
Asia-before		8.10	-3.93	0.56	1.65	11.43	-8.3	0.78	0.97
Asia-after		8.78	-3.04	0.47	2.95	6.42	-3.82	0.24	1.25
Entire-before		9.50	-4.64	0.64	2.01	10.01	-7.15	0.75	1.02
Entire-after		8.79	-2.87	0.53	3.19	5.18	-2.80	0.23	1.14

Table A.2. Statistics for the linear and exponential relationship between estimated LAI and EVI with slope ( $a$ ), intercept ( $b$ ), determination coefficients ( $R^2$ ), and root mean square error (RMSE).

Site	Year	Linear model				Exponential model			
		a	b	$R^2$	RMSE	a	b	$R^2$	RMSE
HK	2010	16.65	-6.99	0.38	2.26	18.28	-9.93	0.72	1.06
MSE	2002-2005	7.94	-1.24	0.59	2.53	8.36	-3.77	0.55	4.38
ESES2	2007-2008	11.87	-2.81	0.82	3.33	6.72	-2.70	0.72	1.98
HK-before	2010	7.74	-3.20	0.34	0.87	17.81	-10.31	0.96	0.32
HK-after	2010	29.98	-13.28	0.78	3.31	10.72	-4.93	0.97	0.30
MSE-before	2002-2005	8.28	-1.59	0.77	1.99	9.73	-4.37	0.72	6.63
MSE-after	2002-2005	4.64	0.86	0.10	3.17	4.62	-1.69	0.08	2.13
ESES2-before	2007-2008	12.26	-3.38	0.89	2.80	7.68	-3.42	0.88	1.22
ESES2-after	2007-2008	7.39	0.25	0.70	3.96	1.70	0.50	0.73	0.53
Asia		7.88	-1.40	0.49	2.48	8.43	-3.96	0.52	3.53
Entire		9.18	-1.85	0.59	2.76	8.07	-3.67	0.55	3.19
Asia-before		7.22	-1.44	0.57	1.85	9.13	-4.40	0.61	3.43
Asia-after		5.72	0.25	0.15	3.19	4.90	-1.82	0.12	2.15
Entire-before		8.88	-2.04	0.67	2.17	8.81	-4.18	0.66	2.88
Entire-after		6.45	0.12	0.24	3.44	4.14	-1.25	0.12	1.82

Table A.3. Parameter sets between  $V_{c_{uptake}}$  and VIs for rice paddy sites with slope (a), intercept (b), determination coefficients ( $R^2$ ), root mean square error (RMSE), akaike information criterion (AIC), difference (Diff., %) between simulated GPP (s.GPP) and observed GPP (o.GPP). 'Version' indicates either estimated LAI (estLAI) or constant LAI (Constant). Mode 1 is LAI estimation model, N is NDVI, E is entire, BA is before and after maximum VIs, V is  $V_{c_{uptake}}$ , N is NDVI, E is 1) located next to 'V' then EVI 2) located on third position then Entire, and BA is before and after maximum VIs. Eq. is an equation of linear (Lm) or exponential (Exp) model.

Site	Year	Version	Mode1	Mode2	Eq.	a	b	$R^2$	RMSE	AIC	s.GPP	o.GPP	Diff. (%)
HK	2010	estLAI	NBA	VNBA	Exp	0.89	1.17	0.86	3.12	30793	648	745	-15
HK	2010	estLAI	NBA	VNE	Lm	0.96	0.90	0.84	3.23	31736	641	745	-16
HK	2010	estLAI	NBA	VNBA	Lm	0.94	0.97	0.86	3.07	30967	645	745	-16
HK	2010	estLAI	NBA	VEE	Lm	0.96	0.90	0.84	3.18	31504	641	745	-16
HK	2010	estLAI	NBA	VEBA	Lm	0.94	0.96	0.86	3.07	30991	644	745	-16
HK	2010	estLAI	NBA	VEBA	Exp	0.90	1.16	0.86	3.12	30889	642	745	-16
HK	2010	estLAI	E	VNE	Lm	0.94	1.00	0.84	3.21	31574	640	745	-16
HK	2010	estLAI	NBA	VNE	Lm	0.96	0.92	0.83	3.33	32126	639	745	-17
HK	2010	estLAI	NBA	VEE	Lm	0.96	0.92	0.83	3.26	31848	638	745	-17
HK	2010	estLAI	NBA	VNBA	Exp	0.93	1.08	0.87	3.01	30575	633	745	-18
HK	2010	estLAI	NBA	VNBA	Lm	0.97	0.92	0.86	3.04	30868	632	745	-18
HK	2010	estLAI	NBA	VEE	Exp	0.95	0.99	0.85	3.12	31168	631	745	-18
HK	2010	estLAI	E	VNE	Exp	0.93	1.10	0.85	3.17	31283	629	745	-18
HK	2010	estLAI	E	VEE	Lm	0.94	1.01	0.83	3.29	31876	634	745	-18
HK	2010	estLAI	NBA	VEBA	Lm	0.98	0.90	0.86	3.05	30917	627	745	-19
HK	2010	estLAI	E	VNBA	Lm	0.96	0.97	0.86	3.07	30944	626	745	-19
HK	2010	estLAI	E	VEE	Exp	0.93	1.14	0.84	3.31	31813	625	745	-19
HK	2010	estLAI	NBA	VNE	Exp	0.98	0.95	0.85	3.11	31115	622	745	-20
HK	2010	estLAI	NBA	VEE	Exp	0.96	1.00	0.85	3.18	31385	622	745	-20
HK	2010	estLAI	NBA	VEBA	Exp	0.95	1.06	0.86	3.02	30658	622	745	-20
HK	2010	estLAI	E	VNBA	Exp	0.93	1.13	0.86	3.06	30763	623	745	-20
HK	2010	estLAI	E	VEBA	Lm	0.97	0.97	0.86	3.08	31009	622	745	-20
MSE	2003	estLAI	NBA	VEBA	Lm	0.67	0.96	0.90	4.83	31930	1090	883	19
MSE	2002	estLAI	E	VEBA	Exp	0.59	1.84	0.80	6.88	38070	1087	938	14
MSE	2003	estLAI	NBA	VNBA	Lm	0.35	3.36	0.41	11.73	44317	991	883	11
MSE	2002	estLAI	NBA	VNE	Lm	0.08	5.37	0.07	28.35	48461	1039	938	10
MSE	2003	estLAI	E	VEBA	Exp	0.67	1.43	0.85	4.93	34914	973	883	9
MSE	2002	estLAI	E	VNBA	Exp	0.71	1.60	0.83	4.99	36752	966	938	3
MSE	2002	estLAI	E	VEBA	Lm	0.77	1.27	0.87	4.09	35027	956	938	2
MSE	2004	estLAI	NBA	VEBA	Exp	0.68	2.20	0.79	6.61	38133	1069	1056	1
MSE	2004	estLAI	NBA	VNBA	Exp	0.71	2.08	0.80	6.11	37672	1048	1056	-1

continued from previous page

Site	Year	Version	Model	Model2	eq.	a	b	R <sup>2</sup>	RMSE	AIC	s.GPP	o.GPP	Diff. ( %)
MSE	2004	estLAI	NBA	VEBA	Exp	0.68	2.32	0.77	6.77	38765	1044	1056	-1
MSE	2003	estLAI	E	VNBA	Exp	0.80	1.13	0.88	3.48	33727	873	883	-1
MSE	2003	estLAI	E	VEBA	Lm	0.83	0.98	0.90	3.05	32143	875	883	-1
MSE	2004	estLAI	NBA	VNBA	Exp	0.71	2.21	0.78	6.31	38389	1023	1056	-3
MSE	2003	estLAI	NBA	VNE	Exp	0.83	1.11	0.88	3.28	33550	846	883	-4
MSE	2002	estLAI	E	VNBA	Lm	0.50	3.04	0.51	8.93	44041	901	938	-4
MSE	2005	estLAI	E	VNBA	Lm	0.19	5.14	0.17	19.19	46398	916	957	-4
MSE	2003	estLAI	E	VEE	Exp	0.80	1.28	0.87	3.59	33995	853	883	-4
MSE	2005	estLAI	E	VEBA	Exp	0.77	1.62	0.83	4.69	35980	922	957	-4
MSE	2003	estLAI	NBA	VEE	Lm	0.93	0.65	0.92	2.41	30617	838	883	-5
MSE	2003	estLAI	NBA	VEE	Exp	0.87	0.92	0.90	2.82	31986	842	883	-5
MSE	2003	estLAI	E	VEE	Lm	0.87	0.96	0.90	2.89	32195	842	883	-5
MSE	2003	estLAI	NBA	VNE	Lm	0.92	0.74	0.92	2.48	30785	832	883	-6
MSE	2003	estLAI	E	VNE	Exp	0.80	1.36	0.84	3.85	35548	830	883	-6
MSE	2005	estLAI	E	VNBA	Exp	0.81	1.49	0.85	4.20	35159	899	957	-6
MSE	2005	estLAI	NBA	VNBA	Exp	0.81	1.50	0.84	4.33	35702	896	957	-7
MSE	2005	estLAI	NBA	VNBA	Lm	0.18	5.21	0.16	19.26	46531	893	957	-7
MSE	2005	estLAI	NBA	VEBA	Exp	0.80	1.57	0.83	4.54	36230	897	957	-7
MSE	2003	estLAI	E	VNE	Lm	0.88	0.99	0.87	3.15	33781	828	883	-7
MSE	2003	estLAI	E	VNBA	Lm	0.92	0.80	0.91	2.59	31465	818	883	-8
MSE	2002	estLAI	NBA	VNBA	Exp	0.88	1.17	0.88	3.30	34343	851	938	-10
MSE	2002	estLAI	NBA	VEBA	Lm	0.93	0.91	0.90	2.94	33219	852	938	-10
MSE	2002	estLAI	NBA	VNE	Exp	0.89	1.16	0.88	3.30	34423	847	938	-11
MSE	2002	estLAI	NBA	VNBA	Exp	0.89	1.20	0.87	3.43	34927	843	938	-11
MSE	2002	estLAI	NBA	VNBA	Lm	0.95	0.86	0.91	2.79	32601	845	938	-11
MSE	2002	estLAI	NBA	VEBA	Exp	0.88	1.24	0.88	3.42	34799	843	938	-11
MSE	2004	estLAI	NBA	VEBA	Lm	0.84	1.75	0.81	5.01	37307	949	1056	-11
MSE	2002	estLAI	E	VNE	Exp	0.83	1.48	0.86	3.84	35726	848	938	-11
MSE	2002	estLAI	E	VEE	Exp	0.83	1.48	0.86	3.78	35519	844	938	-11
MSE	2002	estLAI	NBA	VNE	Exp	0.89	1.22	0.87	3.47	35093	839	938	-12
MSE	2002	estLAI	NBA	VEE	Lm	0.95	0.89	0.89	3.13	34241	834	938	-12
MSE	2002	estLAI	NBA	VEBA	Lm	0.94	0.95	0.89	3.12	34083	841	938	-12
MSE	2002	estLAI	NBA	VEBA	Exp	0.88	1.27	0.87	3.55	35350	837	938	-12
MSE	2002	estLAI	E	VNE	Lm	0.91	1.11	0.89	3.16	33972	837	938	-12
MSE	2004	estLAI	E	VNBA	Exp	0.79	2.06	0.81	5.37	37586	944	1056	-12
MSE	2002	estLAI	E	VEE	Lm	0.90	1.12	0.89	3.18	34002	841	938	-12
MSE	2002	estLAI	NBA	VNBA	Lm	0.95	0.90	0.90	3.00	33609	832	938	-13
MSE	2004	estLAI	NBA	VNBA	Lm	0.86	1.69	0.82	4.84	37095	930	1056	-14
MSE	2002	estLAI	NBA	VEE	Exp	0.90	1.23	0.87	3.49	35303	825	938	-14
MSE	2004	estLAI	NBA	VEBA	Lm	0.84	1.88	0.79	5.33	38174	927	1056	-14
MSE	2002	estLAI	NBA	VEE	Lm	0.97	0.94	0.88	3.26	34777	816	938	-15
MSE	2002	estLAI	NBA	VEE	Exp	0.90	1.29	0.85	3.63	35857	817	938	-15
MSE	2004	estLAI	NBA	VNBA	Lm	0.86	1.83	0.79	5.20	38038	909	1056	-16
MSE	2004	estLAI	E	VEBA	Exp	0.80	2.18	0.78	5.55	38246	908	1056	-16

continued from previous page

Site	Year	Version	Model	Model2	eq.	a	b	R <sup>2</sup>	RMSE	AIC	s.GPP	o.GPP	Diff. ( %)
MSE	2004	estLAI	E	VNE	Exp	0.80	2.23	0.77	5.66	38574	899	1056	-17
MSE	2005	estLAI	E	VNE	Exp	0.84	1.77	0.79	4.76	37538	817	957	-17
MSE	2004	estLAI	E	VNBA	Lm	0.89	1.71	0.83	4.64	36606	904	1056	-17
MSE	2004	estLAI	E	VEBA	Lm	0.89	1.79	0.82	4.80	37070	888	1056	-19
ESES2	2008	estLAI	E	VEBA	Exp	0.62	2.04	0.87	7.46	39195	1400	1208	14
ESES2	2008	estLAI	E	VNBA	Lm	0.52	2.91	0.62	10.50	47033	1391	1208	13
ESES2	2008	estLAI	E	VNBA	Exp	0.63	2.04	0.87	7.26	39276	1380	1208	12
ESES2	2007	estLAI	E	VEBA	Lm	0.63	2.51	0.81	8.38	40672	1546	1364	12
ESES2	2008	estLAI	NBA	VEBA	Exp	0.67	1.83	0.88	6.43	38997	1353	1208	11
ESES2	2008	estLAI	NBA	VNBA	Exp	0.68	1.81	0.88	6.26	39061	1337	1208	10
ESES2	2007	estLAI	E	VNBA	Lm	0.64	2.51	0.80	8.10	40734	1514	1364	10
ESES2	2008	estLAI	NBA	VNBA	Exp	0.68	1.89	0.86	6.31	39846	1312	1208	8
ESES2	2008	estLAI	NBA	VEBA	Exp	0.67	1.92	0.86	6.41	39883	1318	1208	8
ESES2	2008	estLAI	E	VNE	Exp	0.66	2.11	0.85	6.69	40241	1296	1208	7
ESES2	2008	estLAI	E	VEE	Exp	0.66	2.14	0.85	6.72	40467	1289	1208	6
ESES2	2008	estLAI	E	VEBA	Lm	0.70	1.83	0.87	5.88	39190	1291	1208	6
ESES2	2008	estLAI	NBA	VNE	Exp	0.70	1.88	0.85	6.04	40449	1274	1208	5
ESES2	2008	estLAI	NBA	VNE	Exp	0.72	1.79	0.86	5.73	40042	1266	1208	5
ESES2	2008	estLAI	NBA	VEE	Exp	0.70	1.91	0.84	6.08	40725	1266	1208	5
ESES2	2008	estLAI	NBA	VEE	Exp	0.72	1.81	0.85	5.75	40376	1255	1208	4
ESES2	2008	estLAI	E	VNE	Lm	0.72	1.81	0.87	5.63	39506	1260	1208	4
ESES2	2008	estLAI	E	VEE	Lm	0.72	1.82	0.87	5.67	39616	1260	1208	4
ESES2	2008	estLAI	NBA	VEBA	Lm	0.77	1.53	0.86	5.07	39950	1233	1208	2
ESES2	2008	estLAI	NBA	VNBA	Lm	0.78	1.51	0.86	4.99	40002	1223	1208	1
ESES2	2008	estLAI	NBA	VEE	Lm	0.78	1.54	0.85	5.09	40475	1215	1208	1
ESES2	2008	estLAI	NBA	VEBA	Lm	0.79	1.44	0.87	4.74	39333	1219	1208	1
ESES2	2008	estLAI	NBA	VNE	Lm	0.79	1.52	0.85	5.02	40325	1213	1208	0
ESES2	2008	estLAI	NBA	VNBA	Lm	0.81	1.42	0.87	4.64	39435	1203	1208	0
ESES2	2008	estLAI	NBA	VNE	Lm	0.82	1.44	0.86	4.69	40022	1182	1208	-2
ESES2	2008	estLAI	NBA	VEE	Lm	0.82	1.45	0.85	4.77	40237	1184	1208	-2
ESES2	2007	estLAI	NBA	VEBA	Lm	0.75	2.50	0.78	6.75	41521	1308	1364	-4
ESES2	2007	estLAI	NBA	VNE	Lm	0.75	2.53	0.77	6.84	41808	1300	1364	-5
ESES2	2007	estLAI	NBA	VNBA	Lm	0.75	2.50	0.78	6.74	41565	1303	1364	-5
ESES2	2007	estLAI	NBA	VEE	Lm	0.74	2.56	0.76	6.94	42032	1298	1364	-5
ESES2	2007	estLAI	NBA	VEBA	Exp	0.73	2.73	0.77	6.97	41649	1286	1364	-6
ESES2	2007	estLAI	NBA	VNBA	Exp	0.74	2.72	0.77	6.91	41634	1280	1364	-7
ESES2	2007	estLAI	NBA	VNE	Exp	0.73	2.84	0.76	7.11	41993	1267	1364	-8
ESES2	2007	estLAI	NBA	VEE	Exp	0.73	2.89	0.75	7.23	42293	1259	1364	-8
ESES2	2007	estLAI	E	VNE	Lm	0.75	3.09	0.78	6.78	41398	1183	1364	-15
ESES2	2007	estLAI	E	VEE	Lm	0.75	3.10	0.78	6.84	41533	1181	1364	-15
ESES2	2007	estLAI	E	VNE	Exp	0.72	3.41	0.76	7.31	42086	1157	1364	-18
ESES2	2007	estLAI	E	VEE	Exp	0.72	3.45	0.75	7.40	42295	1150	1364	-19
HFK	2008	estLAI	E	VNBA	Lm	0.04	5.64	0.03	40.65	43654	871	854	2
HFK	2008	estLAI	NBA	VNE	Lm	0.94	0.76	0.79	3.90	34262	795	854	-7

continued from previous page

Site	Year	Version	Model	Model2	eq.	a	b	R <sup>2</sup>	RMSE	AIC	s.GPP	o.GPP	Diff. ( %)
HFK	2008	estLAI	E	VNE	Lm	0.92	0.80	0.78	3.97	34422	800	854	-7
HFK	2008	estLAI	NBA	VNBA	Lm	0.94	0.74	0.81	3.68	33516	794	854	-8
HFK	2008	estLAI	E	VEBA	Lm	0.92	0.89	0.72	4.48	35964	784	854	-9
HFK	2008	estLAI	NBA	VNBA	Exp	0.95	0.76	0.82	3.57	33147	778	854	-10
HFK	2008	estLAI	E	VNBA	Exp	0.95	0.79	0.82	3.58	33172	776	854	-10
HFK	2008	estLAI	E	VEE	Lm	0.94	0.86	0.61	5.27	38067	776	854	-10
HFK	2008	estLAI	NBA	VNE	Exp	0.93	0.97	0.78	3.96	34344	767	854	-11
HFK	2008	estLAI	NBA	VEE	Lm	0.96	0.78	0.61	5.23	37965	771	854	-11
HFK	2008	estLAI	NBA	VEBA	Lm	0.94	0.90	0.72	4.46	35911	769	854	-11
HFK	2008	estLAI	E	VNE	Exp	0.92	1.03	0.78	4.02	34496	769	854	-11
HFK	2008	estLAI	E	VEBA	Exp	0.95	1.10	0.71	4.58	36149	727	854	-17
HFK	2008	estLAI	NBA	VEBA	Exp	0.96	1.11	0.71	4.59	36162	719	854	-19
HK	2010	Constant	E	VEE	Exp	0.91	0.93	0.82	3.45	32518	670	745	-11
HK	2010	Constant	E	VNE	Exp	0.94	0.82	0.85	3.12	31323	664	745	-12
HK	2010	Constant	E	VNBA	Lm	0.96	0.81	0.82	3.39	32436	652	745	-14
HK	2010	Constant	E	VNBA	Exp	0.95	0.91	0.86	3.04	30942	648	745	-15
HK	2010	Constant	E	VEBA	Exp	0.97	0.89	0.85	3.12	31247	634	745	-18
MSE	2005	Constant	E	VNBA	Lm	0.01	6.19	0.01	93.22	47571	1137	957	16
MSE	2003	Constant	E	VEBA	Exp	0.76	1.11	0.87	3.87	33920	932	883	5
MSE	2005	Constant	E	VEBA	Exp	0.75	1.31	0.88	4.45	34089	1004	957	5
MSE	2003	Constant	E	VNBA	Lm	0.12	4.85	0.12	21.64	47018	897	883	2
MSE	2005	Constant	E	VNBA	Exp	0.78	1.27	0.88	4.15	33995	973	957	2
MSE	2002	Constant	E	VNE	Exp	0.85	0.86	0.91	3.06	32369	945	938	1
MSE	2002	Constant	E	VEE	Exp	0.83	0.96	0.91	3.24	32751	947	938	1
MSE	2002	Constant	E	VNE	Lm	0.96	0.26	0.93	2.36	30690	935	938	0
MSE	2002	Constant	E	VNBA	Exp	0.87	0.76	0.92	2.80	31654	934	938	0
MSE	2002	Constant	E	VEBA	Exp	0.84	0.95	0.91	3.22	32896	941	938	0
MSE	2003	Constant	E	VEBA	Lm	0.91	0.47	0.93	2.31	29701	887	883	0
MSE	2003	Constant	E	VNE	Exp	0.82	1.05	0.85	3.60	34833	875	883	-1
MSE	2002	Constant	E	VNBA	Lm	0.96	0.27	0.93	2.37	30711	933	938	-1
MSE	2003	Constant	E	VEE	Exp	0.84	0.92	0.89	3.14	33007	874	883	-1
MSE	2002	Constant	E	VEBA	Lm	0.95	0.33	0.95	2.14	29183	933	938	-1
MSE	2004	Constant	E	VEBA	Lm	0.96	0.45	0.92	3.04	31933	1030	1056	-3
MSE	2004	Constant	E	VNBA	Exp	0.87	1.19	0.87	4.10	34884	1014	1056	-4
MSE	2003	Constant	E	VNBA	Exp	0.93	0.67	0.91	2.62	31745	837	883	-5
MSE	2004	Constant	E	VEBA	Exp	0.85	1.35	0.85	4.48	35944	1004	1056	-5
MSE	2004	Constant	E	VNE	Exp	0.87	1.25	0.86	4.32	35672	1000	1056	-6
MSE	2004	Constant	E	VEE	Lm	1.03	0.28	0.86	3.99	35399	985	1056	-7
MSE	2005	Constant	E	VNE	Exp	0.90	1.12	0.86	3.80	35088	874	957	-9
MSE	2005	Constant	E	VEE	Lm	1.01	0.45	0.87	3.52	34559	876	957	-9
MSE	2004	Constant	E	VEE	Exp	0.89	1.36	0.78	5.11	38223	956	1056	-10
MSE	2005	Constant	E	VEE	Exp	0.88	1.37	0.79	4.55	37405	852	957	-12
ESES2	2008	Constant	E	VNE	Exp	0.67	1.18	0.90	6.41	37268	1510	1208	20
ESES2	2008	Constant	E	VEE	Exp	0.66	1.23	0.90	6.59	37430	1517	1208	20

continued from previous page

Site	Year	Version	Model	Model2	eq.	a	b	R <sup>2</sup>	RMSE	AIC	s.GPP	o.GPP	Diff. ( %)
ESES2	2007	Constant	E	VNE	Lm	0.77	0.87	0.85	5.97	39049	1597	1364	15
ESES2	2007	Constant	E	VEE	Lm	0.78	0.87	0.85	5.83	38928	1581	1364	14
ESES2	2007	Constant	E	VEBA	Lm	0.78	0.87	0.85	5.83	38938	1581	1364	14
ESES2	2007	Constant	E	VEBA	Exp	0.72	1.35	0.88	6.20	37474	1594	1364	14
ESES2	2007	Constant	E	VNBA	Lm	0.80	0.87	0.84	5.68	39359	1537	1364	11
ESES2	2007	Constant	E	VNE	Exp	0.76	1.35	0.87	5.61	37812	1510	1364	10
ESES2	2007	Constant	E	VNBA	Exp	0.77	1.26	0.88	5.51	37585	1519	1364	10
ESES2	2007	Constant	E	VEE	Exp	0.76	1.47	0.86	5.78	38402	1495	1364	9
HFK	2008	Constant	E	VNE	Lm	0.93	0.79	0.78	4.00	34569	793	854	-8
HFK	2008	Constant	E	VNBA	Lm	0.94	0.76	0.80	3.75	33755	791	854	-8
HFK	2008	Constant	E	VEE	Lm	0.89	1.12	0.55	5.69	38933	781	854	-9
HFK	2008	Constant	E	VNBA	Exp	0.96	0.77	0.82	3.60	33244	775	854	-10
HFK	2008	Constant	E	VEBA	Lm	0.92	0.96	0.70	4.60	36292	773	854	-10
HFK	2008	Constant	E	VNE	Exp	0.92	1.01	0.78	4.05	34596	766	854	-11
HFK	2008	Constant	E	VEBA	Exp	0.95	1.17	0.70	4.71	36470	717	854	-19



# Appendix B: A case study of dry-land crops

Table B.1. Parameter sets between  $V_{c_{uptake}}$  and VIs, NDVI and EVI for soybean with slope ( $a$ ), intercept ( $b$ ), determination coefficients ( $R^2$ ), root mean square error (RMSE), akaike information criterion (AIC), difference (Diff., %) between simulated GPP (s.GPP) and observed GPP (o.GPP). 'Version' indicates which estimation model used, in detail, B is soybean, N is NDVI, E is EVI, Lm is linear model, Exp is exponential model, Log is logarithm model, Logi is logistic model, nls is nonlinear least squares model. 'Version' is a combination of crop type-NDVI or EVI-entire or BA-model-crop type-NDVI or EVI-entire or BA-model. The combination until the statistical model (Lm, Exp, Log, Logi, and nls) indicates the LAI estimation model, the next combination indicates the  $V_{c_{uptake}}$  estimation model.

Site	Year	Version	a	b	$R^2$	RMSE	AIC	sim.GPP	obs.GPP	Diff. (%)
US-Ne3	2002	BNELmBNBAExp	1.03	1.67	0.83	4.01	36205	637	922	-31
US-Ne3	2002	BNELmBNBALm	1.08	0.86	0.89	3.19	33300	728	922	-21
US-Ne3	2002	BNELmBNEExp	1.12	1.51	0.85	3.98	35267	609	922	-34
US-Ne3	2002	BNELmBNELm	1.09	0.90	0.89	3.30	33650	715	922	-22
US-Ne3	2002	BNELogi	1.07	0.86	0.88	3.23	34389	735	924	-20
US-Ne3	2002	BNElnls	1.07	0.87	0.88	3.23	34359	733	924	-21
US-Ne3	2002	BNEBNBALog	1.08	0.82	0.89	3.11	33715	736	924	-20
US-Ne3	2002	BNEBNBLogAExp	1.10	1.16	0.88	3.52	34843	670	924	-27
US-Ne3	2002	BNEBNBLogALm	1.08	0.84	0.90	3.06	33392	732	924	-21
US-Ne3	2002	BNEBNELog	0.84	1.71	0.66	5.35	41817	772	924	-16
US-Ne3	2002	BEELmBEBAExp	1.49	1.76	0.77	5.80	38395	432	922	-53
US-Ne3	2002	BEELmBEBALm	1.40	0.75	0.88	4.44	34044	573	922	-38

continued from previous page

Site	Year	Version	a	b	R <sup>2</sup>	RMSE	AIC	sim.GPP	obs.GPP	Diff. ( %)
US-Ne3	2002	BEELmBEEExp	1.68	1.26	0.86	5.56	34887	431	922	-53
US-Ne3	2002	BEELmBEELm	1.41	0.70	0.89	4.37	33514	576	922	-38
US-Ne3	2004	BNELmBNBAExp	0.99	1.12	0.92	2.99	31002	801	959	-16
US-Ne3	2004	BNELmBNBALm	1.08	0.43	0.93	2.86	30236	829	959	-14
US-Ne3	2004	BNELmBNEExp	1.05	1.02	0.91	3.31	31958	768	959	-20
US-Ne3	2004	BNELmBNELm	1.08	0.48	0.91	3.21	31814	819	959	-15
US-Ne3	2004	BNELogi	1.08	0.45	0.91	3.26	32131	825	959	-14
US-Ne3	2004	BNEnls	1.08	0.45	0.91	3.26	32105	824	959	-14
US-Ne3	2004	BNEBNBALog	1.09	0.38	0.93	2.97	30709	829	959	-14
US-Ne3	2004	BNEBNBLogAExp	1.08	0.68	0.94	2.82	29451	792	959	-17
US-Ne3	2004	BNEBNBLogALm	1.09	0.40	0.93	2.85	30071	828	959	-14
US-Ne3	2004	BNEBNELog	1.11	0.43	0.91	3.34	32103	808	959	-16
US-Ne3	2004	BEELmBEBAExp	0.89	1.08	0.92	3.10	31199	894	959	-7
US-Ne3	2004	BEELmBEBALm	0.99	0.40	0.93	2.73	30610	910	959	-5
US-Ne3	2004	BEELmBEEExp	0.91	0.97	0.92	3.03	31211	895	959	-7
US-Ne3	2004	BEELmBEELm	0.99	0.41	0.92	2.93	31496	909	959	-5

Table B.2. The parameter sets between  $V_{c_{\text{uptake}}}$  and VIs, NDVI and EVI for sugar beet with slope ( $a$ ), intercept ( $b$ ), determination coefficients ( $R^2$ ), root mean square error (RMSE), akaike information criterion (AIC), difference (Diff., %) between simulated GPP (s.GPP) and observed GPP (o.GPP). 'Version' indicates which estimation model used, in detail, S is sugar beet, N is NDVI, E is EVI, Lm is linear model, Exp is exponential model, and Log is logarithm model. 'Version' is a combination of crop type-NDVI or EVI-entire or BA-model-crop type-NDVI or EVI-entire or BA-model. The combination until the statistical model (Lm, Exp, Log, Logi, and nls) indicates the LAI estimation model, the next combination indicates the  $V_{c_{\text{uptake}}}$  estimation model.

Site	Year	Version	a	b	R <sup>2</sup>	RMSE	AIC	sim.GPP	obs.GPP	Diff. (%)
BE-Lon	2004	SNELmSNBAExp	1.09	1.09	0.91	3.87	46492	1341	1689	-21
BE-Lon	2004	SNELmSNBALm	1.08	0.97	0.91	3.76	46508	1383	1689	-18

continued from previous page

Site	Year	Version	a	b	R <sup>2</sup>	RMSE	AIC	sim.GPP	obs.GPP	Diff. (%)
BE-Lon	2004	SNELmSNEExp	1.95	0.89	0.83	8.23	52506	770	1689	-54
BE-Lon	2004	SNELmSNELm	1.59	0.83	0.83	7.04	52331	953	1689	-44
BE-Lon	2004	SNEnls	1.41	0.96	0.84	6.32	52013	1054	1689	-38
BE-Lon	2004	SNESNBALog	2.1	1.31	0.73	9.24	56515	674	1689	-60
BE-Lon	2004	SNESNBLogAExp	1.08	0.91	0.91	3.78	46557	1384	1689	-18
BE-Lon	2004	SNESNBLogALm	1.07	0.93	0.91	3.76	46677	1394	1689	-17
BE-Lon	2004	SNESNELog	1.51	0.84	0.83	6.71	52269	1005	1689	-40
BE-Lon	2004	SEELmSEBAExp	1.2	1.8	0.77	6.43	55201	1093	1689	-35
BE-Lon	2004	SEELmSEBALm	1.04	1.72	0.78	5.75	54768	1275	1689	-25
BE-Lon	2004	SEELmSEEEExp	1.86	0.75	0.87	7.69	50328	823	1689	-51
BE-Lon	2004	SEELmSEELm	1.53	0.72	0.86	6.5	50636	1008	1689	-40

Table B.3. The parameter sets between  $V_{c_{\text{uptake}}}$  and VIs, NDVI and EVI for potato with slope ( $a$ ), intercept ( $b$ ), determination coefficients ( $R^2$ ), root mean square error (RMSE), akaike information criterion (AIC), difference (Diff., %) between simulated GPP (s.GPP) and observed GPP (o.GPP). 'Version' is indicated which estimation model used, in detail, P is potato, N is NDVI, E is EVI, Lm is linear model, and Exp is exponential model. 'Version' is a combination of crop type-NDVI or EVI-entire or BA-model-crop type-NDVI or EVI-entire or BA-model. The combination until the statistical model (Lm, Exp, Log, Logi, and nls) indicates the LAI estimation model, the next combination indicates the  $V_{c_{\text{uptake}}}$  estimation model.

Site	Year	Version	a	b	R <sup>2</sup>	RMSE	AIC	sim.GPP	obs.GPP	Diff. (%)
HKP	2010	PNELmPNBAExp	1.72	0.77	0.58	6.48	28193	275	555	-50
HKP	2010	PNELmPNBALm	1.46	0.3	0.64	5.64	27449	358	555	-35
HKP	2010	PNELmPNEExp	1.68	0.95	0.55	6.59	28487	270	555	-51
HKP	2010	PNELmPNELm	1.37	0.68	0.59	5.81	27992	351	555	-37
HKP	2010	PEELmPEBAExp	2.82	1.88	0.36	8.31	30074	125	555	-77
HKP	2010	PEELmPEBALm	2.12	1.23	0.46	7.48	29327	200	555	-64
HKP	2010	PEELmPEEEExp	1.95	0.78	0.57	6.82	28277	242	555	-56
HKP	2010	PEELmPEELm	1.56	0.58	0.6	6.05	27876	317	555	-43

Table B.4. The parameter sets between  $V_{c_{uptake}}$  and VIs, NDVI and EVI for maize with slope ( $a$ ), intercept ( $b$ ), determination coefficients ( $R^2$ ), root mean square error (RMSE), akaike information criterion (AIC), difference (Diff., %) between simulated GPP (s.GPP) and observed GPP (o.GPP). 'Version' indicates which estimation model used, in detail M is maize, N is NDVI, E is EVI, Lm is linear model, Exp is exponential model, and Log is logarithm model. 'Version' is a combination of crop type-NDVI or EVI-entire or BA-model-crop type-NDVI or EVI-entire or BA-model. The combination until the statistical model (Lm, Exp, Log, Logi, and nls) indicates the LAI estimation model, the next combination indicates the  $V_{c_{uptake}}$  estimation model.

Site	Year	Version	$a$	$b$	$R^2$	RMSE	AIC	s.GPP	o.GPP	Diff (%)
US-Ne3	2003	MEELmMEBAExp	0.96	0.08	0.94	4.32	28067	1364	1322	3
US-Ne3	2003	MEELmMEBALm	1.09	-0.58	0.93	4.91	29075	1279	1322	-3
US-Ne3	2003	MEELmMEEExp	0.94	0.23	0.93	4.7	28781	1373	1322	4
US-Ne3	2003	MEELmMEELm	1.07	-0.5	0.92	5.04	29467	1287	1322	-3
US-Ne3	2003	MNELmMNBAExp	1.3	0.11	0.9	7.12	30295	1005	1322	-24
US-Ne3	2003	MNELmMNBALm	1.41	-0.52	0.88	8.17	31400	981	1322	-26
US-Ne3	2003	MNELmMNEExp	1.31	-0.18	0.93	6.58	28818	1025	1322	-22
US-Ne3	2003	MNELmMNELm	1.42	-0.78	0.9	7.74	30325	998	1322	-25
US-Ne3	2003	MNEMNBALog	1.45	-0.69	0.88	8.45	31540.71	967	1322	-27
US-Ne3	2003	MNEMNBALogAExp	1.39	-0.43	0.89	8.01	31206.78	984	1322	-26
US-Ne3	2003	MNEMNBALogALm	1.45	-0.67	0.88	8.43	31496.32	967	1322	-27
US-Ne3	2003	MNEMNELog	1.46	-0.87	0.89	8.22	30859.34	975	1322	-26
US-Ne3	2003	MEEMEBAALog	1.13	-0.71	0.92	5.31	29506.3	1246	1322	-6
US-Ne3	2003	MEEMEBAALogAExp	1.04	-0.32	0.91	5.15	29838.98	1301	1322	-2
US-Ne3	2003	MEEMEBAALogALm	1.12	-0.68	0.92	5.27	29479.06	1249	1322	-6
US-Ne3	2003	MEEMEELog	1.12	-0.66	0.91	5.39	29785.17	1251	1322	-5
US-Ne3	2003	MEELmMEBAAnoNE2003	1.02	-0.53	0.9	5.37	30322	1356	1322	3
US-Ne3	2005	MEELmMEBAExp	1.41	0.97	0.84	7.82	49045	1010	1602	-37
US-Ne3	2005	MEELmMEBALm	1.47	-0.04	0.89	7.22	46233	1092	1602	-32
US-Ne3	2005	MEELmMEEExp	1.44	0.95	0.87	7.52	47293	996	1602	-38
US-Ne3	2005	MEELmMEELm	1.49	-0.05	0.92	6.93	43987	1081	1602	-33
US-Ne3	2005	MNELmMNBAExp	1.24	1.09	0.88	6.4	47090	1133	1602	-29
US-Ne3	2005	MNELmMNBALm	1.39	0.14	0.92	6.28	43450	1134	1602	-29

Continued from previous page

Site	Year	Version	$a$	$b$	$R^2$	RMSE	AIC	s.GPP	o.GPP	Diff (%)
US-Ne3	2005	MNELmMNEExp	1.23	1.08	0.86	6.6	48034	1143	1602	-29
US-Ne3	2005	MNELmMNELm	1.37	0.14	0.91	6.45	45057	1149	1602	-28
US-Ne3	2005	MNEMNBALog	1.27	0.88	0.82	7.4	50118.77	1135	1602	-29
US-Ne3	2005	MNEMNBLogAExp	1.34	0.36	0.92	6.07	43999.96	1151	1602	-28
US-Ne3	2005	MNEMNBLogALm	1.43	-0.02	0.93	6.39	42809.26	1123	1602	-30
US-Ne3	2005	MNEMNELog	1.44	-0.09	0.91	6.68	44458.39	1125	1602	-30
US-Ne3	2005	MEEMEBALog	1.49	-0.14	0.9	7.19	45804.52	1094	1602	-32
US-Ne3	2005	MEEMEBLogAExp	1.46	0.15	0.9	7.04	45426.66	1080	1602	-33
US-Ne3	2005	MEEMEBLogALm	1.49	-0.17	0.9	7.2	45808.69	1095	1602	-32
US-Ne3	2005	MEEMEELog	1.52	-0.23	0.92	6.96	43334.57	1081	1602	-33
US-Ne3	2005	MEELmMEBA <sub>noNE2003</sub>	1.36	-0.23	0.92	6.01	43622	1207	1602	-25
DE-Kli	2007	MEELmMEBAExp	1.12	2.14	0.85	4.76	33235	661	1048	-37
DE-Kli	2007	MEELmMEBALm	1.22	1.43	0.9	4.26	30575	692	1048	-34
DE-Kli	2007	MEELmMEEExp	1.13	2.31	0.83	5.03	33904	636	1048	-39
DE-Kli	2007	MEELmMEELm	1.23	1.55	0.9	4.45	31067	674	1048	-36
DE-Kli	2007	MNELmMNBAExp	1	1.8	0.83	4.41	34039	795	1048	-24
DE-Kli	2007	MNELmMNBALm	1.15	1.03	0.9	3.82	30886	783	1048	-25
DE-Kli	2007	MNELmMNEExp	0.99	1.82	0.81	4.62	34697	793	1048	-24
DE-Kli	2007	MNELmMNELm	1.15	1.06	0.88	4.06	31971	782	1048	-25
DE-Kli	2007	MNEMNBALog	1.19	0.88	0.91	3.87	30401.92	772	1048	-26
DE-Kli	2007	MNEMNBLogAExp	1.1	1.23	0.87	4.02	32347.09	794	1048	-24
DE-Kli	2007	MNEMNBLogALm	1.19	0.9	0.9	3.87	30505.69	773	1048	-26
DE-Kli	2007	MNEMNELog	1.2	0.89	0.89	4.08	31313.04	766	1048	-27
DE-Kli	2007	MEEMEBALog	1.23	1.34	0.91	4.26	30389.66	695	1048	-34
DE-Kli	2007	MEEMEBLogAExp	1.17	1.74	0.87	4.55	32362.6	683	1048	-35
DE-Kli	2007	MEEMEBLogALm	1.24	1.35	0.91	4.28	30438.72	692	1048	-34
DE-Kli	2007	MEEMEELog	1.26	1.37	0.91	4.41	30315.59	675	1048	-36
DE-Kli	2007	MEELmMEBA <sub>noNE2003</sub>	1.13	1.41	0.91	3.79	30338	750	1048	-28



# References

- Aber, J. D., P. B. Reich & M. L. Goulden (1996). “Extrapolating leaf CO<sub>2</sub> exchange to the canopy: a generalized model of forest photosynthesis compared with measurements by eddy correlation”. In: *Oecologia* 106.2, pp. 257–265.
- Adiku, S., M. Reichstein, A. Lohila, N. Q. Dinh, M. Aurela, T. Laurila, J. Lueers & J. D. Tenhunen (2006). “PIXGRO: A model for simulating the ecosystem CO<sub>2</sub> exchange and growth of spring barley”. In: *Ecological Modelling* 190.3, pp. 260–276.
- Anthoni, P. M., A. Knohl, C. Rebmann, A. Freibauer, M. Mund, W. Ziegler, O. Kolle & E. .-.D. Schulze (2004). “Forest and agricultural land-use-dependent CO<sub>2</sub> exchange in Thuringia, Germany”. In: *Global Change Biology* 10.12, pp. 2005–2019.
- Aubinet, M., A. Grelle, A. Ibrom, Ü. Rannik, J. Moncrieff, T. Foken, A. S. Kowalski, P. H. Martin, P. Berbigier & C. Bernhofer (1999). “Estimates of the annual net carbon and water exchange of forests: the EUROFLUX methodology”. In: *Advances in ecological research* 30, pp. 113–175.
- Aubinet, M., C. Moureaux, B. Bodson, D. Dufranne, B. Heinesch, M. Suleau, F. Vancutsem & A. Vilret (2009). “Carbon sequestration by a crop over a 4-year sugar beet/winter wheat/seed potato/winter wheat rotation cycle”. In: *Agricultural and Forest Meteorology* 149.3-4, pp. 407–418.
- Baldocchi, D. D. (2003). “Assessing the eddy covariance technique for evaluating carbon dioxide exchange rates of ecosystems: past, present and future”. In: *Global Change Biology* 9.4, pp. 479–492.
- Baldocchi, D. D. & K. B. Wilson (2001). “Modeling CO<sub>2</sub> and water vapor exchange of a temperate broadleaved forest across hourly to decadal time scales”. In: *Ecological Modelling* 142.1, pp. 155–184.

- Baldocchi, D. (1994). "An analytical solution for coupled leaf photosynthesis and stomatal conductance models." In: *Tree physiology* 14, pp. 1069–1079.
- Baldocchi, D. D., B. B. Hincks & T. P. Meyers (1988). "Measuring biosphere-atmosphere exchanges of biologically related gases with micrometeorological methods". In: *Ecology*, pp. 1331–1340.
- Baldocchi, D. & T. Meyers (1998). "On using eco-physiological, micrometeorological and biogeochemical theory to evaluate carbon dioxide, water vapor and trace gas fluxes over vegetation: a perspective". In: *Agricultural and Forest Meteorology* 90.1-2, pp. 1–25.
- Baldocchi, D., R. Valentini, S. Running, W. Oechel & R. DAHLMAN (1996). "Strategies for measuring and modelling carbon dioxide and water vapour fluxes over terrestrial ecosystems". In: *Global Change Biology* 2.3, pp. 159–168.
- Baldocchi, D., E. Falge, L. Gu, R. Olson, D. Hollinger, S. Running, P. Anthoni, C. Bernhofer, K. Davis & R. Evans (2001). "FLUXNET: a new tool to study the temporal and spatial variability of ecosystem-scale carbon dioxide, water vapor, and energy flux densities". In: *Bulletin of the American Meteorological Society* 82.11, pp. 2415–2434.
- Baldocchi, D., J. Finnigan, K. Wilson, K. T. Paw U & E. Falge (2000). "On measuring net ecosystem carbon exchange over tall vegetation on complex terrain". In: *Boundary-Layer Meteorology* 96.1, pp. 257–291.
- Ball, J. T., I. E. Woodrow & J. A. Berry (1987). "A model predicting stomatal conductance and its contribution to the control of photosynthesis under different environmental conditions". In: *Progress in Photosynthesis Research*. Ed. by J. Biggens. Springer Netherlands, pp. 221–224.
- Bannari, A., D. Morin, F. Bonn & A. R. Huete (1995). "A review of vegetation indices". In: *Remote sensing reviews* 13.1-2, pp. 95–120.
- Bastiaanssen, W. G. M., D. J. Molden & I. W. Makin (2000). "Remote sensing for irrigated agriculture: examples from research and possible applications". In: *Agricultural water management* 46.2, pp. 137–155.
- Béziat, P., E. Ceschia & G. Dedieu (2009). "Carbon balance of a three crop succession over two cropland sites in South West France". In: *Agricultural and Forest Meteorology* 149.10, pp. 1628–1645.

- Bonan, G. B. (2002). *Ecological climatology: concepts and applications*. Cambridge, United Kingdom: Cambridge University Press.
- Bonan, G. B., P. J. Lawrence, K. W. Oleson, S. Levis, M. Jung, M. Reichstein, D. M. Lawrence & S. C. Swenson (2011). “Improving canopy processes in the Community Land Model version 4 (CLM4) using global flux fields empirically inferred from FLUXNET data”. In: *Journal of Geophysical Research* 116.G2, G02014.
- Bondeau, A., P. C. Smith, S. Zaehle, S. Schaphoff, W. Lucht, W. Cramer, D. Gerten, H. LOTZE CAMPEN, C. Müller & M. Reichstein (2007). “Modelling the role of agriculture for the 20th century global terrestrial carbon balance”. In: *Global Change Biology* 13.3, pp. 679–706.
- Brantley, S. T., J. C. Zinnert & D. R. Young (2011). “Application of hyperspectral vegetation indices to detect variations in high leaf area index temperate shrub thicket canopies”. In: *Remote Sensing Of Environment* 115.2, pp. 514–523.
- Carrara, A., A. S. Kowalski, J. Neiryneck, I. A. Janssens, J. C. Yuste & R. Ceulemans (2003). “Net ecosystem CO<sub>2</sub> exchange of mixed forest in Belgium over 5 years”. In: *Agricultural and Forest Meteorology* 119.3-4, pp. 209–227.
- Chen, J. M., J. Liu, J. Cihlar & M. L. Goulden (1999). “Daily canopy photosynthesis model through temporal and spatial scaling for remote sensing applications”. In: *Ecological Modelling* 124.2, pp. 99–119.
- Chen, P.-Y., G. Fedosejevs, M. Tiscareño-López & J. G. Arnold (2005). “Assessment of MODIS-EVI, MODIS-NDVI and VEGETATION-NDVI Composite Data Using Agricultural Measurements: An Example at Corn Fields in Western Mexico”. In: *Environmental Monitoring and Assessment* 119.1-3, pp. 69–82.
- Chen, T., G. R. van der Werf, A. J. Dolman & M. Groenendijk (2011). “Evaluation of cropland maximum light use efficiency using eddy flux measurements in North America and Europe”. In: *Geophysical Research Letters* 38.14, p. L14707.
- Christensen, T. R., T. Johansson, M. Olsrud, L. Ström, A. Lindroth, M. Mastepanov, N. Malmer, T. Friberg, P. Crill & T. V. Callaghan (2007). “A catchment-scale carbon and greenhouse gas budget of a subarctic landscape.” In: *Philosophical transactions. Series A, Mathematical, physical, and engineering sciences* 365.1856, pp. 1643–1656.

- Ciais, P., M. Wattenbach, N. Vuichard, P. Smith, S. L. Piao, A. Don, S. Luyssaert, I. A. Janssens, A. Bondeau, R. Dechow, A. Leip, P. C. Smith, C. Beer, G. R. van der Werf, S. Gervois, K. van Oost, E. Tomelleri, A. Freibauer, E. D. Schulze & CARBOEUROPE SYNTHESIS TEAM (2010). "The European carbon balance. Part 2: croplands". In: *Global Change Biology* 16.5, pp. 1409–1428.
- Cuddington, K., M.-J. Fortin, L. R. Gerber, A. Hastings, A. Liebhold, M. O'Connor & C. Ray (2013). "Process-based models are required to manage ecological systems in a changing world". In: *Ecosphere* 4.2.
- Dorigo, W. A., R. Zurita-Milla, A. J. W. de Wit, J. Brazile, R. Singh & M. E. Schaepman (2007). "A review on reflective remote sensing and data assimilation techniques for enhanced agroecosystem modeling". In: *International Journal of Applied Earth Observation and Geoinformation* 9.2, pp. 165–193.
- Falge, E. (1997). "Die Modellierung der Kronendachtranspiration von Fichtenbeständen (*Picea abies* (L.) Karst.)" PhD thesis. Univ. Bayreuth.
- Falge, E., D. Baldocchi, J. Tenhunen, M. Aubinet, P. Bakwin, P. Berbigier, C. Bernhofer, G. Burba, R. Clement & K. J. Davis (2002). "Seasonality of ecosystem respiration and gross primary production as derived from FLUXNET measurements". In: *Agricultural and Forest Meteorology* 113.1, pp. 53–74.
- Falge, E., W. Graber, R. Siegwolf & J. D. Tenhunen (1996). "A model of the gas exchange response of *Picea abies* to habitat conditions". In: *Trees* 10.5, pp. 277–287.
- Falge, E., J. Tenhunen, D. Baldocchi, M. Aubinet, P. Bakwin, P. Berbigier, C. Bernhofer, J. M. Bonnefond, G. Burba & R. Clement (2002). "Phase and amplitude of ecosystem carbon release and uptake potentials as derived from FLUXNET measurements". In: *Agricultural and Forest Meteorology* 113.1, pp. 75–95.
- Falge, E., D. Baldocchi, R. Olson, P. Anthoni, M. Aubinet, C. Bernhofer, G. Burba, R. Ceulemans, R. Clement & H. Dolman (2001). "Gap filling strategies for long term energy flux data sets". In: *Agricultural and Forest Meteorology* 107.1, pp. 71–77.
- Fan, L., Y. Gao, H. Brück & C. Bernhofer (2008). "Investigating the relationship between NDVI and LAI in semi-arid grassland in Inner Mongolia using in-situ measurements". In: *Theoretical and Applied Climatology* 95.1-2, pp. 151–156.

- Farquhar, G. D. & S. Caemmerer (1982). "Modelling of Photosynthetic Response to Environmental Conditions". In: *Physiological Plant Ecology II*. Berlin, Heidelberg: Springer Berlin Heidelberg, pp. 549–587.
- Farquhar, G. D., S. Caemmerer & J. A. Berry (1980). "A biochemical model of photosynthetic CO<sub>2</sub> assimilation in leaves of C3 species". In: *Planta*, pp. 1–13.
- Farquhar, G. D., von Caemmerer S & J. A. Berry (2001). "Models of photosynthesis." In: *Plant physiology* 125.1, pp. 42–45.
- Farquhar, G. D. & T. D. Sharkey (1982). "Stomatal conductance and photosynthesis". In: *Annual Review of Plant Physiology* 33.1, pp. 317–345.
- Flanagan, L., L. Wever & P. Carlson (2002). "Seasonal and interannual variation in carbon dioxide exchange and carbon balance in a northern temperate grassland". In: *Global Change Biology*, pp. 1–17.
- Foken, T. & B. Wichura (1996). "Tools for quality assessment of surface-based flux measurements". In: *Agricultural and Forest Meteorology* 78.1, pp. 83–105.
- Fontana, F., C. Rixen, T. Jonas, G. Aberegg & S. Wunderle (2008). "Alpine grassland phenology as seen in AVHRR, VEGETATION, and MODIS NDVI time series-A comparison with in situ measurements". In: *Sensors* 8.4, pp. 2833–2853.
- Gitelson, A. A., Y. J. Kaufman & M. N. Merzlyak (1996). "Use of a green channel in remote sensing of global vegetation from EOS-MODIS". In: *Remote Sensing Of Environment* 58.3, pp. 289–298.
- Gitelson, A. A., Y. Peng, J. G. Masek, D. C. Rundquist, S. Verma, A. Suyker, J. M. Baker, J. L. Hatfield & T. Meyers (2012). "Remote estimation of crop gross primary production with Landsat data". In: *Remote Sensing Of Environment* 121, pp. 404–414.
- Gobron, N., B. Pinty, M. M. Verstraete & J.-L. Widlowski (2000). "Advanced vegetation indices optimized for up-coming sensors: Design, performance, and applications". In: *Geoscience and Remote Sensing, IEEE Transactions on* 38.6, pp. 2489–2505.
- Goetz, S. J., S. D. Prince, S. N. GOWARD, M. M. Thawley & J. Small (1999). "Satellite remote sensing of primary production: an improved production efficiency modeling approach". In: *Ecological Modelling* 122.3, pp. 239–255.

- Haboudane, D., J. R. Miller, N. Tremblay, P. J. Zarco-Tejada & L. Dextraze (2002). "Integrated narrow-band vegetation indices for prediction of crop chlorophyll content for application to precision agriculture". In: *Remote Sensing Of Environment* 81.2, pp. 416–426.
- Harazono, Y., K. Chikamoto, S. Kikkawa & T. Iwata (2009). "Applications of MODIS-visible bands to estimate CO<sub>2</sub> budget of a rice paddy in Japan". In: *J. Agric. Meteorol.* 4, pp. 365–374.
- Harley, P. C., J. D. Tenhunen, W. Beyschlag & O. L. Lange (1987). "Seasonal changes in net photosynthesis rates and photosynthetic capacity in leaves of *Cistus salvifolius*, a European Mediterranean semi-deciduous shrub". In: *Oecologia* 74.3, pp. 380–388.
- Harley, P. C., J. D. Tenhunen & O. L. Lange (1986). "Use of an analytical model to study limitations on net photosynthesis in *Arbutus unedo* under field conditions". In: *Oecologia* 70.3, pp. 393–401.
- Harley, P. C., J. D. Tenhunen, K. J. Murray & J. Beyers (1989). "Irradiance and temperature effects on photosynthesis of tussock tundra *Sphagnum* mosses from the foothills of the Philip Smith Mountains, Alaska". In: *Oecologia* 79.2, pp. 251–259.
- Harley, P. C. & T. D. Sharkey (1991). "An improved model of C<sub>3</sub> photosynthesis at high CO<sub>2</sub>: reversed O<sub>2</sub> sensitivity explained by lack of glycerate reentry into the chloroplast". In: *Photosynthesis Research* 27.3, pp. 169–178.
- Hashimoto, H., W. Wang, C. Milesi, M. A. White, S. Ganguly, M. Gamo, R. Hirata, R. B. Myneni & R. R. Nemani (2012). "Exploring Simple Algorithms for Estimating Gross Primary Production in Forested Areas from Satellite Data". In: *Remote Sensing* 4.1, pp. 303–326.
- Hastie, T. & R. Tibshirani (1986). "Generalized additive models". In: *Statistical science* 1.3, pp. 297–310.
- Hastie, T. & R. Tibshirani (1990). "Exploring the nature of covariate effects in the proportional hazards model." In: *Biometrics* 46.4, pp. 1005–1016.
- Hicke, J. A., D. B. Lobell & G. P. Asner (2004). "Cropland Area and Net Primary Production Computed from 30 Years of USDA Agricultural Harvest Data". In: *Earth Interactions* 8.10, pp. 1–20.
- Hollinger, D. Y. & A. D. Richardson (2005). "Uncertainty in eddy covariance measurements and its application to physiological models". In: *Tree physiology* 25.7, pp. 873–885.

- Houghton, R. (1999). "The annual net flux of carbon to the atmosphere from changes in land use 1850-1990". In: *Tellus B* 51.2, pp. 298–313.
- Houghton, R. A., J. E. Hobbie, J. M. Melillo, B. Moore, B. J. Peterson, G. R. Shaver & G. M. Woodwell (1983). "Changes in the Carbon Content of Terrestrial Biota and Soils between 1860 and 1980: A Net Release of CO<sub>2</sub> to the Atmosphere". In: *Ecological Monographs* 53.3, p. 235.
- Houghton, R. A. & G. M. Woodwell (1980). "The Flax Pond Ecosystem Study: Exchanges of CO<sub>2</sub> Between a Salt Marsh and the Atmosphere". In: *Ecology*, pp. 1434–1445.
- Hoyaux, J., C. Moureaux, D. Tourneur, B. Bodson & M. Aubinet (2008). "Extrapolating gross primary productivity from leaf to canopy scale in a winter wheat crop". In: *Agricultural and Forest Meteorology* 148.4, pp. 668–679.
- Huete, A. (1997). "A comparison of vegetation indices over a global set of TM images for EOS-MODIS". In: *Remote Sensing Of Environment* 59.3, pp. 440–451.
- Huete, A., K. DIDAN, T. Miura, E. P. Rodriguez, X. Gao & L. G. Ferreira (2002). "Overview of the radiometric and biophysical performance of the MODIS vegetation indices". In: *Remote Sensing Of Environment* 83.1-2, pp. 195–213.
- Huete, A. R. (1988). "A soil-adjusted vegetation index (SAVI)". In: *Remote Sensing Of Environment* 25.3, pp. 295–309.
- Huete, A. R. & H. Q. Liu (1994). "An error and sensitivity analysis of the atmospheric- and soil-correcting variants of the NDVI for the MODIS-EOS". In: *Ieee Transactions On Geoscience And Remote Sensing* 32.4, pp. 897–905.
- Jarvis, P. G., C. W. Rose & J. E. Begg (1967). "An experimental and theoretical comparison of viscous and diffusive resistances to gas flow through amphistomatous leaves". In: *Agricultural Meteorology* 4.2, pp. 103–117.
- Jiang, Z., A. R. Huete, J. Chen, Y. Chen, J. Li, G. Yan & X. Zhang (2006). "Analysis of NDVI and scaled difference vegetation index retrievals of vegetation fraction". In: *Remote Sensing Of Environment* 101.3, pp. 366–378.
- Jonsson, A., G. Algesten, A. K. Bergström, K. Bishop, S. Sobek, L. J. Tranvik & M. Jansson (2007). "Integrating aquatic carbon fluxes in a boreal catchment carbon budget". In: *Journal of Hydrology* 334.1, pp. 141–150.

- Jonsson, P. & L. Eklundh (2004). "TIMESAT—A program for analyzing time-series of satellite sensor data". In: *Computers & Geosciences* 30.8, pp. 833–845.
- Kaminski, T. (2002). "Assimilating atmospheric data into a terrestrial biosphere model: A case study of the seasonal cycle". In: *Global Biogeochemical Cycles* 16.4.
- Kang, S. (2003). "A regional phenology model for detecting onset of greenness in temperate mixed forests, Korea: an application of MODIS leaf area index". In: *Remote Sensing Of Environment* 86.2, pp. 232–242.
- Kimball, J. S., A. R. Keyser, S. W. Running & S. S. Saatchi (2000). "Regional assessment of boreal forest productivity using an ecological process model and remote sensing parameter maps." In: *Tree physiology* 20.11, pp. 761–775.
- Kim, Y., S. Kang, J. H. Lim, D. Lee & J. Kim (2010). "Inter-annual and inter-plot variations of wood biomass production as related to biotic and abiotic characteristics at a deciduous forest in complex terrain, Korea". In: *Ecological research* 25.4, pp. 757–769.
- Knorr, W. (2000). "Annual and interannual CO<sub>2</sub> exchanges of the terrestrial biosphere: process-based simulations and uncertainties". In: *Global Ecology and Biogeography* 9.3, pp. 225–252.
- Kumagai, T., T. Ichie, M. Yoshimura, M. Yamashita, T. Kenzo, T. M. Saitoh, M. Ohashi, M. Suzuki, T. Koike & H. Komatsu (2006). "Modeling CO<sub>2</sub> exchange over a Bornean tropical rain forest using measured vertical and horizontal variations in leaf-level physiological parameters and leaf area densities". In: *Journal of Geophysical Research* 111.D10, p. D10107.
- Kutsch, W. L., M. Aubinet, N. Buchmann, P. Smith, B. Osborne, W. Eugster, M. Wattenbach, M. Schrumpf, E. D. Schulze, E. Tomelleri, E. Ceschia, C. Bernhofer, P. Béziat, A. Carrara, P. Di Di Tommasi, T. Grünwald, M. Jones, V. Magliulo, O. Marloie, C. Moureaux, A. Oliso, M. J. Sanz, M. Saunders, H. Søgaaard, W. Ziegler & P. Di Di Tommasi (2010). "The net biome production of full crop rotations in Europe". In: *Agriculture, Ecosystems & Environment* 139.3, pp. 1–10.
- Kwon, H., J. Kim, J. Hong & J. H. Lim (2010). "Influence of the Asian monsoon on net ecosystem carbon exchange in two major ecosystems in Korea". In: *Biogeosciences* 7, pp. 1493–1504.

- Law, B. E., R. H. Waring, P. M. Anthoni & J. D. Aber (2000). "Measurements of gross and net ecosystem productivity and water vapour exchange of a *Pinus ponderosa* ecosystem, and an evaluation of two generalized models". In: *Global Change Biology* 6.2, pp. 155–168.
- Lee, R., F. Yu, K. Price & J. Ellis (2002). "Evaluating vegetation phenological patterns in Inner Mongolia using NDVI time-series analysis". In: *International Journal of*.
- Leuning, R. (1995). "A critical appraisal of a combined stomatal-photosynthesis model for C3 plants". In: *Plant, Cell & Environment* 18.4, pp. 339–355.
- Leuning, R. (2002). "Temperature dependence of two parameters in a photosynthesis model". In: *Plant, Cell & Environment* 25.9, pp. 1205–1210.
- Liu, H. (2008). "Generalized Additive Model". PhD thesis. University of Minnesota Duluth.
- Li, Y. L., G. Y. Zhou, D. Q. Zhang, K. O. Wenigmann, D. Otieno, J. Tenhunen, Q. M. Zhang & J. H. Yan (2012). "Quantification of ecosystem carbon exchange characteristics in a dominant subtropical evergreen forest ecosystem". In: *Asia-Pacific Journal of Atmospheric Sciences* 48.1, pp. 1–10.
- Li, Y.-L., J. Tenhunen, K. Owen, M. Schmitt, M. Bahn, M. Driesler, D. Otieno, M. Schmidt, T. Gruenwald, M. Z. Hussain, H. Mirzae & C. Bernhofer (2008). "Patterns in CO<sub>2</sub> gas exchange capacity of grassland ecosystems in the Alps". In: *Agricultural and Forest Meteorology* 148.1, pp. 51–68.
- Li, Z., G. Yu, X. Xiao, Y. Li, X. Zhao, C. Ren, L. Zhang & Y. Fu (2007). "Modeling gross primary production of alpine ecosystems in the Tibetan Plateau using MODIS images and climate data". In: *Remote Sensing Of Environment* 107.3, pp. 510–519.
- Lloyd, J. & J. A. Taylor (1994). "On the temperature dependence of soil respiration". In: *Functional ecology*, pp. 315–323.
- Long, S. P., P. K. Farage & R. L. Garcia (1996). "Measurement of leaf and canopy photosynthetic CO<sub>2</sub> exchange in the field". In: *Journal of experimental botany* 47.11, pp. 1629–1642.
- Medlyn, B. E., D. Loustau & S. Delzon (2002). "Temperature response of parameters of a biochemically based model of photosynthesis. I. Seasonal changes in mature maritime pine (*Pinus pinaster* Ait.)" In: *Plant, Cell & Environment* 25.9, pp. 1155–1165.

- Moors, E. J., C. Jacobs, W. Jans, I. Supit, W. L. Kutsch, C. Bernhofer, P. Béziat, N. Buchmann, A. Carrara & E. Ceschia (2010). “Variability in carbon exchange of European croplands”. In: *Agriculture, ecosystems & environment* 139.3, pp. 325–335.
- Moureaux, C., A. Debacq, J. Hoyaux, M. Suleau, D. Tourneur, F. Vancutsem, B. Bodson & M. Aubinet (2008). “Carbon balance assessment of a Belgian winter wheat crop (*Triticum aestivum* L.)” In: *Global Change Biology* 14.6, pp. 1353–1366.
- Moureaux, C., A. Debacq, B. Bodson, B. Heinesch & M. Aubinet (2006). “Annual net ecosystem carbon exchange by a sugar beet crop”. In: *Agricultural and Forest Meteorology* 139.1, pp. 25–39.
- Muraoka, H. & H. Koizumi (2005). “Photosynthetic and structural characteristics of canopy and shrub trees in a cool-temperate deciduous broadleaved forest: implication to the ecosystem carbon gain”. In: *Agricultural and Forest Meteorology* 134.1, pp. 39–59.
- Muraoka, H., H. M. Noda & S. Nagai (2012). “Spectral vegetation indices as the indicator of canopy photosynthetic productivity in a deciduous broadleaf forest”. In: *Journal of Plant Ecology*, pp. 1–15.
- Myneni, R. B., F. G. Hall, P. J. Sellers & A. L. Marshak (1995). “The interpretation of spectral vegetation indexes”. In: *Geoscience and Remote Sensing, IEEE Transactions on* 33.2, pp. 481–486.
- Myneni, R. B., R. Ramakrishna, R. Nemani & S. W. Running (1997). “Estimation of global leaf area index and absorbed PAR using radiative transfer models”. In: *Geoscience and Remote Sensing, IEEE Transactions on* 35.6, pp. 1380–1393.
- Nemani, R. R., C. D. Keeling, H. Hashimoto, W. M. Jolly, S. C. Piper, C. J. Tucker, R. B. Myneni & S. W. Running (2003). “Climate-driven increases in global terrestrial net primary production from 1982 to 1999.” In: *Science* 300.5625, pp. 1560–1563.
- Odum, E. P. (1985). “Biotechnology and the biosphere.” In: *Science* 229.4720, p. 1338.
- Ogutu, B. O., J. Dash & T. P. Dawson (2013). “Developing a diagnostic model for estimating terrestrial vegetation gross primary productivity using the photosynthetic quantum yield and Earth Observation data”. In: *Global Change Biology* 19.9, pp. 2878–2892.

- Osborne, B., M. Saunders, D. Walmsley, M. Jones & P. Smith (2010). "Key questions and uncertainties associated with the assessment of the cropland greenhouse gas balance". In: *Agriculture, Ecosystems & Environment* 139.3, pp. 293–301.
- Owen, K. E., J. Tenhunen, M. Reichstein, Q. Wang, E. Falge, R. Geyer, X. Xiao, P. Stoy, C. Ammann, A. Arain, M. Aubinet, M. Aurela, C. Bernhofer, B. H. Chojnicki, A. Granier, T. Gruenwald, J. Hadley, B. Heinesch, D. Hollinger, A. Knohl, W. Kutsch, A. Lohila, T. Meyers, E. Moors, C. Moureaux, K. Pilegaard, N. Saigusa, S. Verma, T. Vesala & C. Vogel (2007). "Linking flux network measurements to continental scale simulations: ecosystem carbon dioxide exchange capacity under non-water-stressed conditions". In: *Global Change Biology* 13.4, pp. 734–760.
- Pearson, R. L. & L. D. Miller (1972). "Remote Mapping of Standing Crop Biomass for Estimation of the Productivity of the Shortgrass Prairie". In: *Remote Sensing of Environment*, VIII -1, p. 1355.
- Peng, Y. & A. A. Gitelson (2011). "Application of chlorophyll-related vegetation indices for remote estimation of maize productivity". In: *Agricultural and Forest Meteorology* 151.9, pp. 1267–1276.
- Peng, Y. & A. A. Gitelson (2012). "Remote estimation of gross primary productivity in soybean and maize based on total crop chlorophyll content". In: *Remote Sensing Of Environment* 117, pp. 440–448.
- Pettorelli, N., J. O. Vik, A. Mysterud, J.-M. Gaillard, C. J. Tucker & N. C. Stenseth (2005). "Using the satellite-derived NDVI to assess ecological responses to environmental change". In: *Trends in Ecology & Evolution* 20.9, pp. 503–510.
- Physiological Plant Ecology II* (1982). Berlin, Heidelberg: Springer Berlin Heidelberg.
- Pinty, B. & M. M. Verstraete (1992). "GEMI: a non-linear index to monitor global vegetation from satellites". In: *Vegetatio* 101.1, pp. 15–20.
- Potithec, S. (2010). "What is the actual relationship between LAI and VI a deciduous forest?" In: *ISPRS Annals* XXXVIII, pp. 1–6.
- Qi, J., A. Chehbouni, A. R. Huete, Y. H. Kerr & S. Sorooshian (1994). "A modified soil adjusted vegetation index". In: *Remote Sensing Of Environment* 48.2, pp. 119–126.

- Reeves, M. C., M. Zhao & S. W. Running (2005). "Usefulness and limits of MODIS GPP for estimating wheat yield". In: *International Journal of Remote Sensing* 26.7, pp. 1403–1421.
- Reichstein, M. (2001). "Drought effects on ecosystem gas exchange in three Mediterranean Ecosystems—a combined top-down and bottom-up analysis of eddy covariance and sap-flow data". PhD thesis. Univ. Bayreuth.
- Reichstein, M. (2003). "Inverse modeling of seasonal drought effects on canopy CO<sub>2</sub>/H<sub>2</sub> exchange in three Mediterranean ecosystems". In: *Journal of Geophysical Research* 108.D23, p. 4726.
- Reichstein, M., E. Falge, D. Baldocchi, D. Papale, M. Aubinet, P. Berbigier, C. Bernhofer, N. Buchmann, T. Gilmanov & A. Granier (2005). "On the separation of net ecosystem exchange into assimilation and ecosystem respiration: review and improved algorithm". In: *Global Change Biology* 11.9, pp. 1424–1439.
- Revill, A., O. Sus, B. Barrett & M. Williams (2013). "Carbon cycling of European croplands: A framework for the assimilation of optical and microwave Earth observation data". In: *Remote Sensing Of Environment* 137, pp. 84–93.
- Reynolds, R. F., W. L. Bauerle & Y. Wang (2009). "Simulating carbon dioxide exchange rates of deciduous tree species: evidence for a general pattern in biochemical changes and water stress response". In: *Annals of Botany* 104.4, pp. 775–784.
- Rouse, J. W. (1974). "Monitoring the vernal advancement and retrogradation (greenwave effect) of natural vegetation". In: *NASA/GSFCT Type II Report*.
- Rouse, J. W., R. H. Haas, J. A. Schell, D. W. Deering & J. C. Harlan (1974). "Monitoring the vernal advancements and retrogradation of natural vegetation". In: *NASA/GSFC, Final Report, Greenbelt, MD, USA*, pp. 1–137.
- Ruidisch, R., T. T. Nguyen, Y. L. Li, R. Geyer & J. Tenhunen (2014). "Estimation of annual spatial variations in forest production and crop yields at landscape scale in temperate climate regions". In: *Ecological Research* 7, pp. 271–304.
- Running, S. W. & R. R. Nemani (1988). "Relating seasonal patterns of the AVHRR vegetation index to simulated photosynthesis and transpiration of forests in different climates". In: *Remote Sensing Of Environment* 24.2, pp. 347–367.
- Running, S. W., D. D. Baldocchi, D. P. Turner, S. T. Gower, P. S. Bakwin & K. A. Hibbard (1999). "A global terrestrial monitoring network integrating tower fluxes, flask sampling,

- ecosystem modeling and EOS satellite data”. In: *Remote Sensing Of Environment* 70.1, pp. 108–127.
- Saigusa, N. & T. Oikawa (1998). “Seasonal variations of the exchange of CO<sub>2</sub> and H<sub>2</sub>O between a grassland and the atmosphere: an experimental study”. In: *Agricultural and Forest Meteorology* 89, pp. 131–139.
- Saito, M., A. Miyata & H. Nagai (2005). “Seasonal variation of carbon dioxide exchange in rice paddy field in Japan”. In: *Agricultural and forest*.
- Sala, A. & J. D. Tenhunen (1994). “Site-specific water relations and stomatal response of *Quercus ilex* in a Mediterranean watershed.” In: *Tree physiology* 14.6, pp. 601–617.
- Sala, A. & J. D. Tenhunen (1996). “Simulations of canopy net photosynthesis and transpiration in *Quercus ilex* L. under the influence of seasonal drought”. In: *Agricultural and Forest Meteorology* 78.3, pp. 203–222.
- Schulze, E. D. (2006). “Biological control of the terrestrial carbon sink”. In: *Biogeosciences* 3.2, pp. 147–166.
- Schulze, E. D. & A. E. Hall. “Stomatal Responses, Water Loss and CO<sub>2</sub> Assimilation Rates of Plants in Contrasting Environments”. In: *Physiological Plant Ecology II*. Springer Berlin Heidelberg.
- Sellers, P. J., J. A. Berry, G. J. Collatz, C. B. Field & F. G. Hall (1992). “Canopy reflectance, photosynthesis, and transpiration. III. A reanalysis using improved leaf models and a new canopy integration scheme.” In: *Remote Sensing Of Environment* 42.3, pp. 187–216.
- Sellers, P. J., R. E. Dickinson, D. A. Randall, A. K. Betts, F. G. Hall, J. A. Berry, G. J. Collatz, A. S. Denning, H. A. Mooney & C. A. Nobre (1997). “Modeling the exchanges of energy, water, and carbon between continents and the atmosphere”. In: *Science* 275.5299, pp. 502–509.
- Seo, B., C. Bogner, P. Poppenborg, E. Martin, M. Hoffmeister, M. Jun, T. Koellner, B. Reineking, C. Shope & J. Tenhunen (2014). “Deriving a per-field land use and land cover map in an agricultural mosaic catchment”. In: *Earth Syst. Sci. Data Discuss.* 7, pp. 271–304.
- Smith, P., G. Lanigan, W. L. Kutsch, N. Buchmann, W. Eugster, M. Aubinet, E. Ceschia, P. Béziat, J. B. Yeluripati, B. Osborne, E. J. Moors, A. Brut, M. Wattenbach, M. Saunders &

- M. Jones (2010). "Measurements necessary for assessing the net ecosystem carbon budget of croplands". In: *Agriculture, Ecosystems & Environment* 139.3, pp. 302–315.
- Soegaard, H., N. O. Jensen, E. Boegh, C. B. Hasager, K. Schelde & A. Thomsen (2003). "Carbon dioxide exchange over agricultural landscape using eddy correlation and footprint modelling". In: *Agricultural and Forest Meteorology* 114.3, pp. 153–173.
- Stenberg, P., M. Rautiainen, T. Manninen, P. Voipio & H. Smolander (2004). "Reduced simple ratio better than NDVI for estimating LAI in Finnish pine and spruce stands". In: *Silva Fennica* 38.1, pp. 3–14.
- Suyker, A. E. & S. B. Verma (2010). "Coupling of carbon dioxide and water vapor exchanges of irrigated and rainfed maize–soybean cropping systems and water productivity". In: *Agricultural and Forest Meteorology* 150.4, pp. 553–563.
- Suyker, A. E., S. B. Verma, G. G. Burba, T. J. Arkebauer, D. T. Walters & K. G. Hubbard (2004). "Growing season carbon dioxide exchange in irrigated and rainfed maize". In: *Agricultural and Forest Meteorology* 124.1, pp. 1–13.
- Suyker, A. E., S. B. Verma, G. G. Burba & T. J. Arkebauer (2005). "Gross primary production and ecosystem respiration of irrigated maize and irrigated soybean during a growing season". In: *Agricultural and Forest Meteorology* 131.3-4, pp. 180–190.
- Tenhunen, J. D., R. Hanano, M. Abril, E. W. Weiler & W. Hartung (1994). "Above-and below-ground environmental influences on leaf conductance of *Ceanothus thyrsiflorus* growing in a chaparral environment: drought response and the role of abscisic acid". In: *Oecologia* 99.3, pp. 306–314.
- Tenhunen, J. D., A. S. Serra, P. C. Harley, R. L. Dougherty & J. F. Reynolds (1990). "Factors influencing carbon fixation and water use by Mediterranean sclerophyll shrubs during summer drought". In: *Oecologia* 82.3, pp. 381–393.
- Tenhunen, J. D., C. S. Yocum & D. M. Gates (1976). "Development of a photosynthesis model with an emphasis on ecological applications". In: *Oecologia* 26.2, pp. 89–100.
- Tenhunen, J., R. Geyer, S. Adiku, M. Reichstein, U. Tappeiner, M. Bahn, A. Cernusca, N. Q. Dinh, O. Kolcun & A. Lohila (2009). "Influences of changing land use and CO<sub>2</sub> concentration on ecosystem and landscape level carbon and water balances in mountainous terrain of the Stubai Valley, Austria". In: *Global and Planetary Change* 67.1, pp. 29–43.

- Valentini, R. (2003). “EUROFLUX: An Integrated Network for Studying the Long-Term Responses of Biospheric Exchanges of Carbon, Water, and Energy of European Forests”. In: *Fluxes of carbon, water and energy of European forests*. Ed. by R.Valentini. Vol. 163. Springer Berlin Heidelberg.
- Valentini, R., G. Matteucci, A. J. Dolman, E. D. Schulze, C. Rebmann, E. J. Moors, A. Granier, P. Gross, N. O. Jensen, K. Pilegaard, A. Lindroth, A. Grelle, C. Bernhofer, T. Grünwald, M. Aubinet, R. Ceulemans, A. S. Kowalski, T. Vesala, Ü. Rannik, P. Berbigier, D. Loustau, J. Guomundsson, H. Thorgeirsson, A. Ibrom, K. Morgenstern, R. Clement, J. Moncrieff, L. Montagnani, S. Minerbi & P. G. Jarvis (2000). “Respiration as the main determinant of carbon balance in European forests”. In: *Agriculture* 404.6780, pp. 861–865.
- Van der Loo, M. P. (2010). “Distribution based outlier detection for univariate data”. In: *Statistics Netherlands* 10003.
- Verma, S. B., A. Dobermann, K. G. Cassman, D. T. Walters, J. M. Knops, T. J. Arkebauer, A. E. Suyker, G. G. Burba, B. Amos & H. Yang (2005). “Annual carbon dioxide exchange in irrigated and rainfed maize-based agroecosystems”. In: *Agricultural and Forest Meteorology* 131.1, pp. 77–96.
- Veroustraete, F., J. Patyn & R. B. Myneni (1996). “Estimating net ecosystem exchange of carbon using the normalized difference vegetation index and an ecosystem model”. In: *Remote Sensing Of Environment* 58.1, pp. 115–130.
- Vina, A., A. A. Gitelson, D. C. Rundquist, G. Keydan, B. Leavitt & J. Schepers (2004). “Monitoring Maize (L.) Phenology with Remote Sensing”. In: *Agronomy Journal* 96.4, pp. 1139–1147.
- Waddington, J. M., T. J. Griffis & W. R. Rouse (1998). “Northern Canadian Wetlands: Net Ecosystem CO<sub>2</sub> Exchange and Climatic Change - Springer”. In: *Climatic change* 40.2, pp. 267–275.
- Wang, Q., A. Iio & Y. Kakubari (2008). “Broadband simple ratio closely traced seasonal trajectory of canopy photosynthetic capacity”. In: *Geophys Res Lett* 35.7, p. L07401.
- Wang, Q., J. Tenhunen, E. Falge, C. H. Bernhofer, A. Granier & T. Vesala (2003). “Simulation and scaling of temporal variation in gross primary production for coniferous and deciduous temperate forests”. In: *Global Change Biology* 10.1, pp. 37–51.

- Wang, Q., S. Adiku, J. Tenhunen & A. Granier (2005). "On the relationship of NDVI with leaf area index in a deciduous forest site". In: *Remote Sensing of Environment* 94.2, pp. 244–255.
- Wang, Q., J. Tenhunen, N. Q. Dinh, M. Reichstein, T. Vesala & P. Keronen (2004). "Similarities in ground- and satellite-based NDVI time series and their relationship to physiological activity of a Scots pine forest in Finland". In: *Remote Sensing Of Environment* 93.1-2, pp. 225–237.
- WANG, Y., D. BALDOCCHI, R. LEUNING, E. FALGE & T. VESALA (2007). "Estimating parameters in a land-surface model by applying nonlinear inversion to eddy covariance flux measurements from eight FLUXNET sites". In: *Global Change Biology* 13.3, pp. 652–670.
- Wang, Y. P. & R. Leuning (1998). "A two-leaf model for canopy conductance, photosynthesis and partitioning of available energy I: Model description and comparison with a multi-layered model". In: *Agricultural and Forest Meteorology* 91.1, pp. 89–111.
- Wang, Y. P., R. Leuning, H. A. Cleugh & P. A. Coppin (2001). "Parameter estimation in surface exchange models using nonlinear inversion: how many parameters can we estimate and which measurements are most useful?" In: *Global Change Biology* 7.5, pp. 495–510.
- Wang, Y. P. & P. J. Polglase (1995). "Carbon balance in the tundra, boreal forest and humid tropical forest during climate change: scaling up from leaf physiology and soil carbon dynamics". In: *Plant, Cell and Environment* 18.10, pp. 1226–1244.
- Wang, Z., X. Xiao & X. Yan (2010). "Modeling gross primary production of maize cropland and degraded grassland in northeastern China". In: *Agricultural and Forest Meteorology* 150.9, pp. 1160–1167.
- Wardlow, B. D. & S. L. Egbert (2010). "A comparison of MODIS 250-m EVI and NDVI data for crop mapping: a case study for southwest Kansas". In: *International Journal of Remote Sensing* 31.3, pp. 805–830.
- Wattenbach, M., O. Sus, N. Vuichard, S. Lehuger, P. Gottschalk, L. Li, A. Leip, M. Williams, E. Tomelleri, W. L. Kutsch, N. Buchmann, W. Eugster, D. Dietiker, M. Aubinet, E. Ceschia, P. Béziat, T. Grünwald, A. Hastings, B. Osborne, P. Ciais, P. Cellier & P. Smith (2010). "The carbon balance of European croplands: A cross-site comparison of simulation models". In: *Agriculture, ecosystems & environment* 139.3, pp. 419–453.
- Watters, T. R., M. S. Robinson, R. A. Beyer, M. E. Banks, J. F. Bell, M. E. Pritchard, H. Hiesinger, C. H. van der Bogert, P. C. Thomas, E. P. Turtle & N. R. Williams (2010).

- “Evidence of Recent Thrust Faulting on the Moon Revealed by the Lunar Reconnaissance Orbiter Camera”. In: *Science* 329.5994, pp. 936–940.
- White, J. & S. Running (1994). “Testing scale dependent assumptions in regional ecosystem simulations”. In: *Journal of Vegetation Science* 5.5, pp. 687–702.
- Wilby, A. & M. B. Thomas (2005). “Biodiversity and the functioning of selected terrestrial ecosystems: agricultural systems.” In: *BIODIVERSITY: STRUCTURE AND FUNCTION*. Vol. 1. Oxford, United Kingdom: Eolss.
- Wilson, K. B., D. D. Baldocchi & P. J. Hanson (2000). “Spatial and seasonal variability of photosynthetic parameters and their relationship to leaf nitrogen in a deciduous forest.” In: *Tree physiology* 20.9, pp. 565–578.
- Wong, S. C., I. R. Cowan & G. D. Farquhar (1979). “Stomatal conductance correlates with photosynthetic capacity”. In: *Nature* 282.5737, pp. 424–426.
- Wu, C., Z. Niu, Q. Tang, W. Huang, B. Rivard & J. Feng (2009). “Remote estimation of gross primary production in wheat using chlorophyll-related vegetation indices”. In: *Agricultural and Forest Meteorology* 149.6-7, pp. 1015–1021.
- Xiao, J., Q. Zhuang, B. E. Law, J. Chen, D. D. Baldocchi, D. R. Cook, R. Oren, A. D. Richardson, S. Wharton & S. Ma (2010). “A continuous measure of gross primary production for the conterminous United States derived from MODIS and AmeriFlux data”. In: *Remote Sensing Of Environment* 114.3, pp. 576–591.
- Xiao, X., L. He, W. Salas & C. Li (2002). “Quantitative relationships between field-measured leaf area index and vegetation index derived from VEGETATION images for paddy rice fields”. In: *International Journal of Remote Sensing* 23.28, pp. 3595–3604.
- Xiao, X., Q. Zhang, B. Braswell, S. Urbanski, S. Boles, S. Wofsy, B. Moore III & D. Ojima (2004). “Modeling gross primary production of temperate deciduous broadleaf forest using satellite images and climate data”. In: *Remote Sensing Of Environment* 91.2, pp. 256–270.
- Xu, C., R. Fisher, S. D. Wullschleger, C. J. Wilson, M. Cai & N. G. McDowell (2011). “Toward a mechanistic modeling of nitrogen limitation on vegetation dynamics.” In: *PloS one* 7.5, e37914–e37914.
- Xu, Q. & B. Huang (2000). “Effects of differential air and soil temperature on carbohydrate metabolism in creeping bentgrass”. In: *Crop Science* 40.5, pp. 1368–1374.

- Yan, H., Y. Fu, X. Xiao, H. Q. Huang, H. He & L. Ediger (2009). "Modeling gross primary productivity for winter wheat–maize double cropping system using MODIS time series and CO<sub>2</sub> eddy flux tower data". In: *Agriculture, ecosystems & environment* 129.4, pp. 391–400.
- Yee, T. W. & N. D. Mitchell (1991). "Generalized additive models in plant ecology". In: *Journal of vegetation science* 2.5, pp. 587–602.
- Yi, Y., D. Yang, J. Huang & D. Chen (2008). "Evaluation of MODIS surface reflectance products for wheat leaf area index (LAI) retrieval". In: *ISPRS Journal of Photogrammetry and Remote Sensing* 63.6, pp. 661–677.
- Yuan, W., S. Liu, G. Zhou, G. Zhou, L. L. Tieszen, D. Baldocchi, C. Bernhofer, H. Gholz, A. H. Goldstein, M. L. Goulden, D. Y. Hollinger, Y. Hu, B. E. Law, P. C. Stoy, T. Vesala & S. C. Wofsy (2007). "Deriving a light use efficiency model from eddy covariance flux data for predicting daily gross primary production across biomes". In: *Agricultural and Forest Meteorology* 143.3-4, pp. 189–207.
- Zhang, X., M. Friedl, C. Schaaf, A. Strahler, J. Hodges, F. Gao, B. Reed & A. Huete (2003). "Monitoring vegetation phenology using MODIS". In: *Remote Sens Environ* 84.3, pp. 471–475.
- Zhang, X., M. Friedl, C. Schaaf, A. Strahler & Z. Liu (2005). "Monitoring the response of vegetation phenology to precipitation in Africa by coupling MODIS and TRMM instruments". In: *Journal of Geophysical Research* 110.2.
- Zhang, Y., Q. Yu, J. Jiang & Y. Tang (2008). "Calibration of Terra/MODIS gross primary production over an irrigated cropland on the North China Plain and an alpine meadow on the Tibetan Plateau". In: *Global Change Biology* 14.4, pp. 757–767.
- Zhao, M., F. A. Heinsch, R. R. Nemani & S. W. Running (2005). "Improvements of the MODIS terrestrial gross and net primary production global data set". In: *Remote Sensing Of Environment* 95.2, pp. 164–176.



## **(Eidesstattliche) Versicherungen und Erklärungen**

(§ 8 S. 2 Nr. 6 PromO)

Hiermit erkläre ich mich damit einverstanden, dass die elektronische Fassung meiner Dissertation unter Wahrung meiner Urheberrechte und des Datenschutzes einer gesonderten Überprüfung hinsichtlich der eigenständigen Anfertigung der Dissertation unterzogen werden kann.

(§ 8 S. 2 Nr. 8 PromO)

Hiermit erkläre ich eidesstattlich, dass ich die Dissertation selbständig verfasst und keine anderen als die von mir angegebenen Quellen und Hilfsmittel benutzt habe.

(§ 8 S. 2 Nr. 9 PromO)

Ich habe die Dissertation nicht bereits zur Erlangung eines akademischen Grades anderweitig eingereicht und habe auch nicht bereits diese oder eine gleichartige Doktorprüfung endgültig nicht bestanden.

(§ 8 S. 2 Nr. 10 PromO)

Hiermit erkläre ich, dass ich keine Hilfe von gewerbliche Promotionsberatern bzw. -vermittlern in Anspruch genommen habe und auch künftig nicht nehmen werde.

.....  
Ort, Datum, Unterschrift